

國立交通大學

機械工程學系

博士論文

耦合渾沌系統同步、適應同步及廣義同步之部分穩定性理論



Synchronization, Adaptive Synchronization and Generalized
Synchronization of Coupled Chaotic Systems via Partial
Stability Theory

研究生：陳炎生

指導教授：戈正銘 教授

中華民國九十四年六月

耦合渾沌系統同步、適應同步及廣義同步之部分穩定性理論
方法研究

**Synchronization, Adaptive Synchronization and Generalized
Synchronization of Coupled Chaotic Systems via Partial
Stability Theory**

研究生：陳炎生

Student : Yen-Sheng Chen

指導教授：戈正銘

Advisor : Zheng-Ming Ge



A Dissertation

Submitted to Department of Mechanical Engineering

College of Engineering

National Chiao Tung University

In Partial Fulfillment of the Requirements

for the Degree of

Doctor of Philosophy

in

Mechanical Engineering

June 2005

Hsinchu, Taiwan, Republic of China

中華民國九十四年六月

耦合渾沌系統同步、適應同步及廣義同步之部分穩定性理論 方法研究

學生：陳炎生

指導老師：戈正銘 教授

國立交通大學機械工程學系

摘要

渾沌同步可以由許多方法達成。但是，一般來說，並沒有通用的簡單判據。本論文提出一個一般性的解決方案，透過部分變量穩定性理論來達到渾沌同步，並且可以適用於單向及雙向耦合系統。

依照提出方案的程序，首先討論單向耦合系統，共推導出三個判據。一個判據適合系統沒有攝動情況，其他兩個則分別適用於系統存在歸零及非歸零攝動情形。類似於單向耦合系統，針對雙向耦合系統也有三個保證同步發生的定理被推導出來。一個判據適合系統沒有攝動情況，其他兩個則分別適用於系統存在歸零及非歸零攝動情形。

在上述的六個判據中，為了確保同步的出現，必須滿足一個矩陣方程式並且事先估算 Lipschitz 常數。特別地，估算 Lipschitz 常數經常太過於保守。為了克服這兩個缺點，矩陣方程式及估算 Lipschitz 常數分別由一個適應耦合增益值及適應估測器所取代。則對於單向及雙向耦合系統，由此法可實現一簡單又方便的適應同步。

在先前的結果中，同步指的是全等同步(或是完全同步)。接著本論文探討另一種所謂的廣義同步，其意指在無窮長的迭代時間後，驅迫與被驅迫系統的狀態之間存在一個函數關係。類似地，本文提出一個藉由部分變量穩定性理論來達到廣義同步的方案。依此方案的程序，針對單向耦合系統，證出一個透過線性回授來達到廣義同步的定理。

所有在本論文中被推導出的判據都適用於規律及渾沌系統、線性及非線性系統、自治及非自治系統。最後，許多系統被數值模擬用於展示理論分析結果。

Synchronization, Adaptive Synchronization and Generalized Synchronization of Coupled Chaotic Systems via Partial Stability Theory

Student : Yen-Sheng Chen

Advisor : Zheng-Ming Ge

Department of Mechanical Engineering
National Chiao Tung University

Abstract

Chaos synchronization can be achieved by several methods but there is no easy unified criterion in general. Herein, a general scheme for both unidirectional and mutual coupled systems is proposed to achieve chaos synchronization via stability with respect to partial variables.

Follow the procedure of the proposed scheme, the unidirectional coupled systems are discussed first and three sufficient criteria are derived. One of them is suitable for systems without perturbation and the other two are suitable for systems under two kinds of perturbations, vanishing and nonvanishing, respectively. Similar to the unidirectional case, three theorems are proven to ensure occurrence of synchronization for mutual coupled systems. One of them is suitable for systems without perturbation and the other two are suitable for systems under two kinds of perturbations, vanishing and nonvanishing, respectively.

In previous six criteria, to guarantee the emergence of synchronization a matrix equation should be satisfied and the estimation of Lipschitz constant is needed. Specifically, the estimate of Lipschitz constant is often conservative. To overcome these two shortcomings, this matrix equation and the estimation of Lipschitz constant are replaced by adopting an adaptive coupling gain and an adaptive estimator, respectively. As a result, a simple and convenient adaptive synchronization is realized

for both unidirectional and mutual coupled systems.

In the foregoing results, the synchronization discussed indicates the identical synchronization (or complete synchronization). Another kind of synchronization called generalized synchronization which means that there is a functional relation between the states of driving and response systems as time goes to infinity are studied in the chapter 5. Similar, a scheme to achieve chaos generalized synchronization via partial stability is proposed. Follow the procedure of this scheme, one theorem is proven to ensure generalized synchronization for a general kind of unidirectional coupled systems by linear feedback.

All the criteria derived in this dissertation work for regular and chaotic systems, linear and nonlinear systems, autonomous and nonautonomous systems. Finally, several systems are simulated numerically to illustrate the theoretical analyses.



誌謝

從 88 年進入交大機械系就讀碩士乃至 94 年取得博士學位，六個寒暑秋冬不啻是一段漫長的歲月，隨著時空的流轉，我也在此成長。首先我要感謝指導教授 戈正銘教授的悉心指導，由於老師因材施教，使我得以發揮潛能。透過老師嚴謹的治學精神以及不斷追求創新的理念，使我明白做學問無法朝夕竟功，而在於長時間功夫的累積。在此，我要對於老師致上最高的敬意。

我也要感謝幾位口試委員，陳文華教授、張家歐教授、周傳心教授、董必正教授、成維華教授及邵錦昌教授。諸位老師給我許多精闢的建議，使得我的博士論文能夠更加完善，再次致上萬分謝意。

在交大的這幾年，我要感謝研究室所有的學長、同學以及學弟。特別感謝張時明、張萬坤、徐華均、鐘國展、江博容、林俊吉、鮑東昇及王宣智幾位同學對我的幫忙，尤其是時明對我的照顧最多。還有許許多多朋友的支持，無法一一列名，在此一併致謝。

另外，我也要感謝我的母親、父親、兄嫂以及所有的家人，在這段期間他們是我背後的支柱，沒有他們的支持與鼓勵，我無法順利完成博士學位。

最後，我要感恩 師父及十方諸佛菩薩，總是在我最困頓的時候，適時地伸出手來幫助我、引導我、給我希望、給我光明，從此不再行走於黑暗中。當然，還有許多可愛的師兄姐們，就像一家人般的互相扶持。言至於此，內心的感動久久無法平復。僅以此文獻給所有曾經護持我的一切人事物。

CONTENTS

摘要	i
ABSTRACT	ii
誌謝	iv
CONTENTS	v
LIST OF FIGURES	vii
Chapter 1 Introduction	1
Chapter 2 A General Scheme and Synchronization of Unidirectional Coupled Systems	4
2.1 A General Scheme	4
2.2 Unidirectional Coupled Systems without Perturbation	5
2.3 Unidirectional Coupled Systems with Two Kinds of Perturbations	7
2.4 Numerical Illustrated Examples	8
2.4.1 Unidirectional Coupled Systems without Perturbation	10
2.4.2 Unidirectional Coupled Systems with Perturbation $\ \Delta f\ < K \ e\ $	11
2.4.3 Unidirectional Coupled Systems with Perturbation Small on the Average	11
Chapter 3 Synchronization of Mutual Coupled Systems	33
3.1 Mutual Coupled Systems without Perturbation	33
3.2 Mutual Coupled Systems with Two Kinds of Perturbations	34
3.3 Numerical Illustrated Examples	36
3.3.1 Mutual Coupled Systems without Perturbation	37
3.3.2 Mutual Coupled Systems with Perturbation $\ \Delta f\ < K \ e\ $	38
3.3.3 Mutual Coupled Systems with Perturbation Small on the Average	39
Chapter 4 Adaptive Synchronization of Unidirectional and Mutual Coupled Systems	61
4.1 Introduction	61

4.2	Adaptive Synchronization of Unidirectional Coupled Systems.....	61
4.3	Adaptive Synchronization of Mutual Coupled Systems.....	62
4.4	Numerical Illustrated Examples.....	64
Chapter 5	Generalized Synchronization of Coupled Systems.....	78
5.1	Introduction.....	78
5.2	Theoretical Analysis.....	78
5.3	Numerical Illustrated Examples.....	80
Chapter 6	Conclusions.....	94
APPENDIX	96
REFERENCES	100
PAPER LIST	106



List of Figures

Fig. 2.1	Chaotic attractor of the Rössler system.....	13
Fig. 2.2	Chaotic attractor of the Duffing-van der Pol System	14
Fig. 2.3	State errors versus time of unidirectional coupled Rössler systems without perturbation	15
Fig. 2.4	Projections of synchronized manifold for unidirectional Rössler systems without perturbation	16
Fig. 2.5	Lyapunov spectra of unidirectional coupled Rössler systems without perturbation	17
Fig. 2.6	State errors versus time of unidirectional coupled Rössler systems without perturbation while $\gamma = 0.09$	18
Fig. 2.7	State errors versus time of unidirectional coupled Duffing-van der Pol system without perturbation	19
Fig. 2.8	Projections of synchronized manifold of unidirectional coupled Duffing-van der Pol system without perturbation	20
Fig. 2.9	State errors versus time of unidirectional coupled Rössler systems with perturbation $\Delta f_1 = z_2 - z_1$ and $\Delta f_2 = \sin t \cdot (x_1 - x_2)$	21
Fig. 2.10	Projections of synchronized manifold of unidirectional coupled Rössler systems with perturbation $\Delta f_1 = z_2 - z_1$ and $\Delta f_2 = \sin t \cdot (x_1 - x_2)$	22
Fig. 2.11	State errors versus time of unidirectional coupled Duffing-van der Pol system with perturbation $\Delta f_1 = \cos t \sin(y_2 - y_1)$	23
Fig. 2.12	Projections of synchronized manifold of unidirectional coupled Duffing-van der Pol system with perturbation $\Delta f_1 = \cos t \sin(y_2 - y_1)$	24
Fig. 2.13	State errors versus time of unidirectional coupled Rössler systems with perturbation $\Delta f_1 = \text{randn}(t)$ and $\Delta f_2 = 5 \cos 30t$	25
Fig. 2.14	Projections of synchronized manifold of unidirectional coupled Rössler systems with perturbation $\Delta f_1 = \text{randn}(t)$ and $\Delta f_2 = 5 \cos 30t$	26
Fig. 2.15	State errors versus time of unidirectional coupled Rössler systems with $\Delta f_1 = \text{randn}(t)$, $\Delta f_2 = 5 \cos 30t$ and $\gamma = 80$	27
Fig. 2.16	Projections of synchronized manifold of unidirectional coupled Rössler	

	systems with $\Delta f_1 = randn(t)$, $\Delta f_2 = 5 \cos 30t$ and $\gamma = 80$	28
Fig. 2.17	State errors versus time of unidirectional coupled Duffing-van der Pol system with perturbations $\Delta f_1 = \cos 20\pi t$ and $\Delta f_2 = \sin 30\pi t$	29
Fig. 2.18	Projections of synchronized manifold of unidirectional coupled Duffing-van der Pol system with perturbations $\Delta f_1 = \cos 20\pi t$ and $\Delta f_2 = \sin 30\pi t$	30
Fig. 2.19	State errors versus time of unidirectional coupled Duffing-van der Pol system with $\Delta f_1 = \cos 20\pi t$, $\Delta f_2 = \sin 30\pi t$ and $\gamma = 100$	31
Fig. 2.20	Projections of synchronized manifold of unidirectional coupled Duffing-van der Pol system with $\Delta f_1 = \cos 20\pi t$, $\Delta f_2 = \sin 30\pi t$ and $\gamma = 100$	32
Fig. 3.1	Chaotic attractor of the Lorenz system	41
Fig. 3.2	Chaotic attractor of the Ueda system.	42
Fig. 3.3	State errors versus time of mutual coupled Lorenz system without perturbation	43
Fig. 3.4	Projections of synchronized manifold for mutual coupled Lorenz system without perturbation	44
Fig. 3.5	Lyapunov spectra of mutual coupled Lorenz systems without system perturbation	45
Fig. 3.6	State errors versus time of mutual coupled Lorenz systems without perturbation while $\gamma = 0.6$	46
Fig. 3.7	State errors versus time of mutual coupled Ueda system without perturbation	47
Fig. 3.8	Projections of synchronized manifold of mutual coupled Ueda system without perturbation	48
Fig. 3.9	State errors versus time of mutual coupled Lorenz systems with perturbations $\Delta f_1 = \cos t \cdot (y_1 - y_2)$ and $\Delta f_6 = x_1 - x_2$	49
Fig. 3.10	Projections of synchronized manifold of mutual coupled Lorenz systems with perturbations $\Delta f_1 = \cos t \cdot (y_1 - y_2)$ and $\Delta f_6 = x_1 - x_2$	50
Fig. 3.11	State errors versus time of mutual coupled Ueda systems with perturbations $\Delta f_2 = \cos t \sin(x_2 - x_1)$ and $\Delta f_3 = y_2 - y_1$	51

Fig. 3.12	Projections of synchronized manifold of mutual coupled Ueda systems with perturbations $\Delta f_2 = \cos t \sin(x_2 - x_1)$ and $\Delta f_3 = y_2 - y_1$	52
Fig. 3.13	State errors versus time of mutual coupled Lorenz systems with perturbations $\Delta f_2 = 2 \sin(20\pi t)$, $\Delta f_4 = \text{randn}(t)$ and $\Delta f_6 = 5 \cos(30\pi t)$	53
Fig. 3.14	Projections of synchronized manifold of mutual coupled Lorenz systems with perturbations $\Delta f_2 = 2 \sin(20\pi t)$, $\Delta f_4 = \text{randn}(t)$ and $\Delta f_6 = 5 \cos(30\pi t)$	54
Fig. 3.15	State errors versus time of mutual coupled Lorenz systems with $\Delta f_2 = 2 \sin(20\pi t)$, $\Delta f_4 = \text{randn}(t)$, $\Delta f_6 = 5 \cos(30\pi t)$ and $\gamma = 130$	55
Fig. 3.16	Projections of synchronized manifold of mutual coupled Lorenz systems with $\Delta f_2 = 2 \sin(20\pi t)$, $\Delta f_4 = \text{randn}(t)$, $\Delta f_6 = 5 \cos(30\pi t)$ and $\gamma = 130$	56
Fig. 3.17	State errors versus time of mutual coupled Ueda systems with perturbations $\Delta f_2 = \cos(25\pi t)$ and $f_3 = 5 \sin(15\pi t)$	57
Fig. 3.18	Projections of synchronized manifold of mutual coupled Ueda systems with perturbations $\Delta f_2 = \cos(25\pi t)$ and $f_3 = 5 \sin(15\pi t)$	58
Fig. 3.19	State errors versus time of mutual coupled Ueda systems with $\Delta f_2 = \cos(25\pi t)$, $f_3 = 5 \sin(15\pi t)$ and $\gamma = 100$	59
Fig. 3.20	Projections of synchronized manifold of mutual coupled Ueda systems with $\Delta f_2 = \cos(25\pi t)$, $f_3 = 5 \sin(15\pi t)$ and $\gamma = 100$	60
Fig. 4.1	State errors and Estimated Lipschitz constant versus time for $\hat{L}_0 = 1$ and $\varepsilon = 0.1$ of unidirectional coupled Lorenz systems	66
Fig. 4.2	State errors and Estimated Lipschitz constant versus time for $\hat{L}_0 = 25$ and $\varepsilon = 0.1$ of unidirectional coupled Lorenz systems	67
Fig. 4.3	State errors and Estimated Lipschitz constant versus time for $\hat{L}_0 = 1$ and $\varepsilon = 20$ of unidirectional coupled Lorenz systems	68
Fig. 4.4	State errors and Estimated Lipschitz constant versus time for $\hat{L}_0 = 1$ and $\varepsilon = 0.1$ of unidirectional coupled Duffing systems	69
Fig. 4.5	State errors and Estimated Lipschitz constant versus time for $\hat{L}_0 = 5$ and	

	$\varepsilon = 0.1$ of unidirectional coupled Duffing systems.....	70
Fig. 4.6	State errors and Estimated Lipschitz constant versus time for $\hat{L}_0 = 1$ and $\varepsilon = 8$ of unidirectional coupled Duffing systems.....	71
Fig. 4.7	State errors and Estimated Lipschitz constant versus time for $\hat{L}_0 = 1$ and $\varepsilon = 0.1$ of mutual coupled Lorenz systems.....	72
Fig. 4.8	State errors and Estimated Lipschitz constant versus time for $\hat{L}_0 = 20$ and $\varepsilon = 0.1$ of mutual coupled Lorenz systems.....	73
Fig. 4.9	State errors and Estimated Lipschitz constant versus time for $\hat{L}_0 = 1$ and $\varepsilon = 18$ of mutual coupled Lorenz systems.....	74
Fig. 4.10	State errors and Estimated Lipschitz constant versus time for $\hat{L}_0 = 1$ and $\varepsilon = 0.1$ of mutual coupled Duffing systems	75
Fig. 4.11	State errors and Estimated Lipschitz constant versus time for $\hat{L}_0 = 5$ and $\varepsilon = 0.1$ of mutual coupled Duffing systems	76
Fig. 4.12	State errors and Estimated Lipschitz constant versus time for $\hat{L}_0 = 1$ and $\varepsilon = 3$ of mutual coupled Duffing systems	77
Fig. 5.1	e_1, e_2 and e_3 versus time.....	83
Fig. 5.2	Projections of synchronized manifold.....	84
Fig. 5.3	Phase portrait of the driving system.....	85
Fig. 5.4	Phase portrait of the response system	86
Fig. 5.5	e_1, e_2 and e_3 versus time.....	87
Fig. 5.6	Projections of synchronized manifold.....	88
Fig. 5.7	Phase portrait of the response system	89
Fig. 5.8	e_1 and e_2 versus time	90
Fig. 5.9	Projections of synchronized manifold.....	91
Fig. 5.10	Phase portrait of the driving system.....	92
Fig. 5.11	Phase portrait of the response system	93

Chapter 1

Introduction

Chaotic systems exhibit sensitive dependence on initial conditions. Because of this property, chaotic systems are thought difficult to be synchronized or controlled. From the earlier works [1-3], especially after Pecora and Carroll [3], the researchers have realized that synchronization of chaotic motions is possible. From then on, synchronization of chaos was of great interest in these years [4-16]. In particular, it was pointed out that chaos synchronization has the potential in secure communication. Many engineers and scientists were attracted to this discipline [17-36].

Synchronization means that the states of response system approach eventually to the ones of driving system. Two kinds of chaos synchronization are discussed the most often. (1) Duplication (or master-slave): the first kind introduced by Pecora and Carroll [3] consists of a driving system and a response system. The former one evolves chaotic orbits and the latter is identical to the driving system except some partial states replaced by that of the driving one. (2) Coupling: the second kind consists of two identical chaotic systems except coupling term. Coupled systems can be unidirectional or mutual. Under certain conditions (appropriate coupling functions and/or system parameters with enough evolution time) the response system will behave the same orbit with the driving system.

There are many control methods to synchronize chaotic systems such as observer-based design methods [37-44], adaptive control [45-54], sliding mode control (or variable structure control) [41, 43, 44, 55-58], impulsive control [59-65] and other control methods [66-72]. A another kind of more general synchronism called generalized synchronization (GS) is studied in [73-77], this means that there is a functional relation between state variables of driving and response systems as time evolves. This function need not to be defined on the whole phase space but on the attractor only. Three methods were proposed to detect GS in [73-75] respectively while another method measuring the smooth degree of this function in [77].

Zero crossing of Lyapunov exponent which is used widely as a criterion of chaos synchronization is derived from the variational equation. There is a drawback that we can only calculate finite evolution time in computer simulation but infinite evolution

time is needed by definition of Lyapunov exponent. The variational equation itself is also used to ensure the occurrence of synchronism. But its stability is in the sense of Lyapunov first method. Especially, the domain of attraction is infinitesimal, as a result that the stability of synchronization guaranteed by the variational equation is not robust. On other hand, it is difficult to use traditional Lyapunov direct method since the state error equation is not a pure function of state error in general.

In this dissertation, we propose a general scheme to achieve chaos synchronization via partial stability due to Rumjantsev [78]. The previous obstacles will be overcome by our method and it serves as a criterion for chaos synchronization by control methods. Follows the procedure of proposed scheme, the unidirectional coupled systems are discussed and three sufficient criteria are derived in chapter 2. One of them is suitable for systems without perturbation and the other two are suitable for systems under two kinds of perturbations, vanishing and nonvanishing, respectively. In chapter 3, the effort is concentrated on synchronization of mutual coupled systems. Similar to the unidirectional case, three theorems are proven to ensure the occurrence of synchronization. One of them is suitable for systems without perturbation and the other two are suitable for systems under two kinds of perturbations, vanishing and nonvanishing, respectively.

In previous six criteria, to guarantee the emergence of synchronization a matrix equation should be satisfied and the estimation of Lipschitz constant is needed. Moreover, the estimate of Lipschitz constant is often conservative. To overcome these two shortcomings, this matrix equation and the estimation of Lipschitz constant are replaced by adopting an adaptive coupling gain and an adaptive estimator, respectively. As a result, a simple and convenient adaptive synchronization of chaotic systems is realized for both unidirectional and mutual coupled systems in chapter 4. It is easier and more convenient to use this method for synchronization of both unidirectional and mutual coupled systems than the six theorems in chapter 2 and 3. Furthermore, to increase the convergent rate of state error dynamics we only need to set a larger initial condition of the adaptive equation.

The synchronization discussed indicates the identical synchronization (or complete synchronization) in the foregoing results. Another kind of synchronization called generalized synchronization which means that there is a functional relation between the states of driving and response systems as time goes to infinity are studied in the chapter 5. This function can increase the complication of synchronization.

Similar to the chapter 2, a scheme to achieve generalized synchronization of chaos via partial stability is proposed. One theorem is proven to guarantee the occurrence generalized synchronization for a general kind of unidirectional coupled nonautonomous systems by linear feedback. Furthermore, the function between the states of the two coupled systems can be arbitrary assigned.

Superficially, the order of the error dynamic equation is enlarged since it is replaced by an extended equation in this scheme. But only partial variables are manipulated in actual. Furthermore, many control techniques can be applied to synchronize coupled systems in this scheme. All the criteria derived in this dissertation work for regular and chaotic, linear and nonlinear systems, autonomous and nonautonomous systems. Finally, several examples are simulated numerically to illustrate the theoretical analyses.



Chapter 2

A General Scheme and Synchronization of Unidirectional Coupled Systems

2.1 A General Scheme

Consider the following coupled nonautonomous systems

$$\begin{aligned}\dot{\mathbf{x}}_1 &= \mathbf{f}(t, \mathbf{x}_1, \mathbf{x}_2), \\ \dot{\mathbf{x}}_2 &= \mathbf{g}(t, \mathbf{x}_1, \mathbf{x}_2),\end{aligned}\tag{2.1}$$

where $\mathbf{x}_1, \mathbf{x}_2 \in \mathbb{R}^n$ are the states variables and Ω is a domain containing the origin. Assume that the solution of Eq. (2.1) exist for infinite time. That is, for given $(t_0, \mathbf{x}_{10}, \mathbf{x}_{20}) \in \Omega$ the solution $[\varphi_1^T(t; t_0, \mathbf{x}_0, \hat{\mathbf{x}}_0) \ \varphi_2^T(t; t_0, \mathbf{x}_0, \hat{\mathbf{x}}_0)]^T$ of Eq. (2.1) exists for $t \geq t_0$. At the first, we recall the definition of identical synchronization (or complete synchronization).

Definition *The system (2.1) is (identical) synchronized if there is an invariant manifold $S \subset \mathbb{R} \times \mathbb{R}^{2n}$ for the solution $[\varphi_1^T(t; t_0, \mathbf{x}_0, \hat{\mathbf{x}}_0) \ \varphi_2^T(t; t_0, \mathbf{x}_0, \hat{\mathbf{x}}_0)]^T$ of Eq. (2.1) s.t. $\lim_{t \rightarrow \infty} \|\varphi_1(t; t_0, \mathbf{x}_{10}, \mathbf{x}_{20}) - \varphi_2(t; t_0, \mathbf{x}_{10}, \mathbf{x}_{20})\| = 0$ with $(t_0, \mathbf{x}_{10}, \mathbf{x}_{20}) \in \Omega$.*

For convenience, rewrite Eq. (2.1) in a form which contains a coupling term to enhance synchronization

$$\begin{aligned}\dot{\mathbf{x}}_1 &= \mathbf{f}(t, \mathbf{x}_1) + \mathbf{G}_1(t, \mathbf{x}_1, \mathbf{x}_2), \\ \dot{\mathbf{x}}_2 &= \mathbf{f}(t, \mathbf{x}_2) + \mathbf{G}_2(t, \mathbf{x}_1, \mathbf{x}_2),\end{aligned}\tag{2.2}$$

where $\mathbf{f} : \Omega \subset \mathbb{R} \times \mathbb{R}^{2n} \rightarrow \mathbb{R}^n$ satisfy the Lipschitz condition $\|\mathbf{f}(t, \mathbf{x}_1) - \mathbf{f}(t, \mathbf{x}_2)\| \leq L \|\mathbf{x}_1 - \mathbf{x}_2\|$ in \mathbf{x} for all (t, \mathbf{x}_1) and (t, \mathbf{x}_2) in Ω with Lipschitz constants L and $\mathbf{G}_1, \mathbf{G}_2$ are the coupling functions. Assume that $\mathbf{G}_1(t, \mathbf{x}_1, \mathbf{x}_2) = \mathbf{0}$ and $\mathbf{G}_2(t, \mathbf{x}_1, \mathbf{x}_2) = \mathbf{0}$ for $\mathbf{x}_1(t) = \mathbf{x}_2(t), \forall t \geq t_0$. That is the synchronized sub-manifold of Eqs. (2.2) agrees with the original uncoupled one while synchronization occurs. In order to discuss the transversal stability of synchronization manifold, define $\mathbf{e} = \mathbf{x}_2 - \mathbf{x}_1$ to be the state error. Error equations can be written as

$$\dot{\mathbf{e}} = \mathbf{f}(t, \mathbf{x}_2) - \mathbf{f}(t, \mathbf{x}_1) + [\mathbf{G}_2(t, \mathbf{x}_1, \mathbf{x}_2) - \mathbf{G}_1(t, \mathbf{x}_1, \mathbf{x}_2)]. \quad (2.3)$$

Notice that the right hand side of Eqs. (2.3) is not a pure function of \mathbf{e} , as a result that the traditional Lyapunov direct method might hardly be used. The variational equation and zero crossing of Lyapunov exponent are used to clarify transversal stability locally. Moreover, Josić [81] analyzed that synchronization manifolds will persist under perturbation if such manifolds possess a property of k -hyperbolicity.

In our method, the upper half (lower half also works) of Eq. (2.2) is added into Eq. (2.3) with \mathbf{x}_2 replaced by $\mathbf{x}_2 = \mathbf{e} + \mathbf{x}_1$, then an extended equation is obtained as follows

$$\begin{aligned} \dot{\mathbf{x}}_1 &= \mathbf{f}(t, \mathbf{x}_1) + \mathbf{G}_1(t, \mathbf{x}_1, \mathbf{e} + \mathbf{x}_1), \\ \dot{\mathbf{e}} &= \mathbf{f}(t, \mathbf{e} + \mathbf{x}_1) - \mathbf{f}(t, \mathbf{x}_1) + [\mathbf{G}_2(t, \mathbf{x}_1, \mathbf{e} + \mathbf{x}_1) - \mathbf{G}_1(t, \mathbf{x}_1, \mathbf{e} + \mathbf{x}_1)]. \end{aligned} \quad (2.4)$$

If the partial variable \mathbf{e} in Eq. (2.4) are asymptotically stable about $\mathbf{e} = \mathbf{0}$, the synchronization manifold is stable in transversal directions. This means that the system in the form of Eq. (2.2) is synchronized. The determination of whether \mathbf{e} is asymptotically stable can be done via stability with respect to partial variables. The theory of partial stability can be found in appendix or in [78-80]. Note that the same procedure can be developed for Eq. (2.1). But this form of system might too general to be used. The scheme proposed in this section not only satisfies the case of mutual coupled nonlinear systems but also satisfies the unidirectional case. Actually, it works for the case of unidirectional coupled nonlinear systems if $\mathbf{G}_1 = \mathbf{0}$. The rest mission is to choose appropriate controllers \mathbf{G}_1 and \mathbf{G}_2 to guarantee the occurrence of synchronization. In the remainder of this chapter, we will adopt this scheme to develop some criteria of synchronization for unidirectional coupled systems and give some simulated illustrations.

2.2 Unidirectional Coupled Systems without Perturbation

In this section, a theorem will be given for unidirectional coupled nonautonomous system which is a special case of Eq. (2.2). This theorem is suitable for the case without perturbation and will be applied to two examples, the Rössler system and the Duffing-van der Pol system. Choose $\mathbf{G}_1 = \mathbf{0}$ and $\mathbf{G}_2 = \Gamma(\mathbf{x}_1 - \mathbf{x}_2)$, then the Eq. (2.2) becomes

$$\begin{aligned}\dot{\mathbf{x}}_1 &= \mathbf{f}(t, \mathbf{x}_1), \\ \dot{\mathbf{x}}_2 &= \mathbf{f}(t, \mathbf{x}_2) + \Gamma(\mathbf{x}_1 - \mathbf{x}_2),\end{aligned}\tag{2.5}$$

where \mathbf{f} satisfies Lipschitz condition with $\|\mathbf{f}(t, \mathbf{x}_1) - \mathbf{f}(t, \mathbf{x}_2)\| \leq L\|\mathbf{x}_1 - \mathbf{x}_2\|$ in \mathbf{x} for all (t, \mathbf{x}_1) and (t, \mathbf{x}_2) in domain Ω with Lipschitz constant L and $\Gamma \in M_{n \times n}$ is a constant matrix whose entries represent the coupling strength of the linear feedback term $(\mathbf{x}_1 - \mathbf{x}_2)$. The index of entry γ_{ij} means that the j -th component of $(\mathbf{x}_1 - \mathbf{x}_2)$ exerts on the i -th component of $\dot{\mathbf{x}}_2$. Follow the procedure stated in section 2.1. Eq. (2.5) can be rephrased in the form of an extended equation as

$$\begin{aligned}\dot{\mathbf{x}}_1 &= \mathbf{f}(t, \mathbf{x}_1), \\ \dot{\mathbf{e}} &= \mathbf{f}(t, \mathbf{e} + \mathbf{x}_1) - \mathbf{f}(t, \mathbf{x}_1) - \Gamma \mathbf{e}.\end{aligned}\tag{2.6}$$

where $\mathbf{e} = \mathbf{x}_2 - \mathbf{x}_1$.

Theorem 2.1 *The partial state \mathbf{e} is uniformly asymptotically to $\mathbf{0}$ in Eq. (2.6) if $L\mathbf{I}_n - \Gamma$ is negative definite, i.e. the system in the form of Eq. (2.5) is synchronized if $L\mathbf{I}_n - \Gamma$ is negative definite.*

Proof Choose a function $V(\mathbf{x}_1, \mathbf{e}) = \frac{1}{2} \mathbf{e}^T \mathbf{e}$ which is positive definite function with respect to \mathbf{e} and with infinitesimal upper bound. Then its time derivative along the solution of Eq. (2.6) is

$$\begin{aligned}\dot{V} &= \mathbf{e}^T \dot{\mathbf{e}} \\ &= \mathbf{e}^T [\mathbf{f}(t, \mathbf{e} + \mathbf{x}_1) - \mathbf{f}(t, \mathbf{x}_1) - \Gamma \mathbf{e}] \\ &\leq \|\mathbf{e}\| \cdot L \|\mathbf{e}\| - \mathbf{e}^T \Gamma \mathbf{e} \\ &\leq L \|\mathbf{e}\|^2 - \mathbf{e}^T \Gamma \mathbf{e} \\ &= \mathbf{e}^T (L\mathbf{I}_n - \Gamma) \mathbf{e}.\end{aligned}$$

The state error \mathbf{e} uniformly asymptotically approaches $\mathbf{0}$ if $L\mathbf{I}_n - \Gamma$ is negative definite by Theorem A2 in appendix. The Cauchy-Schwarz inequality and the Lipschitz condition were used in the derivation.

Remark 2.1 From the matrix theory, we know that $L\mathbf{I}_n - \Gamma$ is negative definite if and only if all its eigenvalues are negative. For the case $\Gamma = \text{diag}(\gamma_1, \gamma_2, \dots, \gamma_n)$ with $\gamma_i > 0$ for $i = 1, \dots, n$, synchronization occurs if $\gamma_{\min} > L$, where $\gamma_{\min} \leq \gamma_i, i = 1, \dots, n$. This is because the time derivative of $V(\mathbf{x}_1, \mathbf{e})$ can be written as

$\dot{V}(\mathbf{x}_1, \mathbf{e}) \leq (L - \gamma_{\min}) \|\mathbf{e}\|^2$. Moreover, the result is global by Theorem A4 if \mathbf{f} is globally Lipschitzian.

2.3 Unidirectional Coupled Systems with Two Kinds of Perturbations

The criterion given in section 2.2 is suitable for the case without system perturbation. If the system possesses a vanishing perturbation, similar result can be obtained. Consider unidirectional coupled nonautonomous systems with perturbation in the form of

$$\begin{aligned}\dot{\mathbf{x}}_1 &= \mathbf{f}(\mathbf{x}_1), \\ \dot{\mathbf{x}}_2 &= \mathbf{f}(\mathbf{x}_2) + \Delta\mathbf{f}(t, \mathbf{x}_1, \mathbf{x}_2) + \Gamma(\mathbf{x}_1 - \mathbf{x}_2),\end{aligned}\tag{2.7}$$

where \mathbf{f} satisfies Lipschitz condition with $\|\mathbf{f}(t, \mathbf{x}_1) - \mathbf{f}(t, \mathbf{x}_2)\| \leq L\|\mathbf{x}_1 - \mathbf{x}_2\|$ in \mathbf{x} for all (t, \mathbf{x}_1) and (t, \mathbf{x}_2) in domain Ω with Lipschitz constant L and $\Gamma \in M_{n \times n}$ is a constant matrix whose entries represent the coupling strength of the linear feedback term $(\mathbf{x}_1 - \mathbf{x}_2)$. The term $\Delta\mathbf{f}(t, \mathbf{x}_1, \mathbf{x}_2)$ is a vanishing perturbation which means that $\Delta\mathbf{f}(t, \mathbf{x}_1, \mathbf{x}_2) = \mathbf{0}$ with $\mathbf{x}_1(t) = \mathbf{x}_2(t), \forall t$. $\Delta\mathbf{f}(t, \mathbf{x}_1, \mathbf{x}_2)$ can be rephrased to be $\Delta\mathbf{f}(t, \mathbf{x}_1, \mathbf{e})$ while $\mathbf{e} = \mathbf{x}_2 - \mathbf{x}_1$. Then, an extended equation can be obtained as

$$\begin{aligned}\dot{\mathbf{x}}_1 &= \mathbf{f}(\mathbf{x}_1), \\ \dot{\mathbf{e}} &= \mathbf{f}(\mathbf{e} + \mathbf{x}_1) - \mathbf{f}(\mathbf{x}_1) + \Delta\mathbf{f}(t, \mathbf{x}_1, \mathbf{e}) - \Gamma\mathbf{e}.\end{aligned}\tag{2.8}$$

Theorem 2.2 Assume that $\exists K > 0 \Rightarrow \|\Delta\mathbf{f}\| < K\|\mathbf{e}\|$. Then the Eq. (2.8) is uniformly asymptotically \mathbf{e} -stable if $(L + K)\mathbf{I}_n - \Gamma$ is negative definite, i.e. the system in the form of Eq. (2.7) is synchronized if $(L + K)\mathbf{I}_n - \Gamma$ is negative definite.

Proof Choose a function $V(\mathbf{x}_1, \mathbf{e}) = \frac{1}{2}\mathbf{e}^T\mathbf{e}$ which is positive definite function with respect to \mathbf{e} and with infinitesimal upper bound. Then its time derivative along the solution of Eq. (2.6) is

$$\begin{aligned}\dot{V} &= \mathbf{e}^T\dot{\mathbf{e}} \\ &\leq (L + K)\|\mathbf{e}\|^2 - \mathbf{e}^T\Gamma\mathbf{e} \\ &\leq \mathbf{e}^T[(L + K)\mathbf{I}_n - \Gamma]\mathbf{e}.\end{aligned}$$

Hence, the Eq. (2.8) is uniformly asymptotically \mathbf{e} -stable if $(L + K)\mathbf{I}_n - \Gamma$ is negative definite.

Remark 2.2 $(L+K)\mathbf{I}_n - \Gamma$ is negative definite if and only if all its eigenvalues are negative. When $\Gamma = \text{diag}(\gamma_1, \gamma_2, \dots, \gamma_n)$ with $\gamma_i > 0$ for $i = 1, \dots, n$, synchronization occurs if $\gamma_{\min} > L+K$, where γ_{\min} is the minimum one in γ_i . Furthermore, this result is global by Theorem A4 if \mathbf{f} and $\Delta\mathbf{f}(t, \mathbf{x}_1, \mathbf{x}_2)$ are globally Lipschitzian.

If $\Delta\mathbf{f}(t, \mathbf{x}_1, \mathbf{x}_2)$ is not a vanishing perturbation, the origin $\mathbf{0}$ is no longer a trivial solution. It is difficult to design a controller to guarantee the occurrence of asymptotically partial stability like Theorem 2.2. What we called the stable under constantly acting perturbation small on the average will take it over.

Theorem 2.3 Assume that the functions \mathbf{f} and $D\mathbf{f}(\mathbf{x})$ are continuous and bounded in Q . The the Eq. (2.7) is uniformly e-stable under constantly acting perturbation small on the average if $L\mathbf{I}_n - \Gamma$ is negative definite.

Proof From theorem 2.1, the partial state \mathbf{e} is uniformly asymptotically to $\mathbf{0}$ in Eq. (2.6) if $L\mathbf{I}_n - \Gamma$ is negative definite. By corollary A1, the Eq. (2.7) is uniformly e-stable under constantly acting perturbation small on the average if $L\mathbf{I}_n - \Gamma$ is negative definite with the assumption that \mathbf{f} and $D\mathbf{f}(\mathbf{x})$ are continuous and bounded in Q . This completes the proof.

Remark 2.3 Theorem 2.3 means that the coupled structure perturbed systems (2.7) are practical synchronized [82]. If $\Gamma = \text{diag}(\gamma_1, \gamma_2, \dots, \gamma_n)$ with $\gamma_i > 0$ for $i = 1, \dots, n$, practical synchronization occurs if $\gamma_{\min} > L$, where $\gamma_{\min} \leq \gamma_i$, $i = 1, \dots, n$. Moreover, the larger γ_{\min} is, the smaller bounds of the state errors are. This result is global if \mathbf{f} is globally Lipschitzian.

2.4 Numerical Illustrated Examples

In this section, the Rössler system and the Duffing-van der Pol system are adopted to demonstrate the results given in section 2.2 and 2.3. They are simulated for the cases with and without system perturbation, respectively. The system equation of the Rössler system is as following

$$\begin{aligned}\dot{x} &= -y - z \triangleq f_1(\mathbf{x}), \\ \dot{y} &= x + ay \triangleq f_2(\mathbf{x}), \\ \dot{z} &= b + z(x - c) \triangleq f_3(\mathbf{x}),\end{aligned}$$

where $a = b = 0.2$ and $c = 5.7$ ensure that there exists chaotic behavior. The chaotic attractor is shown in Fig. 2.1. To apply the theorem given in this chapter, one needs to estimate the Lipschitz constant at the beginning. By Cauchy-Schwarz inequality, it can be derived for any $\mathbf{x}_2 = [x_2 \ y_2 \ z_2]^T$, $\mathbf{x}_1 = [x_1 \ y_1 \ z_1]^T$, we have

$$\begin{aligned}|f_1(\mathbf{x}_2) - f_1(\mathbf{x}_1)| &\leq \|[0 \ -1 \ -1]\| \|\mathbf{x}_2 - \mathbf{x}_1\|, \\ |f_2(\mathbf{x}_2) - f_2(\mathbf{x}_1)| &\leq \|[1 \ a \ 0]\| \|\mathbf{x}_2 - \mathbf{x}_1\|, \\ |f_3(\mathbf{x}_2) - f_3(\mathbf{x}_1)| &= |z_2x_2 - z_1x_1 - ce_3| \\ &= |z_2x_2 - z_2x_1 + z_2x_1 - z_1x_1 - ce_3| \\ &= |z_2e_1 + x_1e_3 - ce_3| \\ &\leq \|[B_3 \ 0 \ B_1 - c]\| \|\mathbf{x}_2 - \mathbf{x}_1\|,\end{aligned}$$

where $|x_i(t)| \leq B_1$, $|y_i(t)| \leq B_2$, $|z_i(t)| \leq B_3$, $\forall t > t_0$, $i = 1, 2$. Hence, a Lipschitz constant can be obtained as

$$L = \sqrt{\|[0 \ -1 \ -1]\|^2 + \|[1 \ a \ 0]\|^2 + \|[B_3 \ 0 \ B_1 - c]\|^2}.$$

From numerical simulation, $B_1 = 12$, $B_2 = 8$, $B_3 = 23$, then $L = 23.55$.

The governing equation of the Duffing-van der Pol system is

$$\begin{aligned}\dot{x} &= y \triangleq f_1(\mathbf{x}), \\ \dot{y} &= \mu(1 - \gamma x^2)y - x^3 + A \sin \Omega t \triangleq f_2(\mathbf{x}).\end{aligned}$$

The chaotic behavior exists while $\mu = 0.2$, $\gamma = 8$, $A = 5$ and $\Omega = 1.02$. The chaotic attractor is shown in Fig. 2.2. Apply the Cauchy-Schwarz inequality to estimate the Lipschitz constant. For any $\mathbf{x}_2 = [x_2 \ y_2]^T$, $\mathbf{x}_1 = [x_1 \ y_1]^T$, it can be derived

$$\begin{aligned}|f_1(\mathbf{x}_2) - f_1(\mathbf{x}_1)| &\leq \|\mathbf{x}_2 - \mathbf{x}_1\|, \\ |f_2(\mathbf{x}_2) - f_2(\mathbf{x}_1)| &\leq |\mu e_1 - \gamma x_2^2 y_2 + \gamma x_1^2 y_1 - x_2^3 + x_1^3| \\ &\leq \|[2\gamma B_1 B_2 + 3B_1^2 \ \mu + \gamma B_1^2]\| \|\mathbf{x}_2 - \mathbf{x}_1\|,\end{aligned}$$

where $|x_i(t)| \leq B_1$, $|y_i(t)| \leq B_2$, $\forall t > t_0$, $i = 1, 2$. Hence, one Lipschitz constant can be obtained as

$$L = \sqrt{1 + \|[2\gamma B_1 B_2 + 3B_1^2 \ \mu + \gamma B_1^2]\|^2}.$$

From numerical simulation, $B_1 = 1, B_2 = 1$, then $L = 20.72$.

2.4.1 Unidirectional Coupled Systems without Perturbation

Example 2.1 Autonomous case: Consider the following unidirectional coupled Rössler systems without perturbation in the form of Eq. (2.5) as

$$\begin{aligned}\dot{x}_1 &= -y_1 - z_1, \\ \dot{y}_1 &= x_1 + ay_1, \\ \dot{z}_1 &= b + z_1(x_1 - c), \\ \dot{x}_2 &= -y_2 - z_2 + \gamma(x_1 - x_2), \\ \dot{y}_2 &= x_2 + ay_2 + \gamma(y_1 - y_2), \\ \dot{z}_2 &= b + z_2(x_2 - c) + \gamma(z_1 - z_2),\end{aligned}$$

where $\Gamma = \text{diag}\{\gamma, \gamma, \gamma\}$ and $\gamma = 24$. The initial value is $\mathbf{x}_0 = [-9, 0, 0, 0, -1, -1]^T$.

The simulated results are shown in Fig. 2.3-2.5. In Fig. 2.3, three state errors versus time are shown and the state errors approach zero as time evolves. Since $x_2 \rightarrow x_1$, $y_2 \rightarrow y_1$, $z_2 \rightarrow z_1$ as $t \rightarrow \infty$, the projections of synchronized manifold shown in Fig. 2.4 represent diagonal-like. The three Lyapunov exponents versus coupling strength γ are shown in Fig. 2.5. There is a zero-crossing of a Lyapunov spectrum while $\gamma \approx 0.074$. This value of γ is a threshold value which synchronization occurs. Choose $\gamma = 0.09$, the simulated result in Fig. 2.6 shows that the state errors still converge but the transient time of convergence is long. This agrees with our intuition. Moreover, it also demonstrates that the estimate of Lipschitz constant is conservative. In chapter 4, the estimation of Lipschitz constant will be replaced by a simple and convenient adaptive estimator.

Example 2.2 Nonautonomous case: The unidirectional coupled Duffing-van der Pol systems without perturbation is

$$\begin{aligned}\dot{x}_1 &= y_1, \\ \dot{y}_1 &= \mu(1 - \gamma x_1^2)y_1 - x_1^3 + A \sin \Omega t, \\ \dot{x}_2 &= y_2 + \gamma(x_2 - x_1), \\ \dot{y}_2 &= \mu(1 - \gamma x_2^2)y_2 - x_2^3 + A \sin \Omega t + \gamma(y_2 - y_1).\end{aligned}$$

where $\Gamma = \text{diag}\{\gamma, \gamma\}$ and $\gamma = 21$. The initial value is $\mathbf{x}_0 = [-0.2, 0.2, 1, 1]^T$. The simulated results are shown in Fig. 2.7 and Fig. 2.8. In Fig. 2.7, the state errors approach zero as time evolves. Since $x_2 \rightarrow x_1$, $y_2 \rightarrow y_1$ as $t \rightarrow \infty$, the projections

of synchronized manifold shown in Fig. 2.8 represent diagonal-like.

2.4.2 Unidirectional Coupled Systems with Perturbation $\|\Delta\mathbf{f}\| < K\|\mathbf{e}\|$

Example 2.3 Autonomous case: Consider the following unidirectional coupled Rössler systems with some perturbations in the form of Eq. (2.7) as

$$\begin{aligned}\dot{x}_1 &= -y_1 - z_1, \\ \dot{y}_1 &= x_1 + ay_1, \\ \dot{z}_1 &= b + z_1(x_1 - c), \\ \dot{x}_2 &= -y_2 - z_2 + (z_2 - z_1) + \gamma(x_1 - x_2), \\ \dot{y}_2 &= x_2 + ay_2 + \sin t \cdot (x_1 - x_2) + \gamma(y_1 - y_2), \\ \dot{z}_2 &= b + z_2(x_2 - c) + \gamma(z_1 - z_2).\end{aligned}$$

The system perturbation is $|\Delta f_1| = |z_2 - z_1| \leq \|\mathbf{e}\|$ and $|\Delta f_2| = |\sin t \cdot (x_1 - x_2)| \leq \|\mathbf{e}\|$. Then $\|\Delta\mathbf{f}\| \leq \sqrt{2}\|\mathbf{e}\|$. Choose $\gamma = 25$ to satisfy $\gamma > L + K$. With the same initial condition in example 2.1, the state errors approach zero as time goes to infinite in Fig. 2.9 although there exists perturbation. The projections of synchronized manifold shown in Fig. 2.10 still represent diagonal-like.

Example 2.4 Nonautonomous case: The unidirectional coupled Duffing-van der Pol systems with some perturbations is

$$\begin{aligned}\dot{x}_1 &= y_1, \\ \dot{y}_1 &= \mu(1 - \gamma x_1^2)y_1 - x_1^3 + A \sin \Omega t, \\ \dot{x}_2 &= y_2 + \cos t \sin(y_2 - y_1) + \gamma(x_2 - x_1), \\ \dot{y}_2 &= \mu(1 - \gamma x_2^2)y_2 - x_2^3 + A \sin \Omega t + \gamma(y_2 - y_1).\end{aligned}$$

The system perturbation is $|\Delta f_1| = |\cos t \sin(y_2 - y_1)| \leq \|\mathbf{e}\|$. The initial value is also $\mathbf{x}_0 = [-0.2, 0.2, 1, 1]^T$. Choose $\gamma = 22$ to satisfy $\gamma > L + K$. The simulated results are shown in Fig. 2.11 and Fig. 2.12. In Fig. 2.11, the state errors approach zero as time evolves. Since $x_2 \rightarrow x_1$, $y_2 \rightarrow y_1$ as $t \rightarrow \infty$, the projections of synchronized manifold shown in Fig. 2.12 represent diagonal-like.

2.4.3 Unidirectional Coupled Systems with Perturbation Small on the Average

Example 2.5 Autonomous case: Consider the following unidirectional coupled Rössler systems with nonvanishing perturbation as

$$\begin{aligned}
\dot{x}_1 &= -y_1 - z_1, \\
\dot{y}_1 &= x_1 + ay_1, \\
\dot{z}_1 &= b + z_1(x_1 - c), \\
\dot{x}_2 &= -y_2 - z_2 + \text{randn}(t) + \gamma(x_1 - x_2), \\
\dot{y}_2 &= x_2 + ay_2 + 5 \cos 30t + \gamma(y_1 - y_2), \\
\dot{z}_2 &= b + z_2(x_2 - c) + \gamma(z_1 - z_2).
\end{aligned}$$

The first error dynamics is $\dot{e}_1 = e_1 + ae_2 + \text{randn}(t)$, where $\text{randn}(t)$ is the unit normal random variable. Thus, the first system perturbation is bounded on the average as $\int_0^T \sup\{|\Delta f_1|\}d\tau \leq T$. Similar, the second system perturbation is bounded on the average as $\int_0^T \sup\{|\Delta f_2|\}d\tau \leq 5T$. The initial condition and $\gamma = 24$ are the same as in the example 2.1. Three state errors versus time are shown in Fig. 2.13 and they are bounded by a constant as time evolves. The projections of synchronized manifold are shown in Fig. 2.14. They do not represent exact diagonal-like since the state errors are stable but not asymptotically stable. For $\gamma = 80$, state errors dynamics and synchronized sub-manifolds are shown in Fig. 2.15 and Fig. 2.16, respectively. As coupling strength γ increases, the error bounds decrease and the synchronized sub-manifolds look more diagonal.

Example 2.6 Nonautonomous case: The unidirectional coupled Duffing-van der Pol systems with nonvanishing perturbations is

$$\begin{aligned}
\dot{x}_1 &= y_1, \\
\dot{y}_1 &= \mu(1 - \gamma x_1^2)y_1 - x_1^3 + A \sin \Omega t, \\
\dot{x}_2 &= y_2 + \cos 20\pi t + \gamma(x_2 - x_1), \\
\dot{y}_2 &= \mu(1 - \gamma x_2^2)y_2 - x_2^3 + \sin 30\pi t + A \sin \Omega t + \gamma(y_2 - y_1).
\end{aligned}$$

The nonvanishing perturbations are bounded as $|\Delta f_1| = |\cos 20\pi t| \leq 1$ and $|\Delta f_2| = |\sin 30\pi t| \leq 1$. The initial condition and $\gamma = 21$ are the same as in the example 2.2. The simulated results are shown in Fig. 2.17 and Fig. 2.18. The state errors versus time are shown in Fig. 2.17 and they are bounded by a constant as time evolves. The projections of synchronized manifold are shown in Fig. 2.18. They look like vague diagonal lines since the state errors are stable but not asymptotically stable. Choose $\gamma = 100$, the results are shown in Fig. 2.19 and Fig. 2.20, respectively. As coupling strength γ increases, the error bounds decrease and the projections of synchronized manifold look clear.

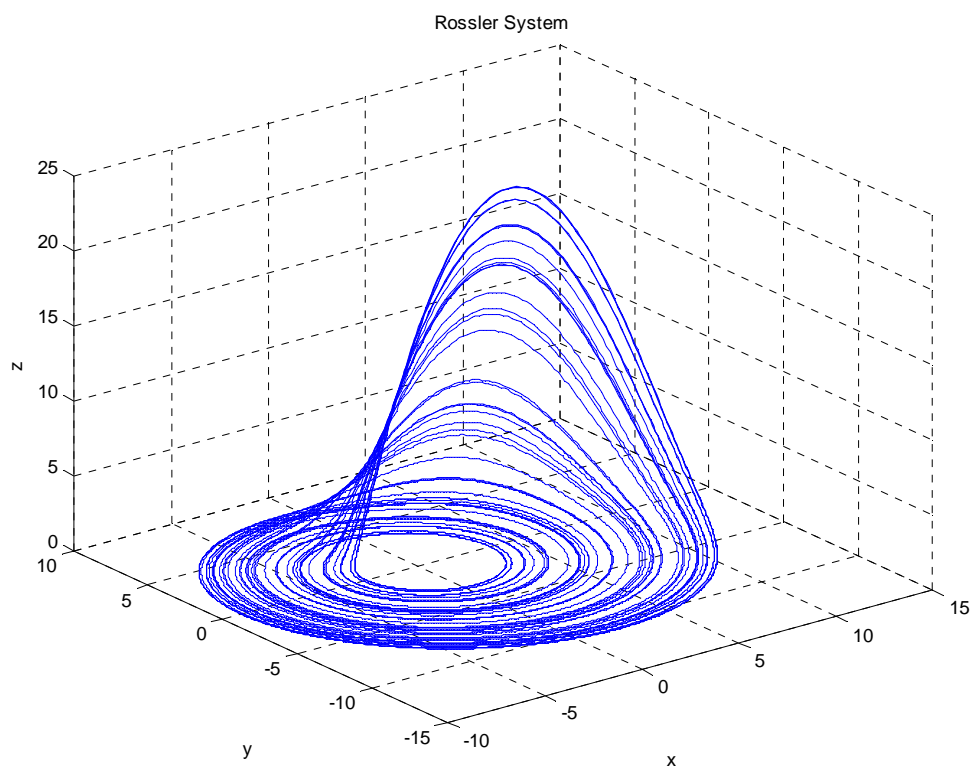


Fig. 2.1 Chaotic attractor of the Rössler system.

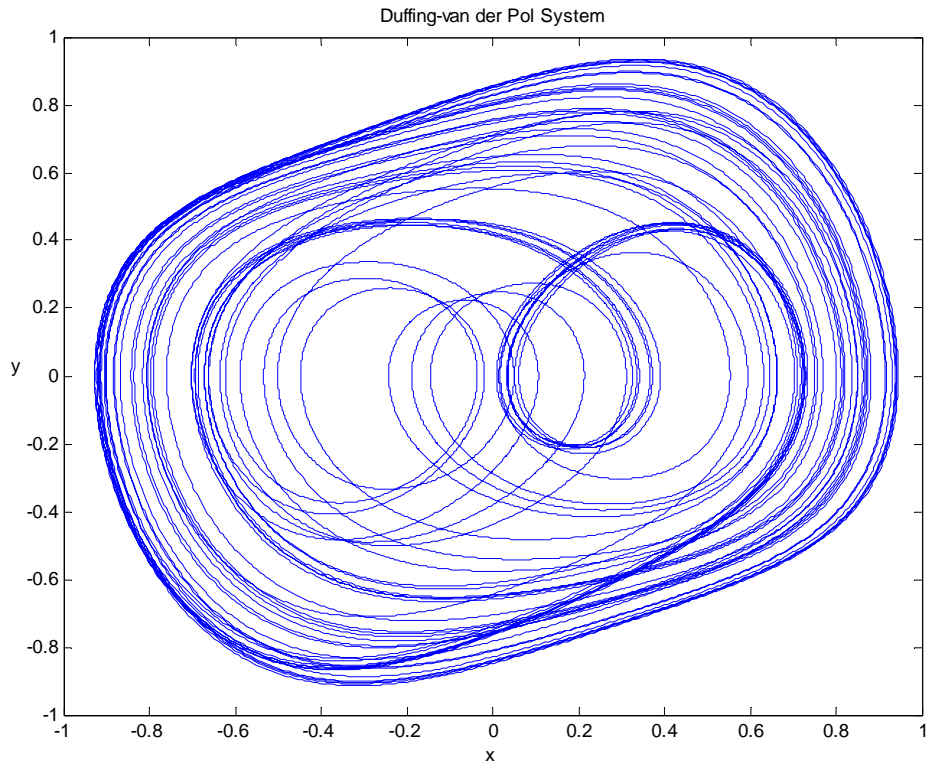


Fig. 2.2 Chaotic attractor of the Duffing-van der Pol System.

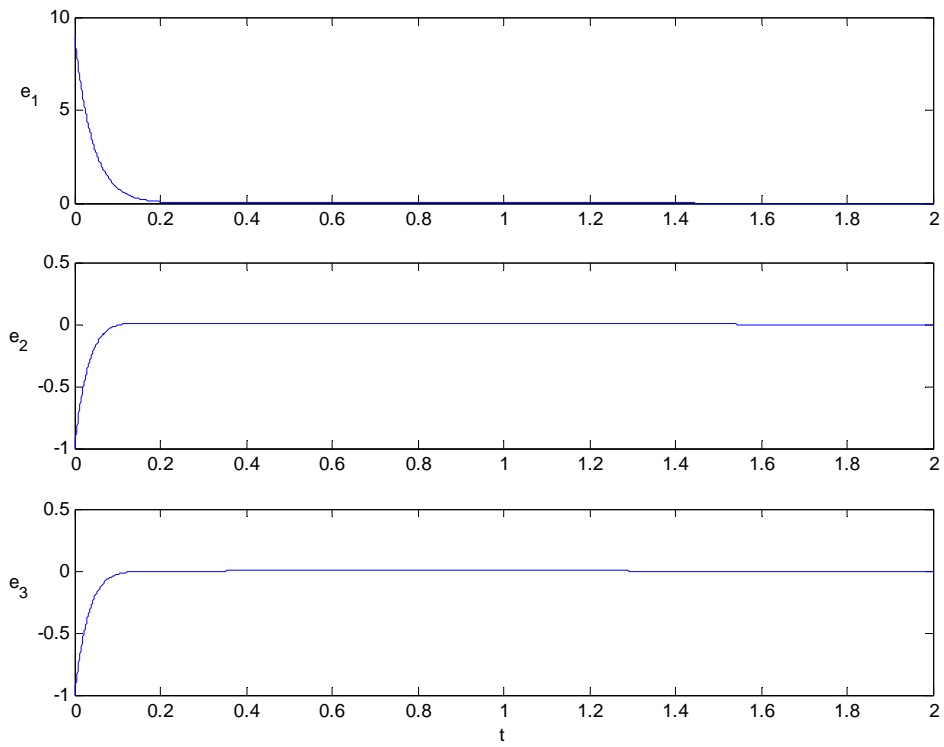


Fig. 2.3 State errors versus time of unidirectional coupled Rössler systems without perturbation.

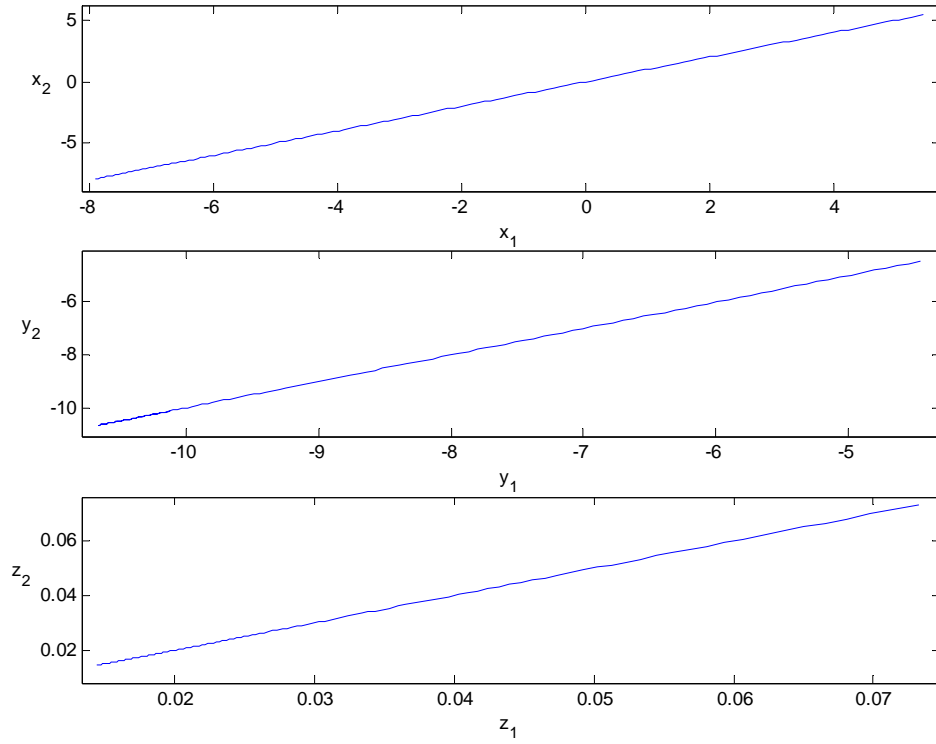


Fig. 2.4 Projections of synchronized manifold for unidirectional Rössler systems without perturbation.

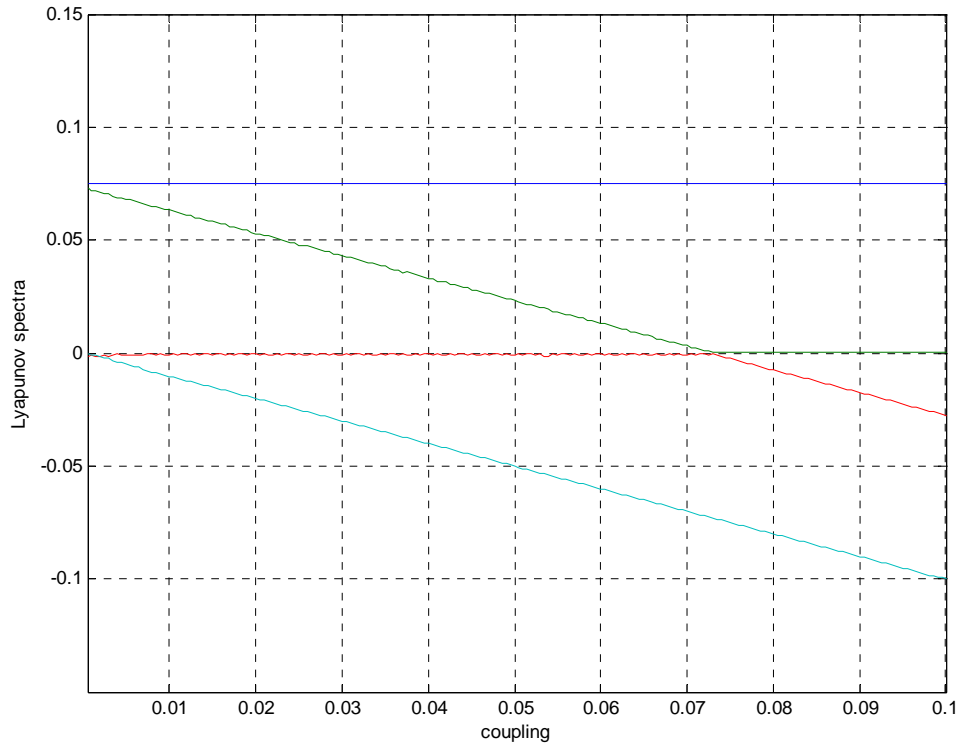


Fig. 2.5 Lyapunov spectra of unidirectional coupled Rössler systems without perturbation.

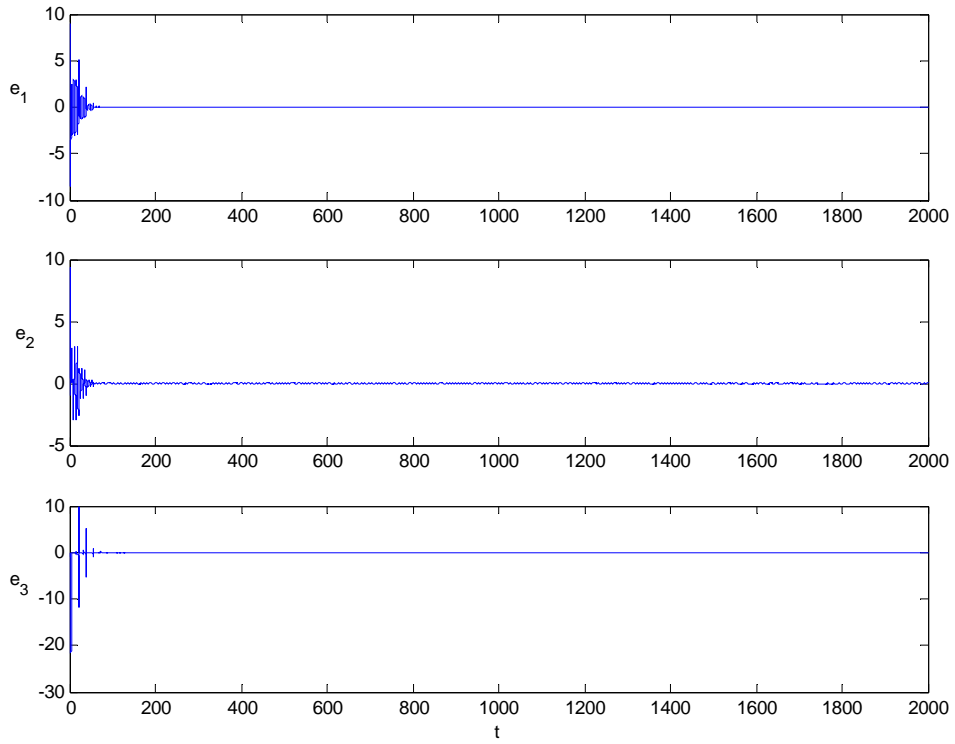


Fig. 2.6 State errors versus time of unidirectional coupled Rössler systems without perturbation while $\gamma = 0.09$.

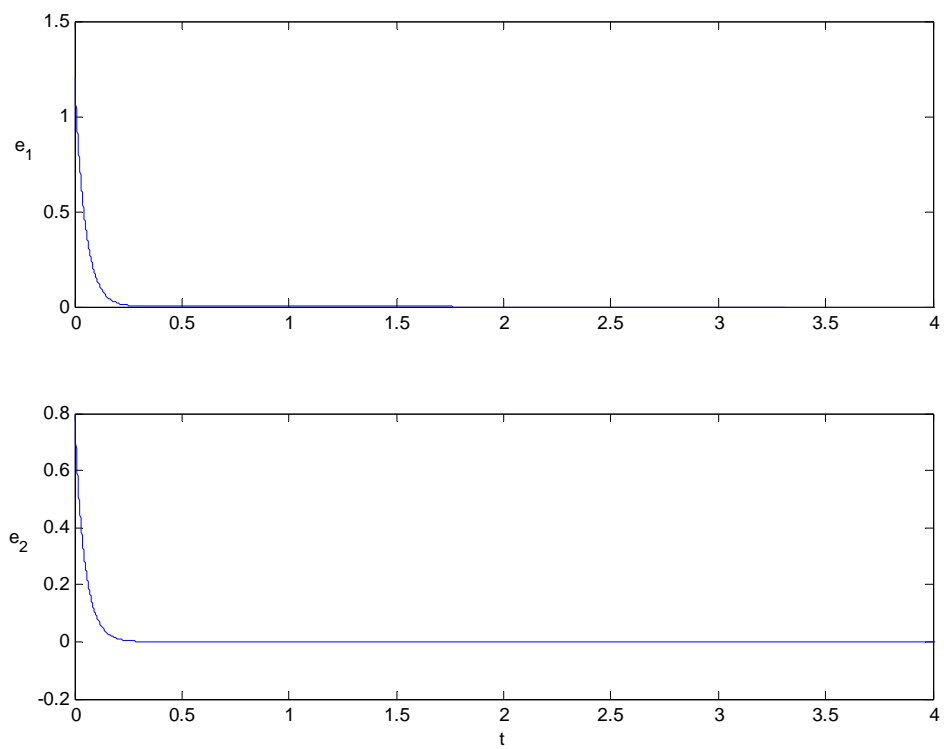


Fig. 2.7 State errors versus time of unidirectional coupled Duffing-van der Pol system without perturbation.

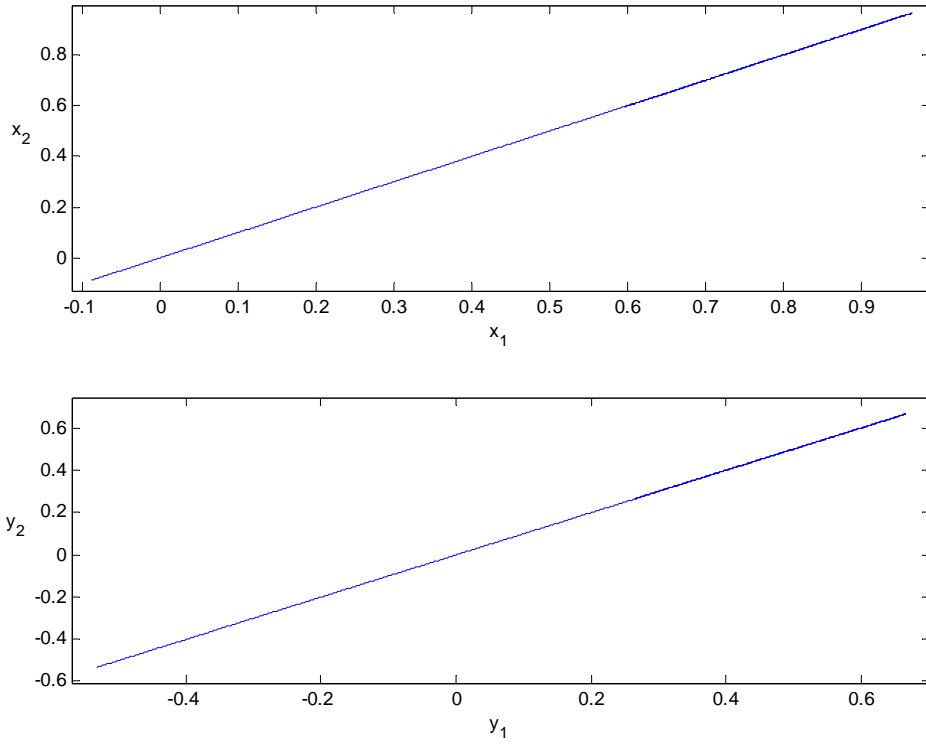


Fig. 2.8 Projections of synchronized manifold of unidirectional coupled Duffing-van der Pol system without perturbation.

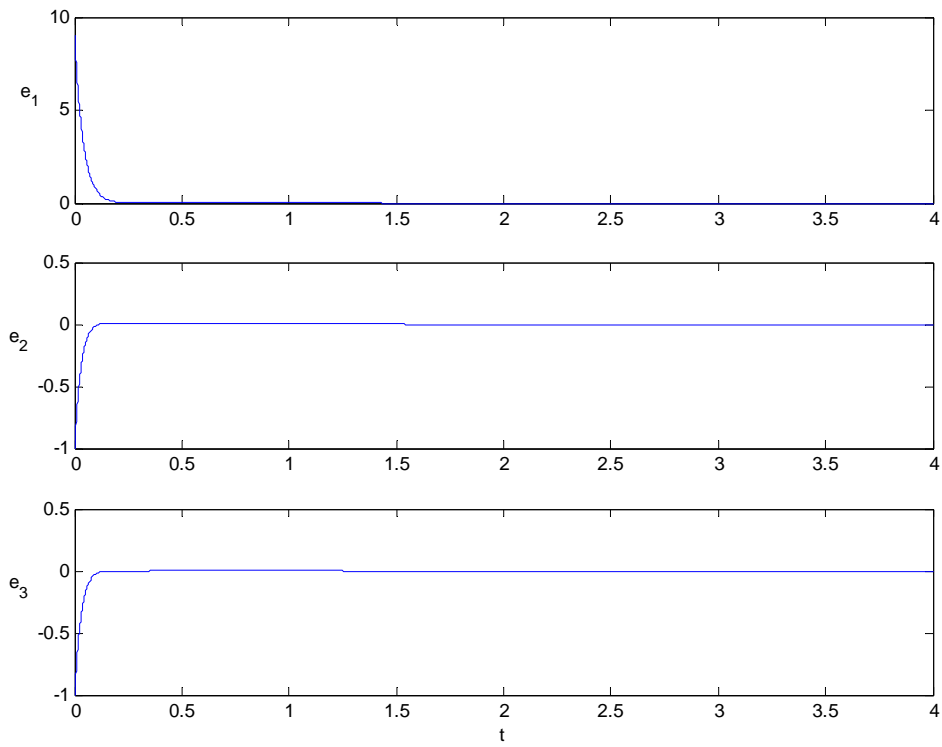


Fig. 2.9 State errors versus time of unidirectional coupled Rössler systems with perturbation $\Delta f_1 = z_2 - z_1$ and $\Delta f_2 = \sin t \cdot (x_1 - x_2)$.

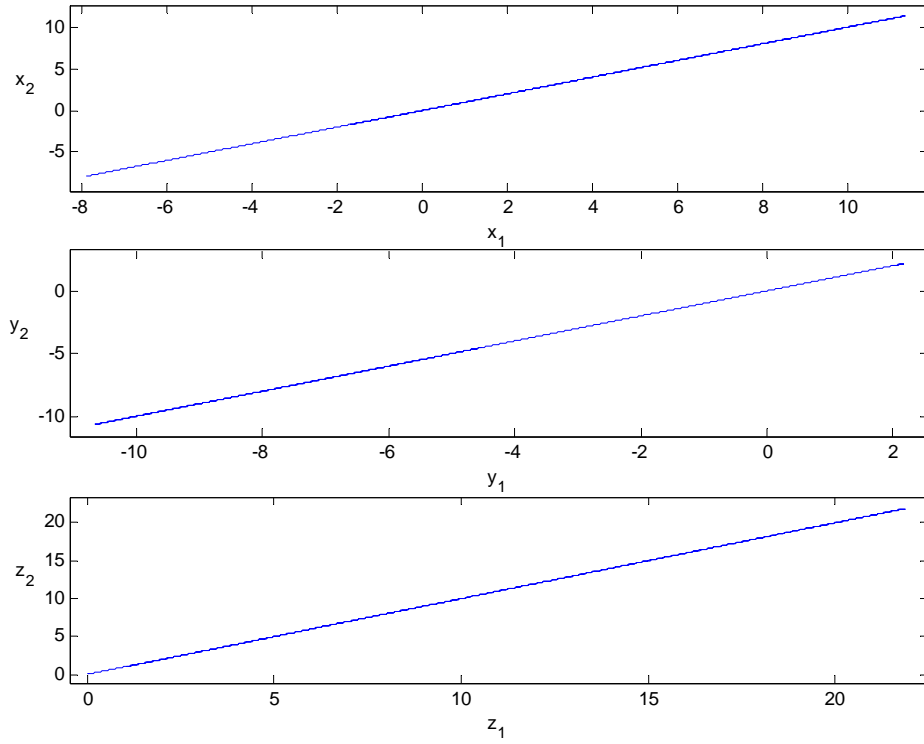


Fig. 2.10 Projections of synchronized manifold of unidirectional coupled Rössler systems with perturbation $\Delta f_1 = z_2 - z_1$ and $\Delta f_2 = \sin t \cdot (x_1 - x_2)$.

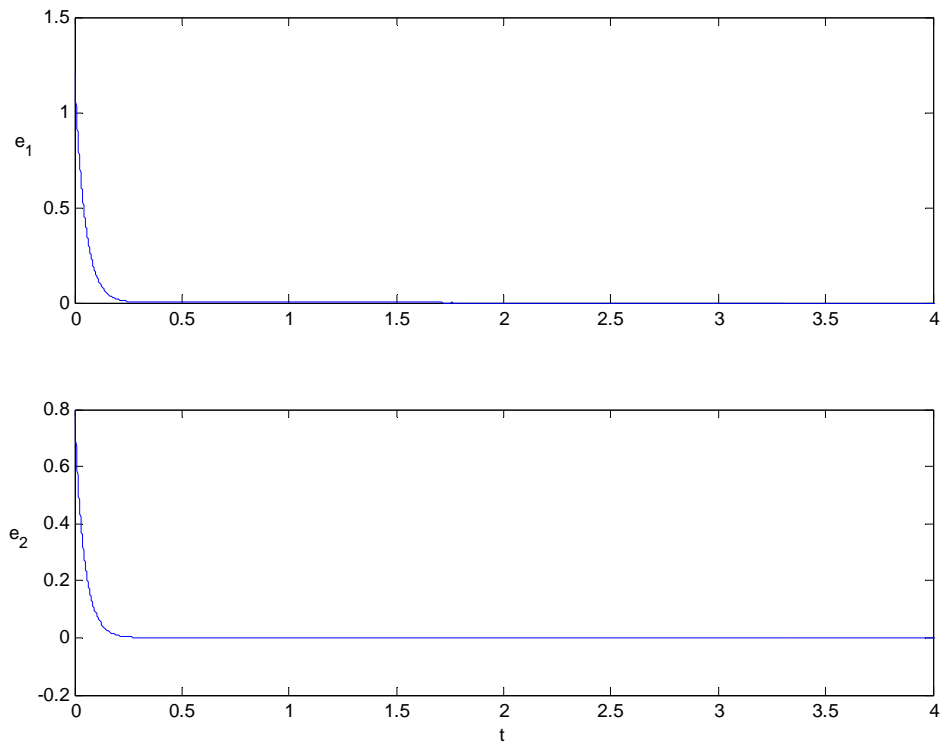


Fig. 2.11 State errors versus time of unidirectional coupled Duffing-van der Pol system with perturbation $\Delta f_1 = \cos t \sin(y_2 - y_1)$.

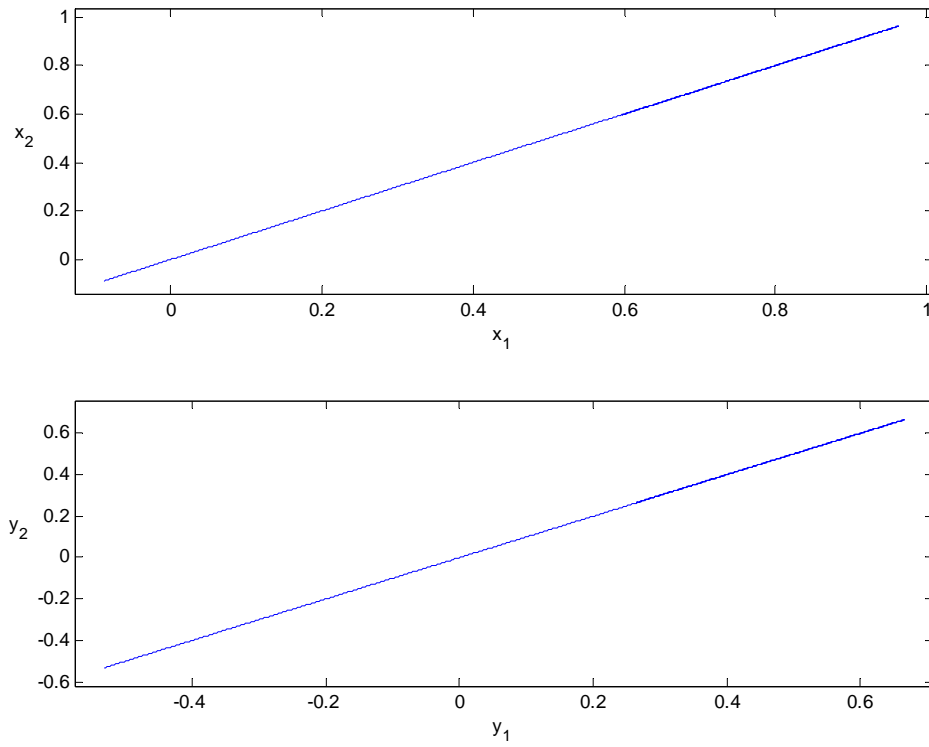


Fig. 2.12 Projections of synchronized manifold of unidirectional coupled Duffing-vander Pol system with perturbation $\Delta f_1 = \cos t \sin(y_2 - y_1)$.

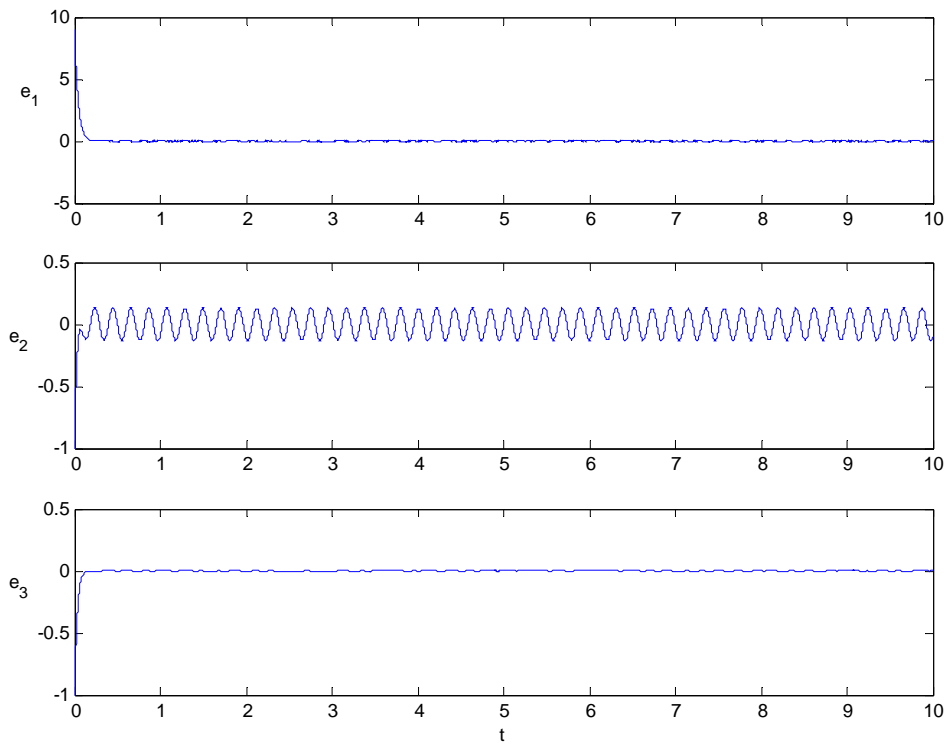


Fig. 2.13 State errors versus time of unidirectional coupled Rössler systems with perturbation $\Delta f_1 = randn(t)$ and $\Delta f_2 = 5 \cos 30t$.

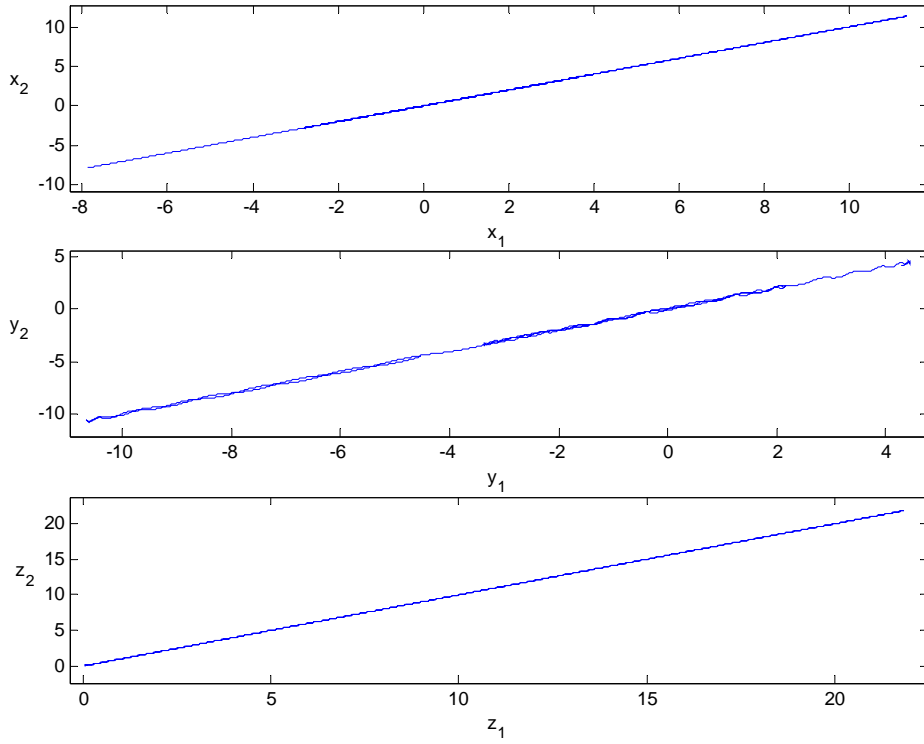


Fig. 2.14 Projections of synchronized manifold of unidirectional coupled Rössler systems with perturbation $\Delta f_1 = randn(t)$ and $\Delta f_2 = 5 \cos 30t$.

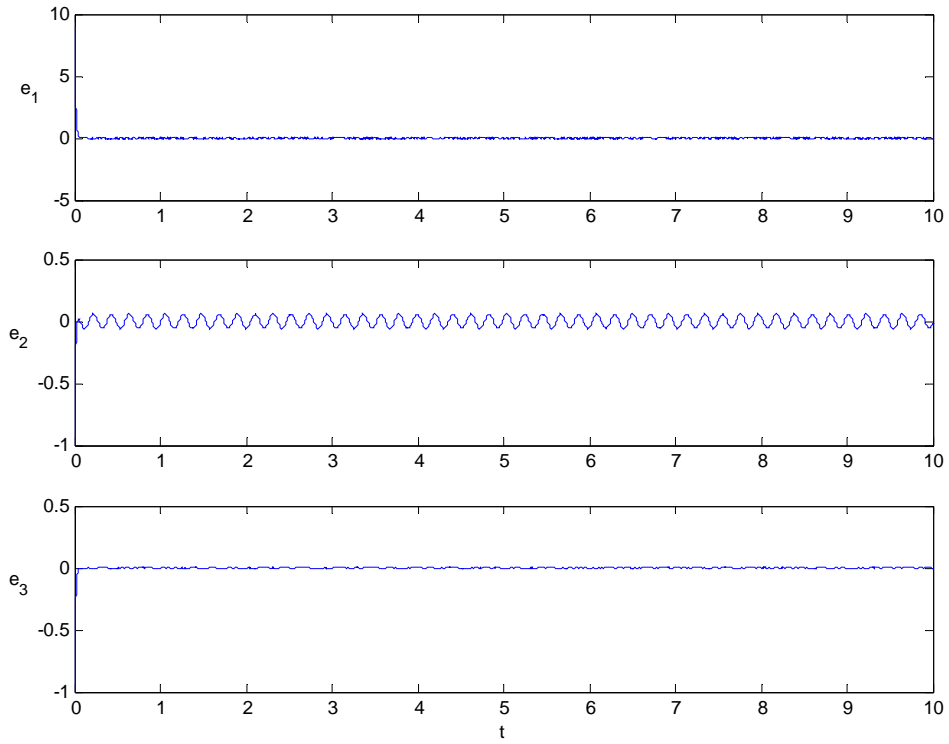


Fig. 2.15 State errors versus time of unidirectional coupled Rössler systems with $\Delta f_1 = \text{randn}(t)$, $\Delta f_2 = 5 \cos 30t$ and $\gamma = 80$.

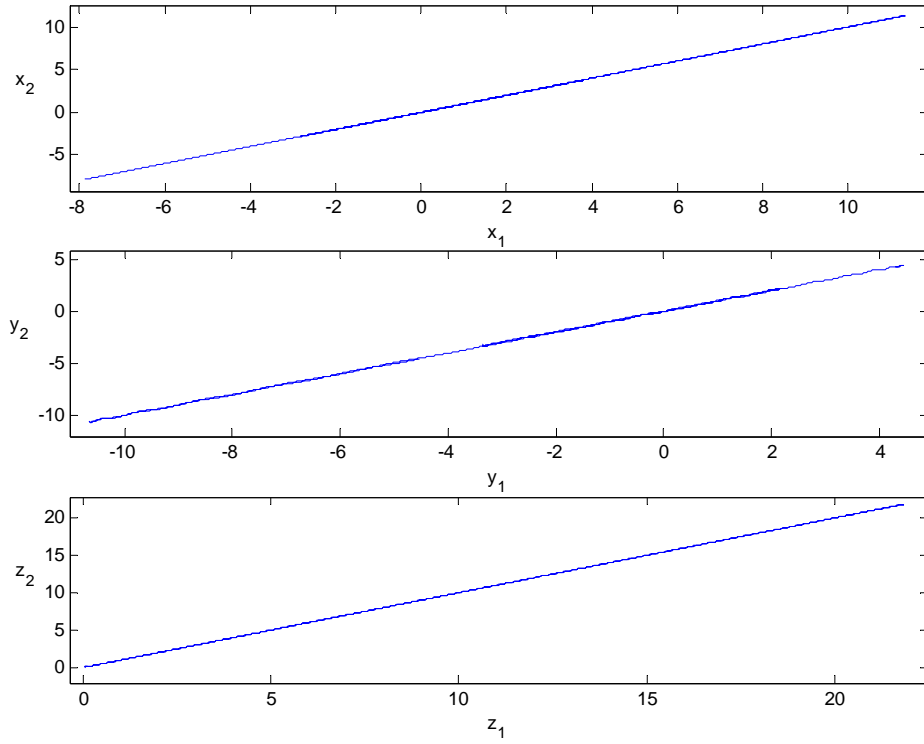


Fig. 2.16 Projections of synchronized manifold of unidirectional coupled Rössler systems with $\Delta f_1 = \text{randn}(t)$, $\Delta f_2 = 5 \cos 30t$ and $\gamma = 80$.

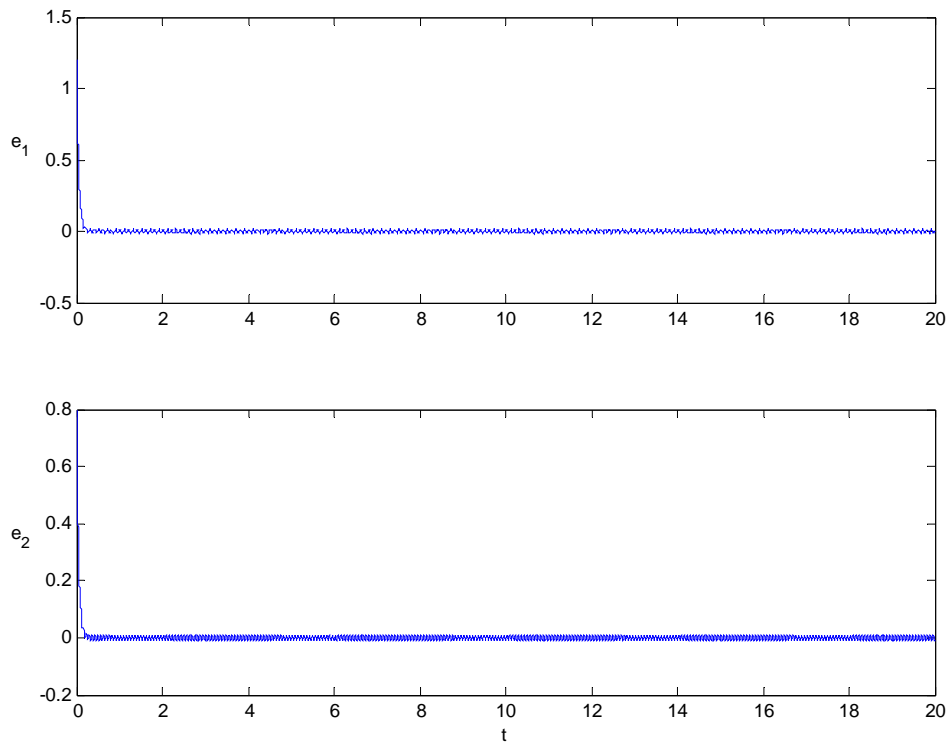


Fig. 2.17 State errors versus time of unidirectional coupled Duffing-van der Pol system with perturbations $\Delta f_1 = \cos 20\pi t$ and $\Delta f_2 = \sin 30\pi t$.

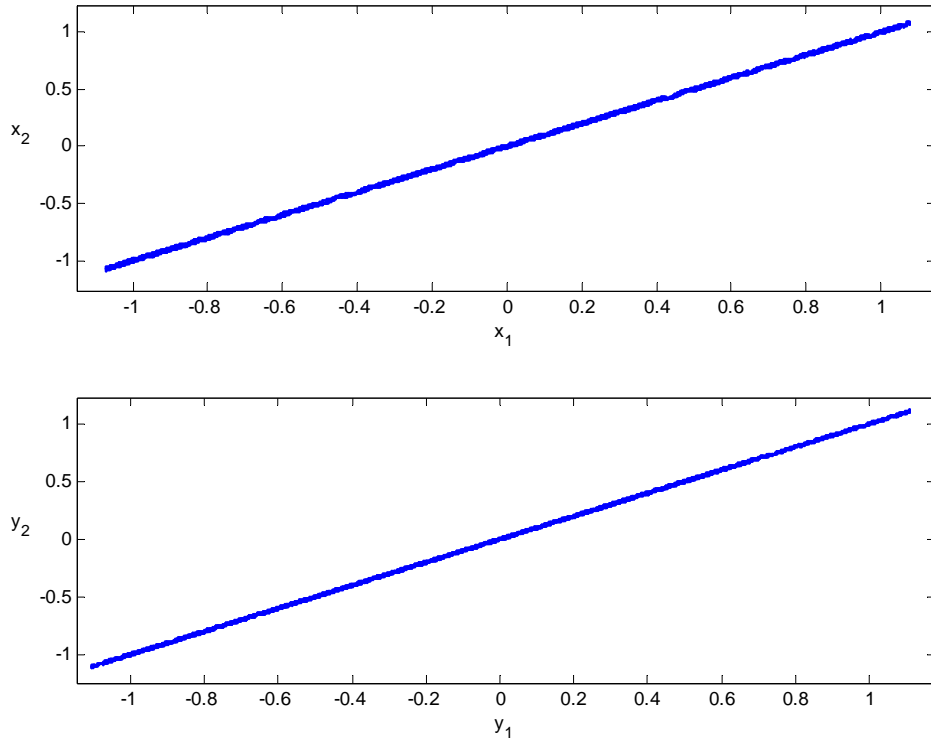


Fig. 2.18 Projections of synchronized manifold of unidirectional coupled Duffing-van der Pol system with perturbations $\Delta f_1 = \cos 20\pi t$ and $\Delta f_2 = \sin 30\pi t$.

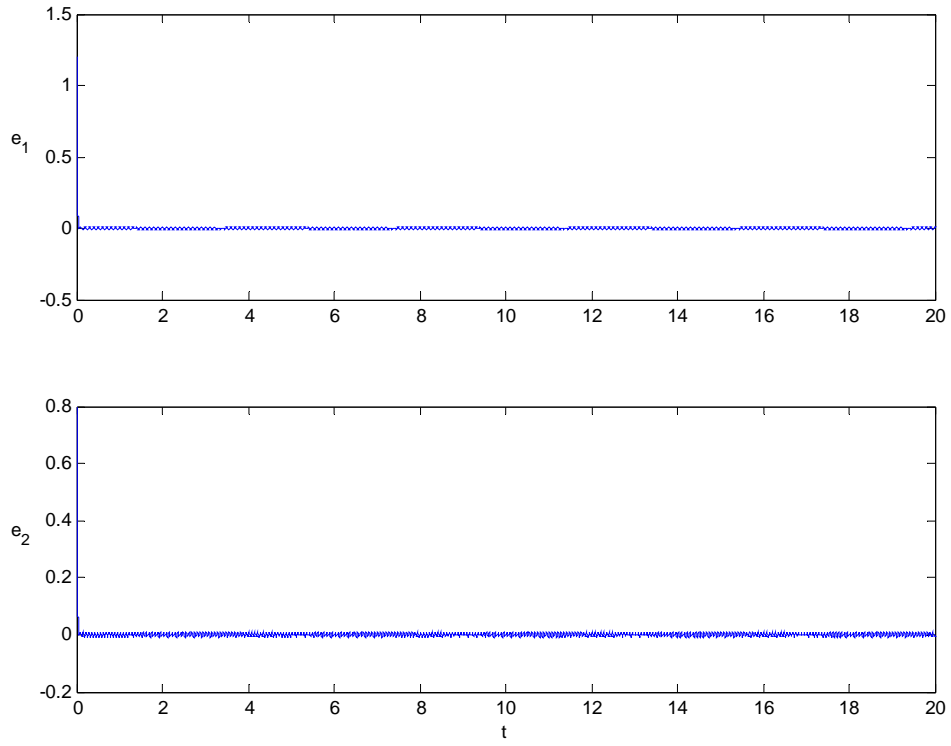


Fig. 2.19 State errors versus time of unidirectional coupled Duffing-van der Pol system with $\Delta f_1 = \cos 20\pi t$, $\Delta f_2 = \sin 30\pi t$ and $\gamma = 100$.

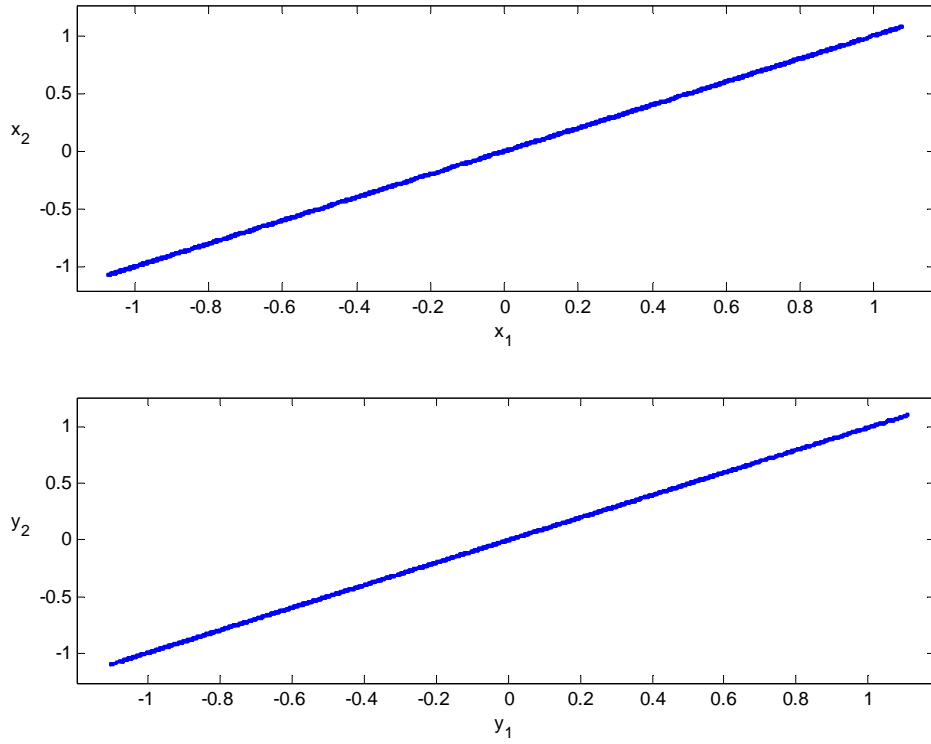


Fig. 2.20 Projections of synchronized manifold of unidirectional coupled Duffing-vander Pol system with $\Delta f_1 = \cos 20\pi t$, $\Delta f_2 = \sin 30\pi t$ and $\gamma = 100$.

Chapter 3

Synchronization of Mutual Coupled Systems

3.1 Mutual Coupled Systems without Perturbation

The proposed scheme to achieve synchronization in the chapter 2, it is suitable for both unidirectional and mutual coupled systems. The unidirectional case is discussed in chapter 2. Three sufficient theorems, one for systems without perturbation and two for systems with perturbations, are derived. In this chapter, the effort will be concentrated on synchronization of mutual coupled nonautonomous systems. Similar to the results in the chapter 2, three theorems will be proven to ensure synchronization for a general kind of mutual coupled nonautonomous systems by linear feedback coupling term. One of them is suitable for the case without system perturbation and the other two are suitable for systems under two kinds of perturbations, vanishing and nonvanishing, respectively. Finally, six numerical examples are simulated to illustrate the theoretical analysis.

Consider a mutual coupled nonautonomous system as

$$\begin{aligned}\dot{\mathbf{x}}_1 &= \mathbf{f}(t, \mathbf{x}_1) + \Gamma(\mathbf{x}_2 - \mathbf{x}_1), \\ \dot{\mathbf{x}}_2 &= \mathbf{f}(t, \mathbf{x}_2) + \Gamma(\mathbf{x}_1 - \mathbf{x}_2),\end{aligned}\tag{3.1}$$

where $\mathbf{x}_1, \mathbf{x}_2 \in \mathbb{R}^n$ are the states variables and $\mathbf{f} : \Omega \subset \mathbb{R} \times \mathbb{R}^{2n} \rightarrow \mathbb{R}^n$ satisfy the Lipschitz condition $\|\mathbf{f}(t, \mathbf{x}_1) - \mathbf{f}(t, \mathbf{x}_2)\| \leq L\|\mathbf{x}_1 - \mathbf{x}_2\|$ in \mathbf{x} for all (t, \mathbf{x}_1) and (t, \mathbf{x}_2) in Ω with Lipschitz constants L . $\Gamma \in M_{n \times n}$ is a constant matrix whose entries represent the coupling strength of the linear feedback term $(\mathbf{x}_1 - \mathbf{x}_2)$ and $(\mathbf{x}_2 - \mathbf{x}_1)$. The index of entry γ_{ij} means that the j -th component of $(\mathbf{x}_1 - \mathbf{x}_2)$ or $(\mathbf{x}_2 - \mathbf{x}_1)$ exert on the i -th component of $\dot{\mathbf{x}}_2$ or $\dot{\mathbf{x}}_1$, respectively. Follow the procedure stated in section 2.1. Define $\mathbf{e} = \mathbf{x}_2 - \mathbf{x}_1$, an extended equation can be obtained as

$$\begin{aligned}\dot{\mathbf{x}}_1 &= \mathbf{f}(t, \mathbf{x}_1) + \Gamma\mathbf{e}, \\ \dot{\mathbf{e}} &= \mathbf{f}(t, \mathbf{x}_1 + \mathbf{e}) - \mathbf{f}(t, \mathbf{x}_1) - 2\Gamma\mathbf{e}.\end{aligned}\tag{3.2}$$

Theorem 3.1 *The partial state \mathbf{e} in Eq. (3.2) asymptotically approaches to $\mathbf{0}$ uniformly if $L\mathbf{I}_n - 2\Gamma$ is negative definite, i.e. the system in the form of Eq. (3.1) is*

synchronized if $L\mathbf{I}_n - 2\Gamma$ is negative definite.

Proof Choose a function $V(\mathbf{x}_1, \mathbf{e}) = \frac{1}{2} \mathbf{e}^T \mathbf{e}$ which is positive definite function with respect to \mathbf{e} and with infinitesimal upper bound. Then its time derivative along the solution of Eq. (3.2) is

$$\begin{aligned} \dot{V} &= \mathbf{e}^T \dot{\mathbf{e}} \\ &= \mathbf{e}^T [\mathbf{f}(t, \mathbf{x}_1 + \mathbf{e}) - \mathbf{f}(t, \mathbf{x}_1)] - 2\mathbf{e}^T \Gamma \mathbf{e} \\ &\leq L \|\mathbf{e}\|^2 - \mathbf{e}^T \Gamma \mathbf{e} \\ &= \mathbf{e}^T (L\mathbf{I}_n - 2\Gamma) \mathbf{e}. \end{aligned}$$

The state error \mathbf{e} asymptotically approaches $\mathbf{0}$ uniformly if $L\mathbf{I}_n - 2\Gamma$ is negative definite by Theorem A2 in appendix.

Remark 3.1 $L\mathbf{I}_n - 2\Gamma$ is negative definite if and only if all its eigenvalues are negative. For the case $\Gamma = \text{diag}(\gamma_1, \gamma_2, \dots, \gamma_n)$ with $\gamma_i > 0$, $i = 1, \dots, n$, synchronization occurs if $\gamma_{\min} > \frac{L}{2}$, $\gamma_{\min} \leq \gamma_i, i = 1, \dots, n$. This is because the time derivative of $V(\mathbf{x}_1, \mathbf{e})$ can be written as $\dot{V}(\mathbf{x}_1, \mathbf{e}) \leq (L - 2\gamma_{\min}) \|\mathbf{e}\|^2$. Moreover, the result is global by Theorem A4 if \mathbf{f} is globally Lipschitzian.

3.2 Mutual Coupled Systems with Two Kinds of Perturbations

The criterion given in section 3.1 is suitable for the case without system perturbation. If the system possesses perturbation, similar result can be obtained. Consider mutual coupled nonautonomous systems with perturbation in the form of

$$\begin{aligned} \dot{\mathbf{x}}_1 &= \mathbf{f}(t, \mathbf{x}_1) + \Delta \mathbf{f}_1(t, \mathbf{x}_1, \mathbf{x}_2) + \Gamma(\mathbf{x}_2 - \mathbf{x}_1), \\ \dot{\mathbf{x}}_2 &= \mathbf{f}(t, \mathbf{x}_2) + \Delta \mathbf{f}_2(t, \mathbf{x}_1, \mathbf{x}_2) + \Gamma(\mathbf{x}_1 - \mathbf{x}_2), \end{aligned} \quad (3.3)$$

where \mathbf{f} satisfies Lipschitz condition with $\|\mathbf{f}(t, \mathbf{x}_1) - \mathbf{f}(t, \mathbf{x}_2)\| \leq L \|\mathbf{x}_1 - \mathbf{x}_2\|$ in \mathbf{x} for all (t, \mathbf{x}_1) and (t, \mathbf{x}_2) in domain Ω with Lipschitz constant L and $\Gamma \in M_{n \times n}$ is a constant matrix whose entries represent the coupling strength of the linear feedback term $(\mathbf{x}_1 - \mathbf{x}_2)$. The terms $\Delta \mathbf{f}_1(t, \mathbf{x}_1, \mathbf{x}_2)$ and $\Delta \mathbf{f}_2(t, \mathbf{x}_1, \mathbf{x}_2)$ are vanishing perturbations which means that $\Delta \mathbf{f}_1(t, \mathbf{x}_1, \mathbf{x}_2) = \mathbf{0}$ and $\Delta \mathbf{f}_2(t, \mathbf{x}_1, \mathbf{x}_2) = \mathbf{0}$ with $\mathbf{x}_1(t) = \mathbf{x}_2(t), \forall t$. $\Delta \mathbf{f}_1(t, \mathbf{x}_1, \mathbf{x}_2)$ and $\Delta \mathbf{f}_2(t, \mathbf{x}_1, \mathbf{x}_2)$ can be rephrased to be

$\Delta \mathbf{f}_1(t, \mathbf{x}_1, \mathbf{e})$ and $\Delta \mathbf{f}_2(t, \mathbf{x}_1, \mathbf{e})$, where $\mathbf{e} = \mathbf{x}_2 - \mathbf{x}_1$. Then, an extended equation can be obtained as

$$\begin{aligned}\dot{\mathbf{x}}_1 &= \mathbf{f}(t, \mathbf{x}_1) + \Delta \mathbf{f}_1 + \Gamma \mathbf{e}, \\ \dot{\mathbf{e}} &= \mathbf{f}(t, \mathbf{e} + \mathbf{x}_1) - \mathbf{f}(t, \mathbf{x}_1) + \Delta \mathbf{f}_2 - \Delta \mathbf{f}_1 + 2\Gamma \mathbf{e}.\end{aligned}\quad (3.4)$$

Theorem 3.2 Assume that $\exists K_i > 0 \Rightarrow \|\Delta \mathbf{f}_i\| < K_i \|\mathbf{e}\|, i=1, 2$. Then the Eq. (3.4) is uniformly asymptotically \mathbf{e} -stable if $(L + K_1 + K_2)\mathbf{I}_n - 2\Gamma$ is negative definite, i.e. the system in the form of Eq. (3.3) is synchronized if $(L + K_1 + K_2)\mathbf{I}_n - 2\Gamma$ is negative definite.

Proof Choose a function $V(\mathbf{x}_1, \mathbf{e}) = \frac{1}{2} \mathbf{e}^T \mathbf{e}$ which is positive definite function with respect to \mathbf{e} and with infinitesimal upper bound. Then its time derivative along the solution of Eq. (3.4) is

$$\begin{aligned}\dot{V} &= \mathbf{e}^T \dot{\mathbf{e}} \\ &= \mathbf{e}^T [\mathbf{f}(t, \mathbf{e} + \mathbf{x}_1) - \mathbf{f}(t, \mathbf{x}_1) + \Delta \mathbf{f}_2 - \Delta \mathbf{f}_1] - 2\mathbf{e}^T \Gamma \mathbf{e} \\ &\leq (L + K_1 + K_2) \mathbf{e}^T \mathbf{e} - 2\mathbf{e}^T \Gamma \mathbf{e} \\ &= \mathbf{e}^T [(L + K_1 + K_2)\mathbf{I}_n - 2\Gamma] \mathbf{e}.\end{aligned}$$

Hence, the Eq. (3.4) is uniformly asymptotically \mathbf{e} -stable if $(L + K_1 + K_2)\mathbf{I}_n - 2\Gamma$ is negative definite.

Remark 3.2 $(L + K_1 + K_2)\mathbf{I}_n - 2\Gamma$ is negative definite if and only if all its eigenvalues are negative. When $\Gamma = \text{diag}(\gamma_1, \gamma_2, \dots, \gamma_n)$ with $\gamma_i > 0$ for $i=1, \dots, n$, synchronization occurs if $\gamma_{\min} > \frac{L + K_1 + K_2}{2}$, where γ_{\min} is the minimum one in γ_i .

Furthermore, the result is global by Theorem A4 if \mathbf{f} is globally Lipschitzian.

If $\Delta \mathbf{f}_1(t, \mathbf{x}_1, \mathbf{x}_2)$ and $\Delta \mathbf{f}_2(t, \mathbf{x}_1, \mathbf{x}_2)$ are not vanishing perturbations, it is difficult to design a controller to guarantee the occurrence of asymptotically partial stability like Theorem 3.2. The stable under constantly acting perturbation small on the average will take it over.

Theorem 3.3 Assume that the functions \mathbf{f} and $D\mathbf{f}(\mathbf{x})$ are continuous and bounded in Q . The the Eq. (3.4) is uniformly \mathbf{e} -stable under constantly acting perturbation small on the average if $L\mathbf{I}_n - 2\Gamma$ is negative definite.

Proof From theorem 3.1, the partial state \mathbf{e} is uniformly asymptotically to $\mathbf{0}$ in Eq. (3.1) if $L\mathbf{I}_n - 2\Gamma$ is negative definite. By corollary A1, the Eq. (3.4) is uniformly e-stable under constantly acting perturbation small on the average if $L\mathbf{I}_n - 2\Gamma$ is negative definite with the assumption that \mathbf{f} and $D\mathbf{f}(\mathbf{x})$ are continuous and bounded in Q . This completes the proof.

Remark 3.3 Theorem 3.3 means that the coupled structure perturbed systems (3.3) are practical synchronized [82]. If $\Gamma = \text{diag}(\gamma_1, \gamma_2, \dots, \gamma_n)$ with $\gamma_i > 0$ for $i = 1, \dots, n$, practical synchronization occurs if $\gamma_{\min} > L$, where $\gamma_{\min} \leq \gamma_i$, $i = 1, \dots, n$. Moreover, the larger γ_{\min} is, the smaller bounds of the state errors are. This criterion is global if \mathbf{f} is globally Lipschitzian.

3.3 Numerical Illustrated Examples

In this section, the Lorenz system and the Ueda system are adopted to demonstrate the results given in section 3.1 and 3.2. They are simulated for the cases with and without system perturbation, respectively. The system equation of the Lorenz system is

$$\begin{aligned}\dot{x} &= -\sigma(x - y) \triangleq f_1(\mathbf{x}), \\ \dot{y} &= rx - y - xz \triangleq f_2(\mathbf{x}), \\ \dot{z} &= xy - bz \triangleq f_3(\mathbf{x}),\end{aligned}$$

where $\sigma = 10$, $r = 28$ and $b = 8/3$ ensure that there exists chaotic behavior. The chaotic attractor is shown in Fig. 3.1. To apply the theorem given in this chapter, estimation of the Lipschitz constant is needed. By Cauchy-Schwarz inequality, it can be derived for any $\mathbf{x}_2 = [x_2 \ y_2 \ z_2]^T$, $\mathbf{x}_1 = [x_1 \ y_1 \ z_1]^T$, we have

$$\begin{aligned}|f_1(\mathbf{x}_2) - f_1(\mathbf{x}_1)| &= |-\sigma e_1 + \sigma e_2| \leq \left\| \begin{bmatrix} -\sigma & \sigma & 0 \end{bmatrix} \right\| \|\mathbf{x}_2 - \mathbf{x}_1\|, \\ |f_2(\mathbf{x}_2) - f_2(\mathbf{x}_1)| &= |re_1 - e_2 - x_2z_2 + x_1z_1| \\ &= |re_1 - e_2 - x_2z_2 + x_2z_1 - x_2z_1 + x_1z_1| \|\mathbf{x}_2 - \mathbf{x}_1\| \\ &= |re_1 - e_2 - x_2e_3 - z_1e_1| \|\mathbf{x}_2 - \mathbf{x}_1\| \\ &\leq \left\| \begin{bmatrix} r + B_3 & -1 & B_1 \end{bmatrix} \right\| \|\mathbf{x}_2 - \mathbf{x}_1\|,\end{aligned}$$

$$\begin{aligned}
|f_3(\mathbf{x}_2) - f_3(\mathbf{x}_1)| &= |x_2 y_2 - x_1 y_1 - b e_3| \\
&= |x_2 y_2 - x_1 y_2 + x_1 y_2 - x_1 y_1 - b e_3| \\
&= |y_2 e_1 + x_1 e_2 - b e_3| \\
&\leq \|[B_2 \ B_1 \ -b]\| \|\mathbf{x}_2 - \mathbf{x}_1\|,
\end{aligned}$$

where $|x_i(t)| \leq B_1$, $|y_i(t)| \leq B_2$, $|z_i(t)| \leq B_3$, $\forall t > t_0$, $i = 1, 2$. Hence, a Lipschitz constant can be obtained as

$$L = \sqrt{\|[-\sigma \ \sigma \ 0]\|^2 + \|[r + B_3 \ -1 \ B_1]\|^2 + \|[B_2 \ B_1 \ -b]\|^2}.$$

From numerical simulation, $B_1 = 20$, $B_2 = 28$, $B_3 = 49$, then $L = 87.87$.

The governing equation of the Ueda system is

$$\begin{aligned}
\dot{x} &= y \triangleq f_1(\mathbf{x}), \\
\dot{y} &= -x^3 - by + A \sin \Omega t \triangleq f_2(\mathbf{x}).
\end{aligned}$$

The chaotic behavior exists while $b = 0.05$, $A = 5$ and $\Omega = 1$. The chaotic attractor is shown in Fig. 3.2. Apply the Cauchy-Schwarz inequality to estimate the Lipschitz constant. For any $\mathbf{x}_2 = [x_2 \ y_2]^T$, $\mathbf{x}_1 = [x_1 \ y_1]^T$, it can be derived

$$\begin{aligned}
|f_1(\mathbf{x}_2) - f_1(\mathbf{x}_1)| &\leq \|\mathbf{x}_2 - \mathbf{x}_1\|, \\
|f_2(\mathbf{x}_2) - f_2(\mathbf{x}_1)| &= |-x_2^3 + x_1^3 - b e_2| \\
&\leq \|[3B_1^2 \ -b]\| \|\mathbf{x}_2 - \mathbf{x}_1\|,
\end{aligned}$$

where $|x_i(t)| \leq B_1$, $|y_i(t)| \leq B_2$, $\forall t > t_0$, $i = 1, 2$. Hence, one Lipschitz constant can be obtained as

$$L = \sqrt{1 + \|[3B_1^2 \ -b]\|^2}.$$

From numerical simulation, $B_1 = 3.5$, $B_2 = 7$, then $L = 36.77$.

3.3.1 Mutual Coupled Systems without Perturbation

Example 3.1 Autonomous case: Consider the following mutual coupled simplest quadratic chaotic system without system perturbation as in the form of Eq. (3.1)

$$\begin{aligned}
\dot{x}_1 &= -\sigma(x_1 - y_1) + \gamma(x_2 - x_1), \\
\dot{y}_1 &= rx_1 - y_1 - x_1 z_1 + \gamma(y_2 - y_1), \\
\dot{z}_1 &= x_1 y_1 - bz_1 + \gamma(z_2 - z_1),
\end{aligned}$$

$$\begin{aligned}\dot{x}_2 &= -\sigma(x_2 - y_2) + \gamma(x_1 - x_2), \\ \dot{y}_2 &= rx_2 - y_2 - x_2z_2 + \gamma(y_1 - y_2), \\ \dot{z}_2 &= x_2y_2 - bz_2 + \gamma(z_1 - z_2),\end{aligned}$$

where $\Gamma = \text{diag}\{\gamma, \gamma, \gamma\}$ and $\gamma = 44 > L/2$. The initial value is $\mathbf{x}_0 = [1, -0.01, 3, 0, 0, 5]^T$. The simulated results are shown in Fig. 3.3-3.6. In Fig. 3.3, three state errors versus time are shown and the state errors approach zero as time evolves. Since $x_2 \rightarrow x_1$, $y_2 \rightarrow y_1$, $z_2 \rightarrow z_1$ as $t \rightarrow \infty$, the projections of synchronized manifold shown in Fig. 3.4 represent diagonal-like. The three Lyapunov exponents versus coupling strength γ are shown in Fig. 3.5. There is a zero-crossing of a Lyapunov spectrum while $\gamma \approx 0.41$. This value of γ is a threshold value which synchronization occurs. Fujisaka and Yamada [1] proved that synchronization of linear coupled autonomous systems occurs if the coupling strength larger than half of the largest Lyapunov exponent. The largest Lyapunov exponent is 0.82 and its half is 0.41. This coincides with the values of zero-crossing of a Lyapunov spectrum. Choose $\gamma = 0.6$, the simulated result in Fig. 3.6 shows that the state errors still converge but the transient time of convergence is long. This agrees with our intuition.

Example 3.2 Nonautonomous case: The mutual coupled Ueda systems without perturbation is

$$\begin{aligned}\dot{x}_1 &= y_1 + \gamma(x_2 - x_1), \\ \dot{y}_1 &= -x_1^3 - by_1 + A \sin \Omega t + \gamma(y_2 - y_1), \\ \dot{x}_2 &= y_2 + \gamma(x_1 - x_2), \\ \dot{y}_2 &= -x_2^3 - by_2 + A \sin \Omega t + \gamma(y_1 - y_2),\end{aligned}$$

where $\Gamma = \text{diag}\{\gamma, \gamma\}$ and $\gamma = 18.5$. The initial value is $\mathbf{x}_0 = [2.5, 0, 1, 1]^T$. The simulated results are shown in Fig. 3.7 and Fig. 2.8. In Fig. 3.7, the state errors approach zero as time evolves. Since $x_2 \rightarrow x_1$, $y_2 \rightarrow y_1$ as $t \rightarrow \infty$, the projections of synchronized manifold shown in Fig. 3.8 represent diagonal-like.

3.3.2 Mutual Coupled Systems with Perturbation $\|\Delta \mathbf{f}\| < K \|\mathbf{e}\|$

Example 3.3 Autonomous case: Consider the following mutual coupled Lorenz systems with system perturbation as

$$\begin{aligned}
\dot{x}_1 &= -\sigma(x_1 - y_1) + \cos t \cdot (y_1 - y_2) + \gamma(x_2 - x_1), \\
\dot{y}_1 &= rx_1 - y_1 - x_1 z_1 + \gamma(y_2 - y_1), \\
\dot{z}_1 &= x_1 y_1 - bz_1 + \gamma(z_2 - z_1), \\
\dot{x}_2 &= -\sigma(x_2 - y_2) + \gamma(x_1 - x_2), \\
\dot{y}_2 &= rx_2 - y_2 - x_2 z_2 + \gamma(y_1 - y_2), \\
\dot{z}_2 &= x_2 y_2 - bz_2 + (x_1 - x_2) + \gamma(z_1 - z_2).
\end{aligned}$$

The system perturbations are bounded as $|\Delta f_1| = |\cos t \cdot (y_1 - y_2)| \leq \|\mathbf{e}\|$ and $|\Delta f_6| = |x_1 - x_2| \leq \|\mathbf{e}\|$. Choose $\gamma = 45$ to satisfy $\gamma > (L + K_1 + K_2)/2$ and the initial condition is the same as in example 3.1. In Fig. 3.9, the state errors approach zero as time goes to infinite although there is persistent acting perturbation. The projections of synchronized manifold shown in Fig. 3.10 represent diagonal-like.

Example 3.4 Nonautonomous case: The mutual coupled Ueda systems with some perturbations is

$$\begin{aligned}
\dot{x}_1 &= y_1 + \gamma(x_2 - x_1), \\
\dot{y}_1 &= -x_1^3 - by_1 + A \sin \Omega t + \cos t \sin(x_2 - x_1) + \gamma(y_2 - y_1), \\
\dot{x}_2 &= y_2 + (y_2 - y_1) + \gamma(x_1 - x_2), \\
\dot{y}_2 &= -x_2^3 - by_2 + A \sin \Omega t + \gamma(y_1 - y_2).
\end{aligned}$$

The system perturbations are bounded as $|\Delta f_2| = |\cos t \sin(x_2 - x_1)| \leq \|\mathbf{e}\|$ and $|\Delta f_3| = |y_2 - y_1| \leq \|\mathbf{e}\|$. Choose $\gamma = 19.5$ to satisfy $\gamma > (L + K_1 + K_2)/2$. The initial value is also $\mathbf{x}_0 = [0.2, -0.2, 1, 1]^T$. The simulated results are shown in Fig. 3.11 and Fig. 3.12. In Fig. 3.11, the state errors approach zero as time evolves. Since $x_2 \rightarrow x_1$, $y_2 \rightarrow y_1$ as $t \rightarrow \infty$, the projections of synchronized manifold shown in Fig. 3.12 represent diagonal-like.

3.4.3 Mutual Coupled Systems with Perturbation Small on the Average

Example 3.5 Autonomous case: Consider the following mutual coupled Lorenz systems with nonvanishing perturbation in the form of Eq. (3.3) as

$$\begin{aligned}
\dot{x}_1 &= -\sigma(x_1 - y_1) + \gamma(x_2 - x_1), \\
\dot{y}_1 &= rx_1 - y_1 - x_1 z_1 + 2 \sin(20\pi t) + \gamma(y_2 - y_1), \\
\dot{z}_1 &= x_1 y_1 - bz_1 + \gamma(z_2 - z_1),
\end{aligned}$$

$$\begin{aligned}\dot{x}_2 &= -\sigma(x_2 - y_2) + randn(t) + \gamma(x_1 - x_2), \\ \dot{y}_2 &= rx_2 - y_2 - x_2z_2 + \gamma(y_1 - y_2), \\ \dot{z}_2 &= x_2y_2 - bz_2 + 5\cos(30\pi t) + \gamma(z_1 - z_2),\end{aligned}$$

where $randn(t)$ is the unit normal random variable. The second system perturbation is $\Delta f_2 = 2\sin(20\pi t)$. It is bounded on the average since $\int_t^{t+T} \sup\{|\Delta f_2|\}d\tau \leq 2T$, $\forall t \in [0, \infty)$. Similar, for $t \in [0, \infty)$ the fourth system perturbation $\Delta f_4 = randn(t)$ and the sixth system perturbation $\Delta f_6 = 5\cos(30\pi t)$ are bounded on the average by $\int_t^{t+T} \sup\{|\Delta f_4|\}d\tau \leq T$ and $\int_t^{t+T} \sup\{|\Delta f_6|\}d\tau \leq 5T$, respectively. The initial condition and $\gamma = 44$ are the same as in the example 3.1. Three state errors versus time are shown in Fig. 3.13 and they are bounded by a constant as time evolves. The projections of synchronized manifold are shown in Fig. 3.14. They look like a little vague since the state errors are stable but not asymptotically stable. If $\gamma = 130$, the results are shown in Fig. 3.15 and Fig. 3.16, respectively. As coupling strength γ increases, the error bounds decrease and the projections of synchronized manifold look clear.

Example 3.6 Nonautonomous case: The mutual coupled Ueda systems with nonvanishing perturbations is

$$\begin{aligned}\dot{x}_1 &= y_1 + \gamma(x_2 - x_1), \\ \dot{y}_1 &= -x_1^3 - by_1 + A\sin\Omega t + \cos(25\pi t) + \gamma(y_2 - y_1), \\ \dot{x}_2 &= y_2 + 5\sin(15\pi t) + \gamma(x_1 - x_2), \\ \dot{y}_2 &= -x_2^3 - by_2 + A\sin\Omega t + \gamma(y_1 - y_2).\end{aligned}$$

The system perturbations are $\Delta f_2 = \cos(25\pi t)$ and $f_3 = 5\sin(15\pi t)$, then $\int_t^{t+T} \sup\{|\Delta f_2|\}d\tau \leq T$ and $\int_t^{t+T} \sup\{|\Delta f_3|\}d\tau \leq 5T$, $\forall t \in [0, \infty)$. The initial condition and $\gamma = 18.5$ are the same as in the example 3.2. The simulated results are shown in Fig. 3.17 and 3.18. The state errors versus time are shown in Fig. 3.17 and they are bounded by a constant as time evolves. The projections of synchronized manifold are shown in Fig. 3.18. They do not look like exact diagonal lines since the state errors are stable but not asymptotically stable. Choose $\gamma = 100$, the results are shown in Fig. 3.19 and Fig. 3.20, respectively. As coupling strength γ increases, the error bounds decrease and the projections of synchronized manifold look clear.

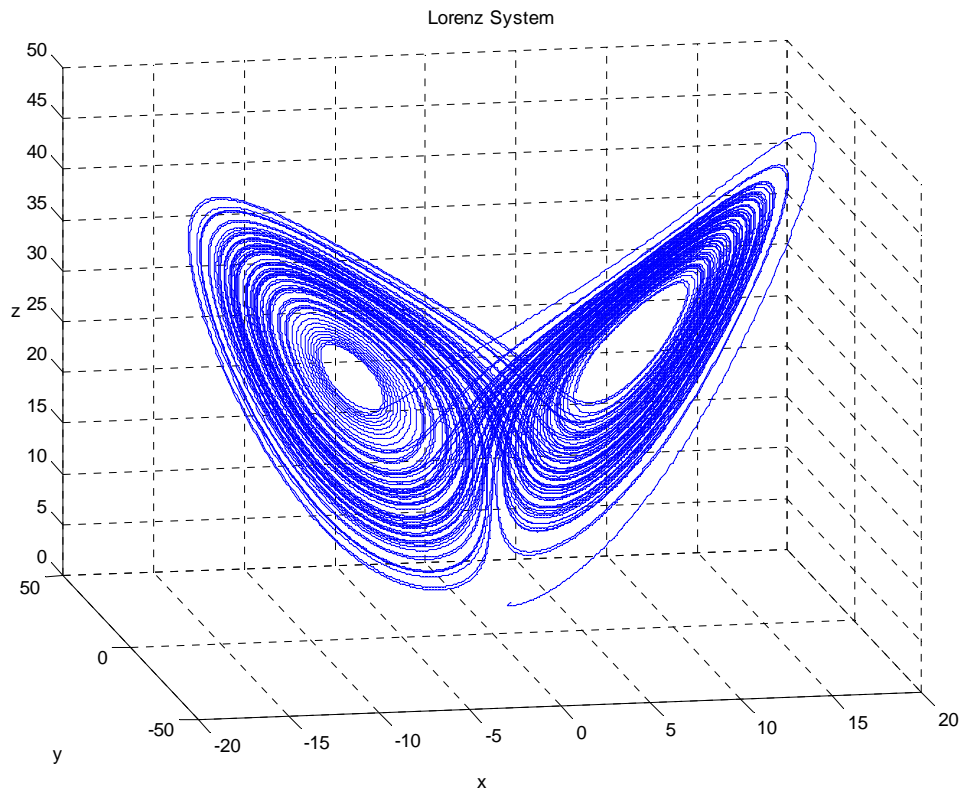


Fig. 3.1 Chaotic attractor of the Lorenz system.

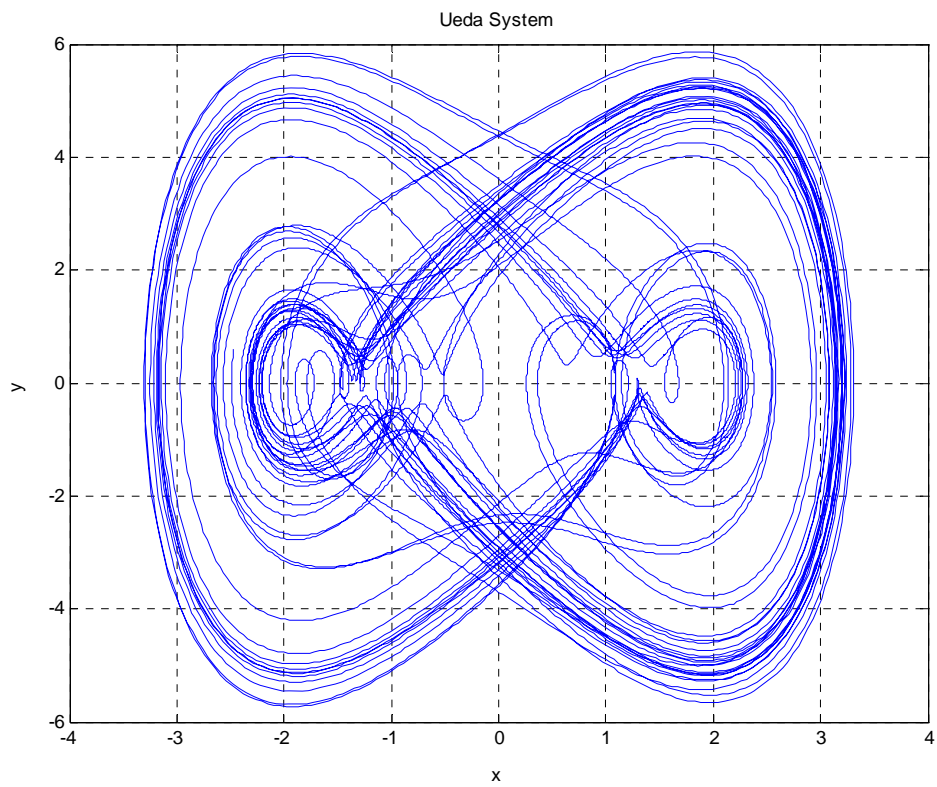


Fig. 3.2 Chaotic attractor of the Ueda system.

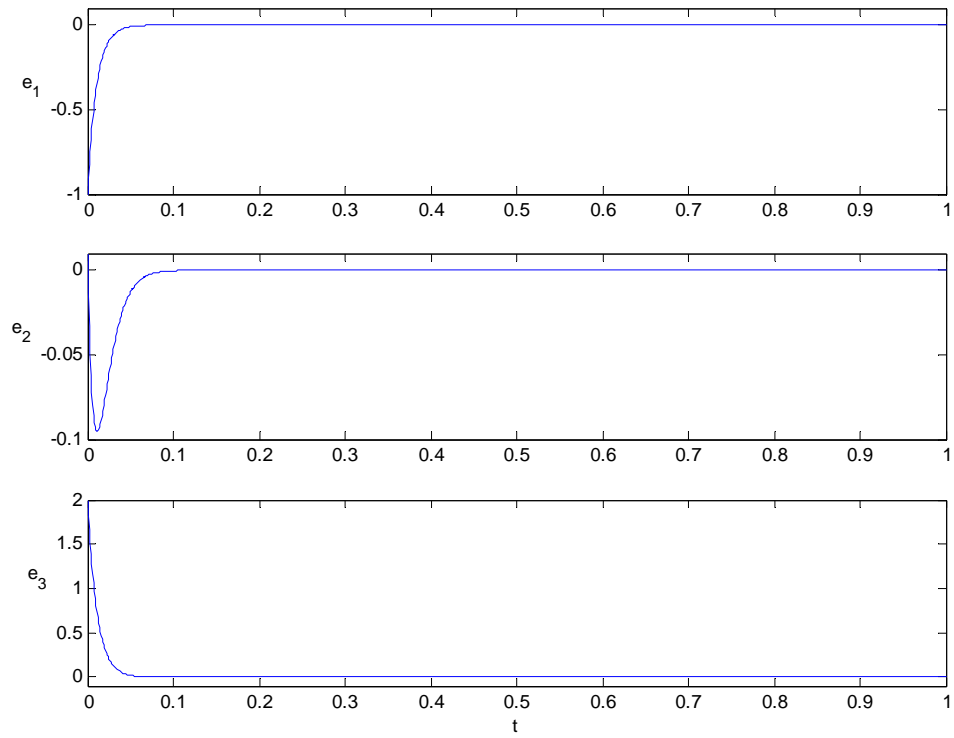


Fig. 3.3 State errors versus time of mutual coupled Lorenz system without perturbation.

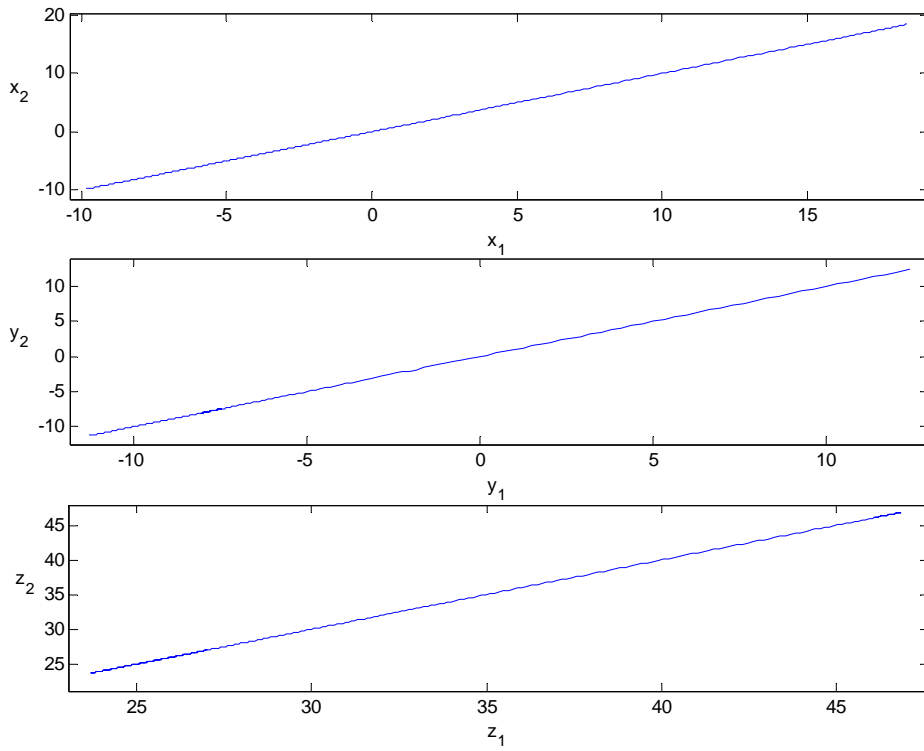


Fig. 3.4 Projections of synchronized manifold for mutual coupled Lorenz system without perturbation.

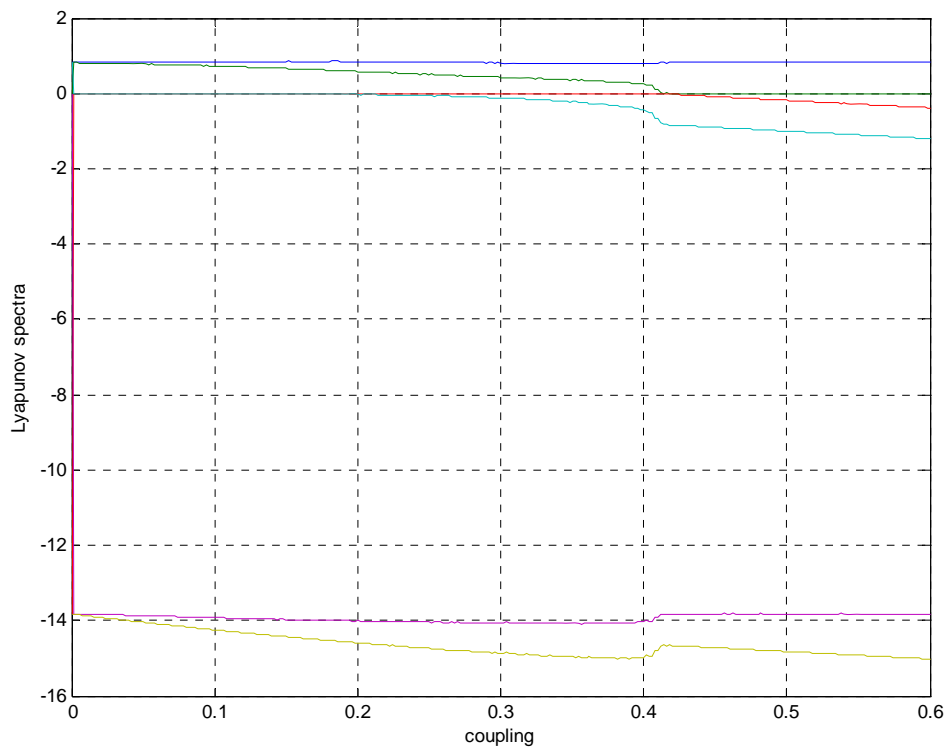


Fig. 3.5 Lyapunov spectra of mutual coupled Lorenz systems without system perturbation.

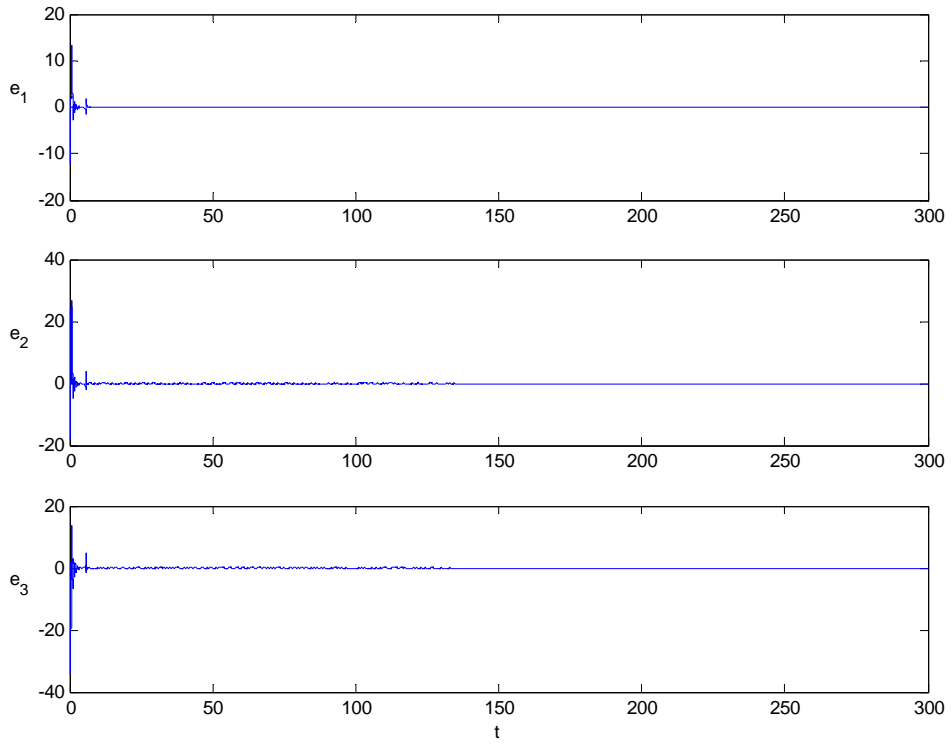


Fig. 3.6 State errors versus time of mutual coupled Lorenz systems without perturbation while $\gamma = 0.6$.

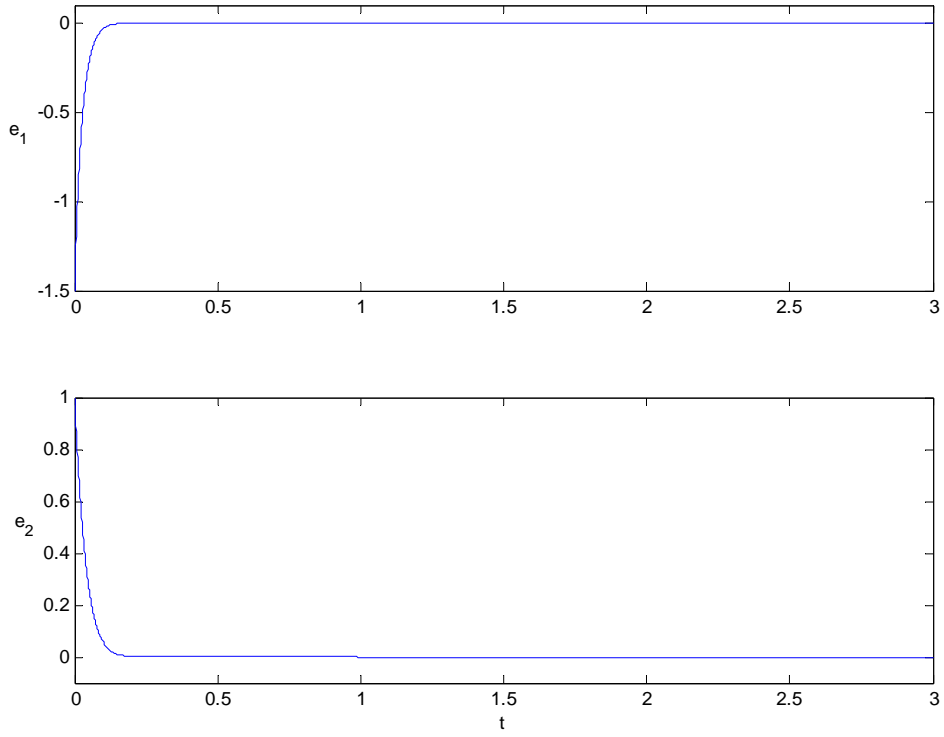


Fig. 3.7 State errors versus time of mutual coupled Ueda system without perturbation.

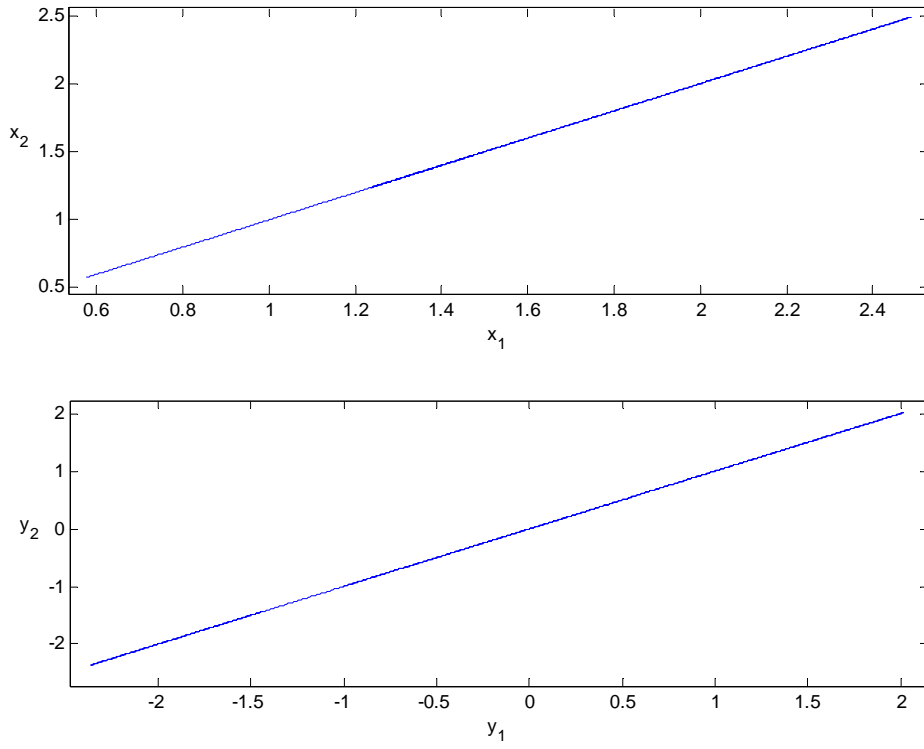


Fig. 3.8 Projections of synchronized manifold of mutual coupled Ueda system without perturbation.

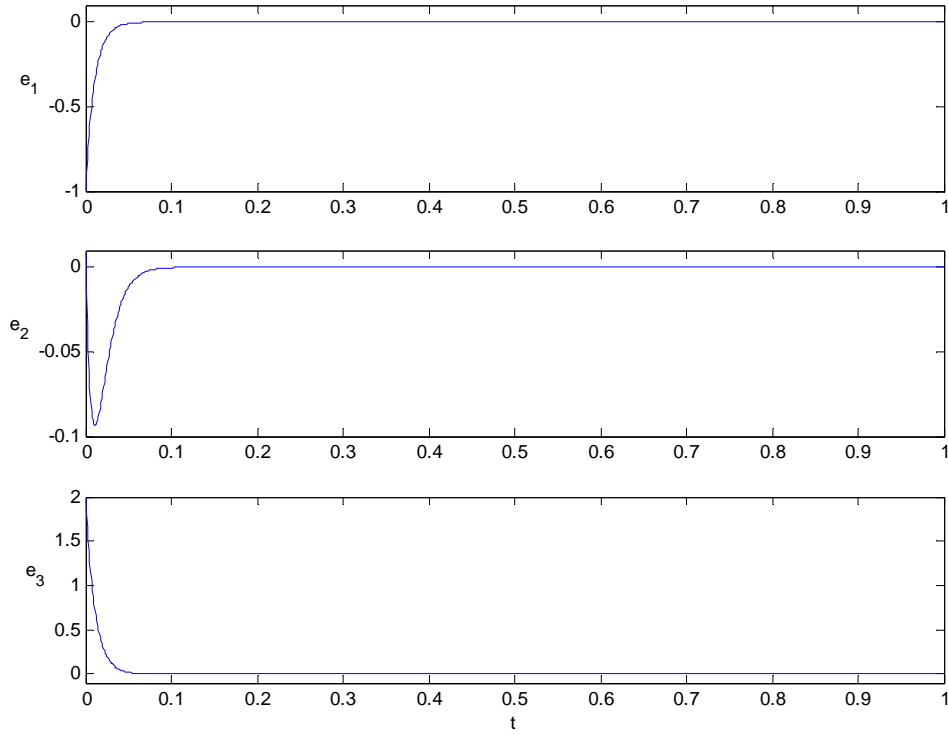


Fig. 3.9 State errors versus time of mutual coupled Lorenz systems with perturbations
 $\Delta f_1 = \cos t \cdot (y_1 - y_2)$ and $\Delta f_6 = x_1 - x_2$.

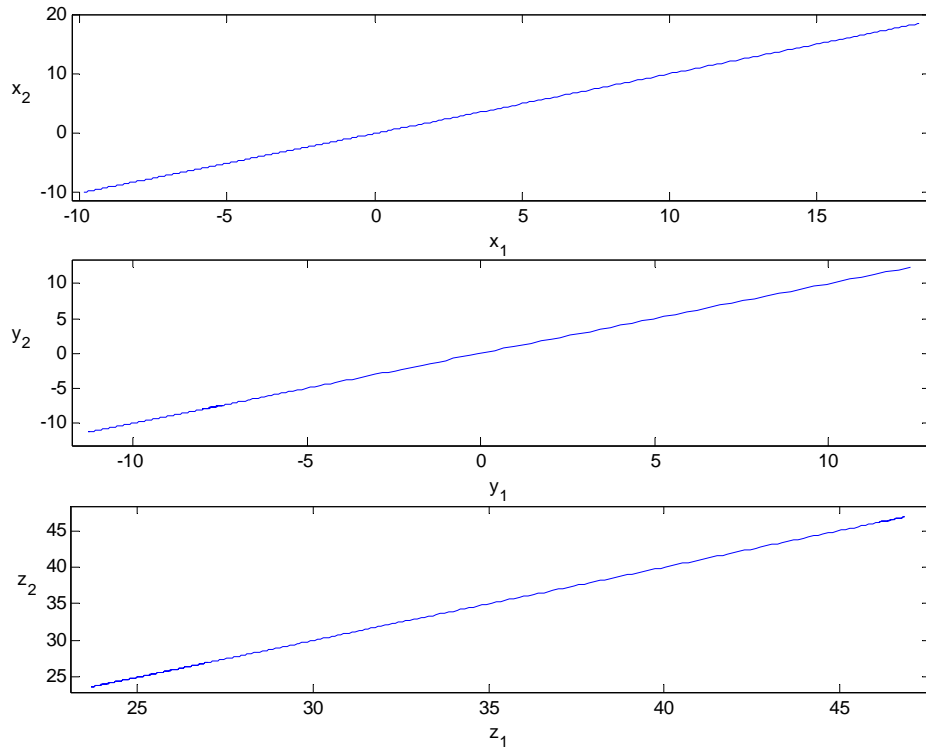


Fig. 3.10 Projections of synchronized manifold of mutual coupled Lorenz systems with perturbations $\Delta f_1 = \cos t \cdot (y_1 - y_2)$ and $\Delta f_6 = x_1 - x_2$.

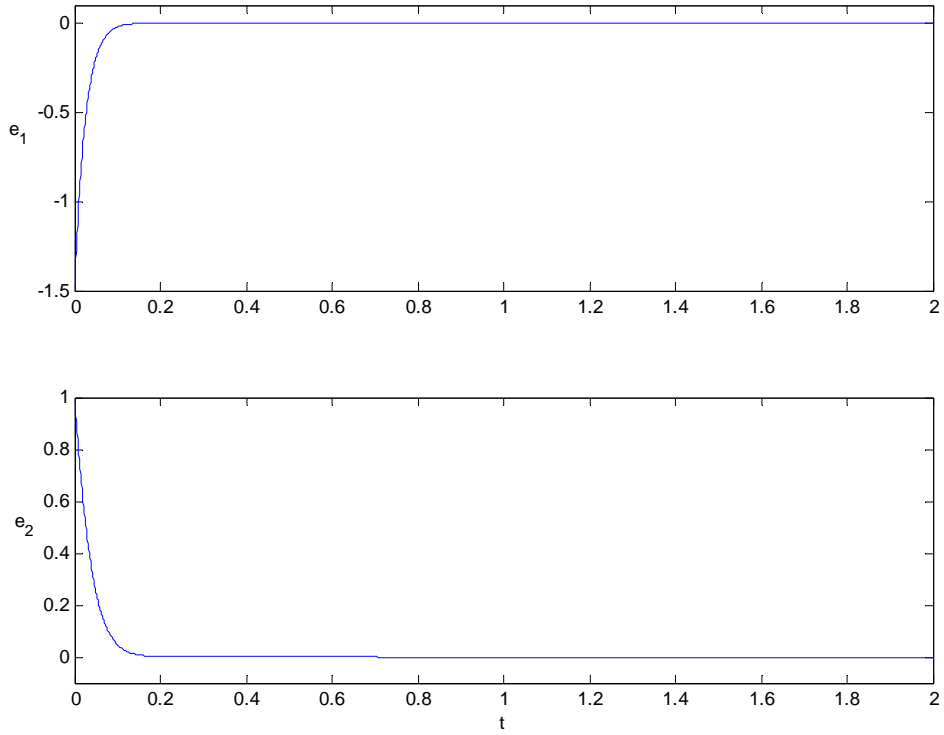


Fig. 3.11 State errors versus time of mutual coupled Ueda systems with perturbations
 $\Delta f_2 = \cos t \sin(x_2 - x_1)$ and $\Delta f_3 = y_2 - y_1$.

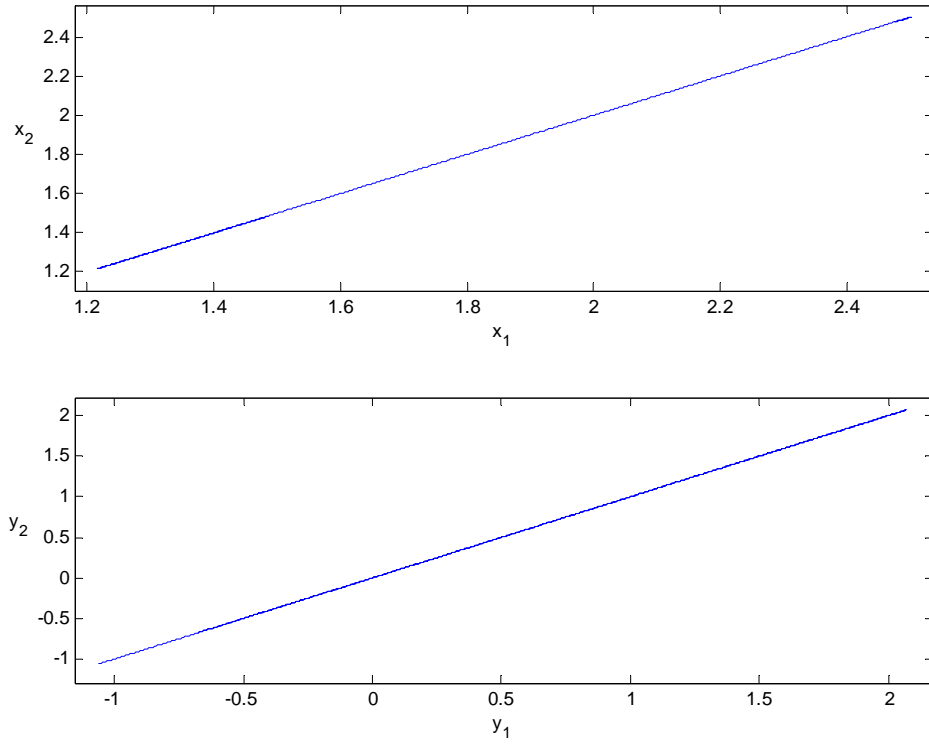


Fig. 3.12 Projections of synchronized manifold of mutual coupled Ueda systems with perturbations $\Delta f_2 = \cos t \sin(x_2 - x_1)$ and $\Delta f_3 = y_2 - y_1$.

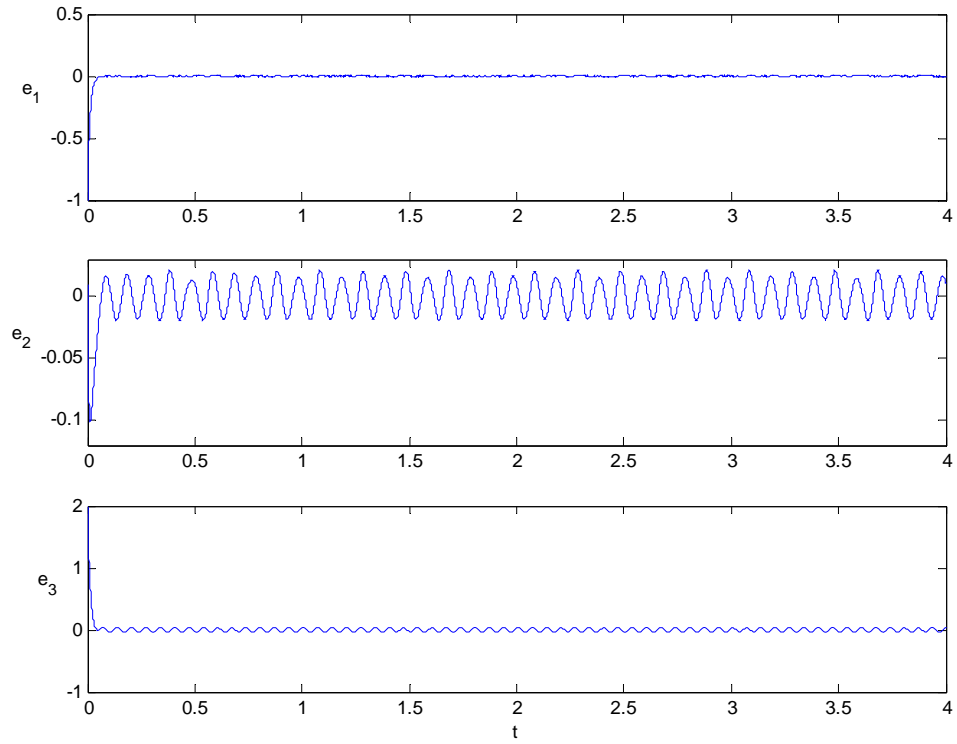


Fig. 3.13 State errors versus time of mutual coupled Lorenz systems with perturbations $\Delta f_2 = 2 \sin(20\pi t)$, $\Delta f_4 = \text{randn}(t)$ and $\Delta f_6 = 5 \cos(30\pi t)$.

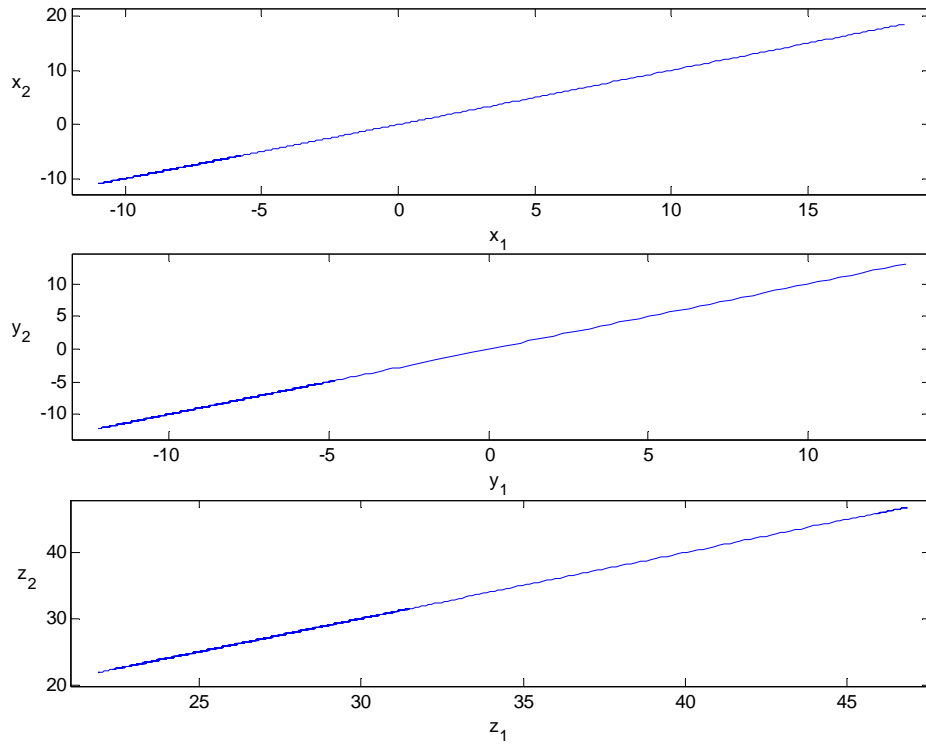


Fig. 3.14 Projections of synchronized manifold of mutual coupled Lorenz systems with perturbations $\Delta f_2 = 2 \sin(20\pi t)$, $\Delta f_4 = \text{randn}(t)$ and $\Delta f_6 = 5 \cos(30\pi t)$.

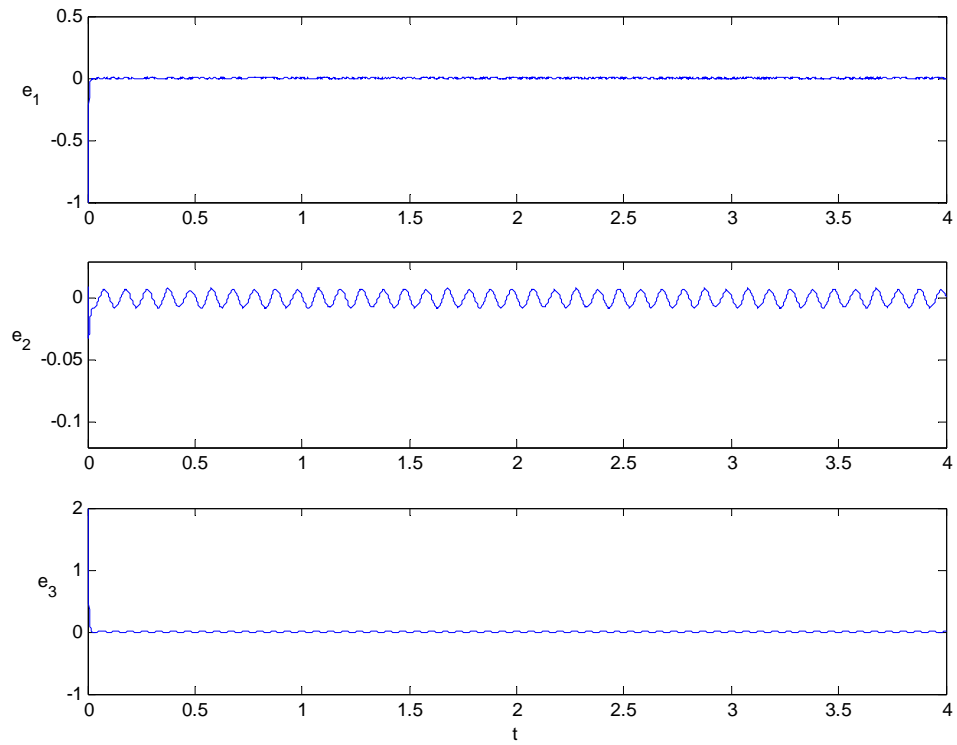


Fig. 3.15 State errors versus time of mutual coupled Lorenz systems with $\Delta f_2 = 2 \sin(20\pi t)$, $\Delta f_4 = \text{randn}(t)$, $\Delta f_6 = 5 \cos(30\pi t)$ and $\gamma = 130$.

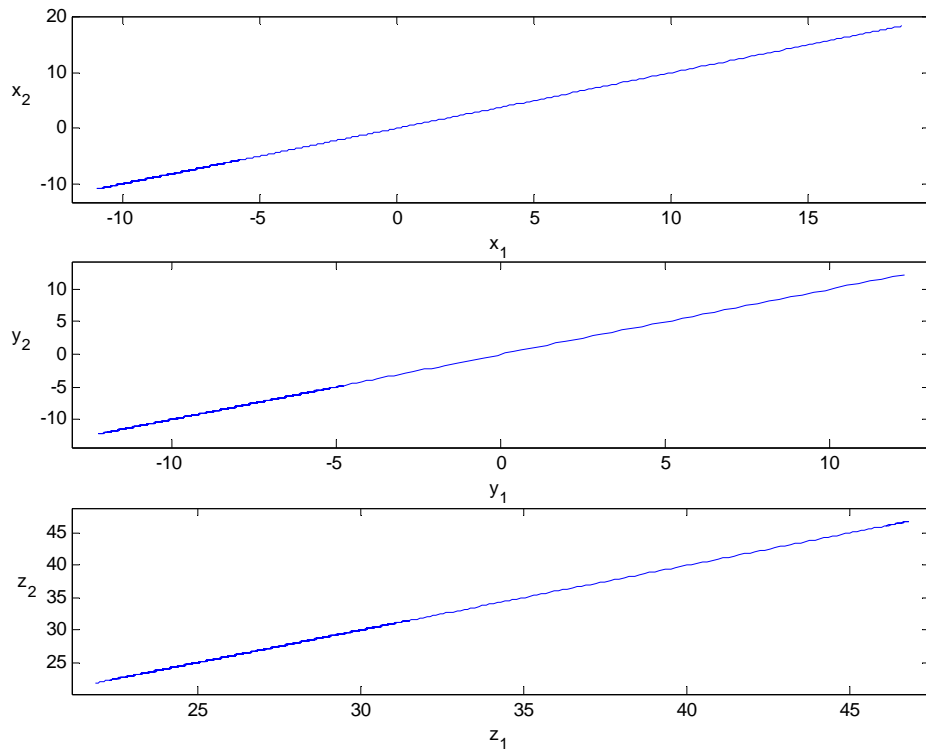


Fig. 3.16 Projections of synchronized manifold of mutual coupled Lorenz systems with $\Delta f_2 = 2 \sin(20\pi t)$, $\Delta f_4 = \text{randn}(t)$, $\Delta f_6 = 5 \cos(30\pi t)$ and $\gamma = 130$.

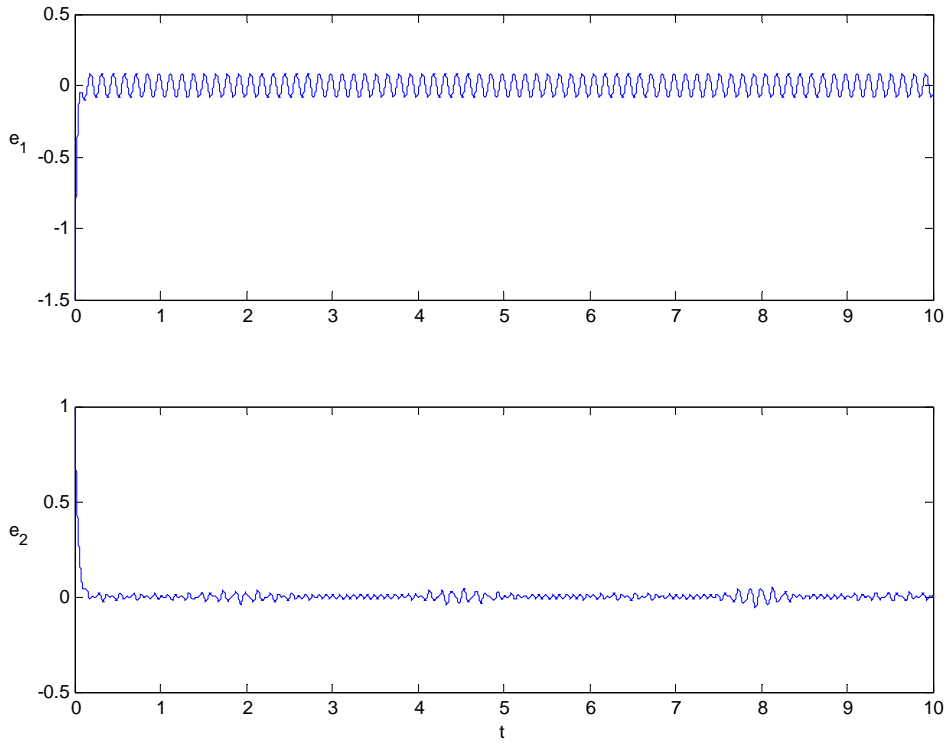


Fig. 3.17 State errors versus time of mutual coupled Ueda Systems with perturbations

$$\Delta f_2 = \cos(25\pi t) \quad \text{and} \quad f_3 = 5 \sin(15\pi t).$$

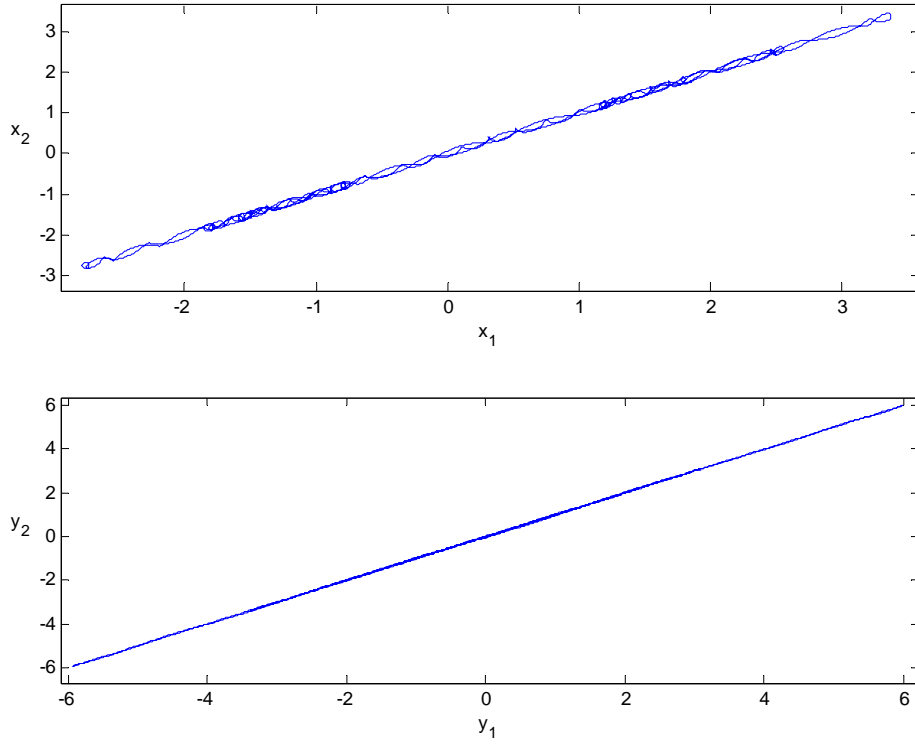


Fig. 3.18 Projections of synchronized manifold of mutual coupled Ueda Systems with perturbations $\Delta f_2 = \cos(25\pi t)$ and $f_3 = 5 \sin(15\pi t)$.

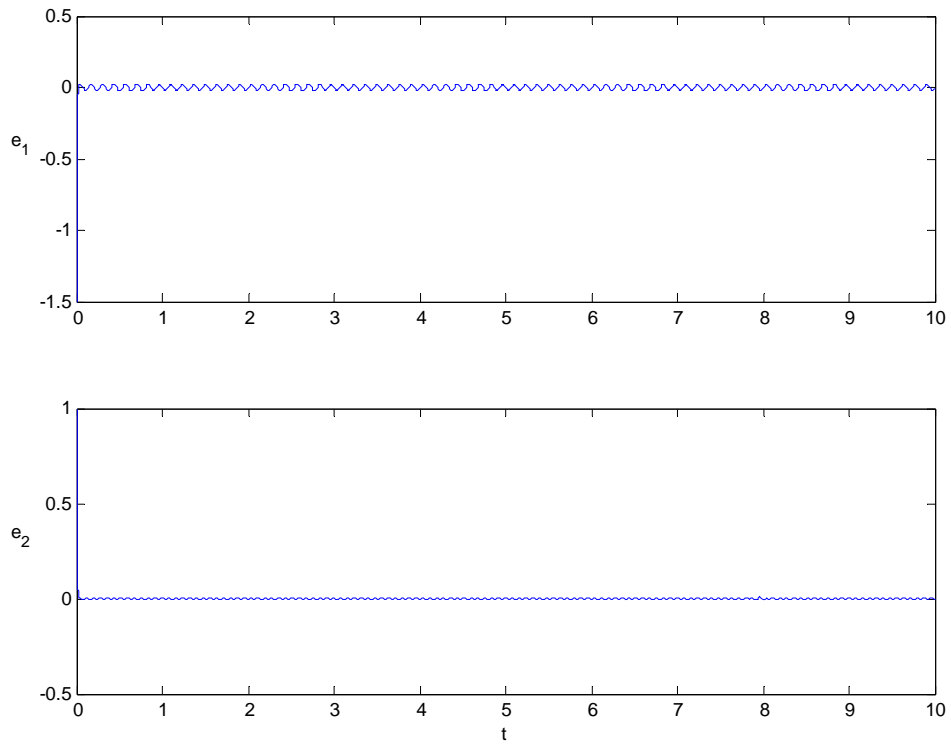


Fig. 3.19 State errors versus time of mutual coupled Ueda Systems with

$$\Delta f_2 = \cos(25\pi t), \quad f_3 = 5 \sin(15\pi t) \quad \text{and} \quad \gamma = 100.$$

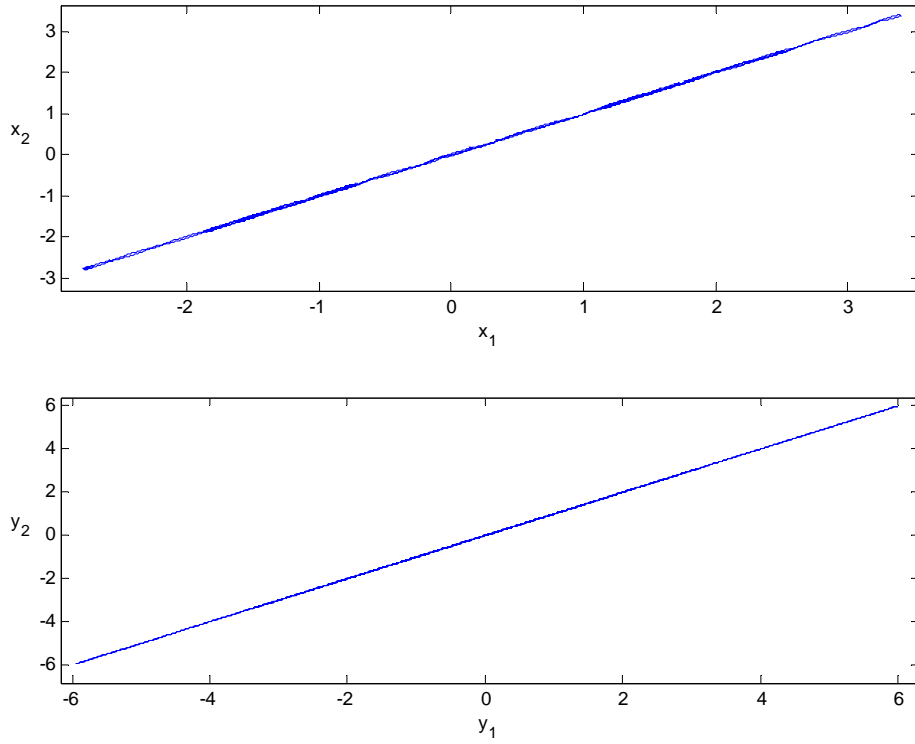


Fig. 3.20 Projections of synchronized manifold of mutual coupled Ueda Systems with $\Delta f_2 = \cos(25\pi t)$, $f_3 = 5 \sin(15\pi t)$ and $\gamma = 100$.

Chapter 4

Adaptive Synchronization of Unidirectional and Mutual Coupled Systems

4.1 Introduction

In chapter 2, it is proposed a general scheme to achieve chaos synchronization of unidirectional coupled nonautonomous systems via partial stability theory due to Rumjantsev [78]. Three theorems are derived to achieve synchronization for unidirectional coupled systems by linear feedback. This scheme is also applied to mutual coupled systems in chapter 3. Three theorems are also derived to achieve synchronization for mutual coupled systems by linear feedback.

To use these theorems a relation about coupling gain matrix must be satisfied in advance since these theorems are sufficient. Moreover, the estimate of Lipschitz constant is needed and it is often conservative. In this chapter, an adaptive coupling gain replaces this coupling gain matrix. To implement this adaptive coupling gain an adaptive law is adopted to estimate the Lipschitz constant of the chaotic system. It is easier and more convenient to use this adaptive method for synchronization of both unidirectional and mutual coupled systems than the theorems in previous two chapters. Furthermore, to increase the convergent rate of state errors we only set a larger initial condition of the adaptive equation.

The theoretical analyses are arranged in section 2 and section 3 for both unidirectional and mutual coupled systems, respectively. Two theorems for adaptive synchronization of unidirectional and mutual coupled nonautonomous chaotic systems are derived individually. An adaptive coupling gain is realized by adopting an adaptive law to estimate the Lipschitz constant of the chaotic system. In section 4, the Lorenz system and the Duffing system are simulated to demonstrate analytical results for unidirectional and mutual coupled chaotic systems, respectively.

4.2 Adaptive Synchronization of Unidirectional Coupled Systems

Consider the following unidirectional coupled nonautonomous systems

$$\begin{aligned}\dot{\mathbf{x}} &= \mathbf{f}(t, \mathbf{x}), \\ \dot{\hat{\mathbf{x}}} &= \mathbf{f}(t, \hat{\mathbf{x}}) + \mathbf{u}(t, \mathbf{x}, \hat{\mathbf{x}}),\end{aligned}\tag{4.1}$$

where $\mathbf{x}, \hat{\mathbf{x}} \in \mathbb{R}^n$ and $\mathbf{f} : \Omega_1 \subset \mathbb{R} \times \mathbb{R}^n \rightarrow \mathbb{R}^n$ satisfy Lipschitz condition $\|\mathbf{f}(t, \mathbf{x}_1) - \mathbf{f}(t, \mathbf{x}_2)\| \leq L\|\mathbf{x}_1 - \mathbf{x}_2\|$ in \mathbf{x} for all (t, \mathbf{x}_1) and (t, \mathbf{x}_2) in Ω_1 with Lipschitz constant L . $\mathbf{u} : \Omega_2 \subset \mathbb{R} \times \mathbb{R}^n \times \mathbb{R}^n \rightarrow \mathbb{R}^n$ is the coupling function. Ω_1, Ω_2 are domains containing the origin. Assume that the solution of Eq. (4.1) exists for infinite time. That is, for given $(t_0, \mathbf{x}_0, \hat{\mathbf{x}}_0) \in \Omega_1 \cap \Omega_2$ the solution $[\mathbf{x}^T(t; t_0, \mathbf{x}_0, \hat{\mathbf{x}}_0) \quad \hat{\mathbf{x}}^T(t; t_0, \mathbf{x}_0, \hat{\mathbf{x}}_0)]^T$ of Eq. (4.1) exists for $t \geq t_0$.

To ensure diagonal-like synchronized manifold, assume $\mathbf{u}(t, \mathbf{x}, \hat{\mathbf{x}}) = \mathbf{0}$ if $\mathbf{x}(t) = \hat{\mathbf{x}}(t)$, $\forall t$. Define $\mathbf{e} = \hat{\mathbf{x}} - \mathbf{x}$ to be the state error. Then an extended equation can be obtained as

$$\begin{aligned}\dot{\mathbf{x}} &= \mathbf{f}(t, \mathbf{x}), \\ \dot{\mathbf{e}} &= \mathbf{f}(t, \mathbf{e} + \mathbf{x}) - \mathbf{f}(t, \mathbf{x}) + \mathbf{u}(t, \mathbf{x}, \mathbf{e} + \mathbf{x}).\end{aligned}\tag{4.2}$$

Our goal is to choose an appropriate \mathbf{u} so that the partial state $\mathbf{e} = \mathbf{0}$ of equation (4.2) is asymptotically stable. This means that $\hat{\mathbf{x}}$ synchronizes to \mathbf{x} .

Theorem 4.1 *The partial state $\mathbf{e} = \mathbf{0}$ of Eq. (4.2) is uniformly asymptotically stable if $\mathbf{u} = -(\hat{L} + \varepsilon)\mathbf{e}$ with $\varepsilon > 0$ and adaptation $\dot{\hat{L}} = \|\mathbf{e}\|^2$, i.e. the system in the form of Eq. (4.1) is synchronized if $\mathbf{u} = -(\hat{L} + \varepsilon)\mathbf{e}$ with $\varepsilon > 0$ and adaptation $\dot{\hat{L}} = \|\mathbf{e}\|^2$.*

Proof Choose a positive definite function as

$$V = \frac{1}{2}\mathbf{e}^T\mathbf{e} + \frac{1}{2}(\hat{L} - L)^2,$$

then its time derivative along the solution of Eq.(4.2) is

$$\begin{aligned}\dot{V} &= \mathbf{e}^T [\mathbf{f}(t, \mathbf{e} + \mathbf{x}) - \mathbf{f}(t, \mathbf{x}) + \mathbf{u}(t, \mathbf{x}, \mathbf{e} + \mathbf{x})] + (\hat{L} - L)\dot{\hat{L}} \\ &\leq L\|\mathbf{e}\|^2 + \mathbf{e}^T\mathbf{u} + (\hat{L} - L)\dot{\hat{L}}.\end{aligned}$$

Let the adaptive law be $\dot{\hat{L}} = \|\mathbf{e}\|^2$ and $\mathbf{u} = -(\hat{L} + \varepsilon)\mathbf{e}$ with $\varepsilon > 0$. We obtain $\dot{V} < -\varepsilon\|\mathbf{e}\|^2$. Hence the equilibrium $\mathbf{e} = \mathbf{0}$ is uniformly asymptotically stable by partial stability theory [78-80].

4.3 Adaptive Synchronization of Mutual Coupled Systems

For the mutual coupled nonautonomous systems, consider the systems in the form as follows

$$\begin{aligned}\dot{\mathbf{x}} &= \mathbf{f}(t, \mathbf{x}) - \mathbf{u}(t, \mathbf{x}, \hat{\mathbf{x}}), \\ \dot{\hat{\mathbf{x}}} &= \mathbf{f}(t, \hat{\mathbf{x}}) + \mathbf{u}(t, \mathbf{x}, \hat{\mathbf{x}}),\end{aligned}\quad (4.3)$$

where $\mathbf{x}, \hat{\mathbf{x}} \in \mathbb{R}^n$ and $\mathbf{f} : \Omega_1 \subset \mathbb{R} \times \mathbb{R}^n \rightarrow \mathbb{R}^n$ satisfy Lipschitz condition $\|\mathbf{f}(t, \mathbf{x}_1) - \mathbf{f}(t, \mathbf{x}_2)\| \leq L\|\mathbf{x}_1 - \mathbf{x}_2\|$ in \mathbf{x} for all (t, \mathbf{x}_1) and (t, \mathbf{x}_2) in Ω_1 with Lipschitz constant L . $\mathbf{u} : \Omega_2 \subset \mathbb{R} \times \mathbb{R}^n \times \mathbb{R}^n \rightarrow \mathbb{R}^n$ is the coupling function. Ω_1, Ω_2 are domains containing the origin. Assume that the solution of Eq. (4.3) exists for infinite time. That is, for given $(t_0, \mathbf{x}_0, \hat{\mathbf{x}}_0) \in \Omega_1 \cap \Omega_2$ the solution $[\mathbf{x}^T(t; t_0, \mathbf{x}_0, \hat{\mathbf{x}}_0) \quad \hat{\mathbf{x}}^T(t; t_0, \mathbf{x}_0, \hat{\mathbf{x}}_0)]^T$ of Eqs. (4.3) exist for $t \geq t_0$.

To ensure diagonal-like synchronized manifold, assume that $\mathbf{u}(t, \mathbf{x}, \mathbf{x}) = \mathbf{0}$ for $\mathbf{x}(t) = \hat{\mathbf{x}}(t)$, $\forall t$. Define $\mathbf{e} = \hat{\mathbf{x}} - \mathbf{x}$ to be the state error. Then an extended equation can be obtained as

$$\begin{aligned}\dot{\mathbf{x}} &= \mathbf{f}(t, \mathbf{x}) - \mathbf{u}(t, \mathbf{x}, \mathbf{e} + \mathbf{x}), \\ \dot{\mathbf{e}} &= \mathbf{f}(t, \mathbf{e} + \mathbf{x}) - \mathbf{f}(t, \mathbf{x}) + 2\mathbf{u}(t, \mathbf{x}, \mathbf{e} + \mathbf{x}).\end{aligned}\quad (4.4)$$

Theorem 4.2 *The partial state $\mathbf{e} = \mathbf{0}$ of Eq. (4.4) is uniformly asymptotically stable if $\mathbf{u} = -0.5(\hat{L} + \varepsilon)\mathbf{e}$ with $\varepsilon > 0$ and adaptation $\dot{\hat{L}} = \|\mathbf{e}\|^2$, i.e. the system in the form of Eq. (4.3) is synchronized if $\mathbf{u} = -0.5(\hat{L} + \varepsilon)\mathbf{e}$ with $\varepsilon > 0$ and adaptation $\dot{\hat{L}} = \|\mathbf{e}\|^2$.*

Proof Choose a positive definite function as

$$V = \frac{1}{2}\mathbf{e}^T\mathbf{e} + \frac{1}{2}(\hat{L} - L)^2,$$

then its time derivative along the solution of Eq.(4.4) is

$$\begin{aligned}\dot{V} &= \mathbf{e}^T [\mathbf{f}(t, \mathbf{e} + \mathbf{x}) - \mathbf{f}(t, \mathbf{x}) + 2\mathbf{u}(t, \mathbf{x}, \mathbf{e} + \mathbf{x})] + (\hat{L} - L)\dot{\hat{L}} \\ &\leq L\|\mathbf{e}\|^2 + 2\mathbf{e}^T\mathbf{u} + (\hat{L} - L)\dot{\hat{L}}.\end{aligned}$$

Let the adaptation be $\dot{\hat{L}} = \|\mathbf{e}\|^2$ and $\mathbf{u} = -0.5(\hat{L} + \varepsilon)\mathbf{e}$ with $\varepsilon > 0$. We can obtain $\dot{V} < -0.5\varepsilon\|\mathbf{e}\|^2$. Hence the partial state $\mathbf{e} = \mathbf{0}$ is uniformly asymptotically stable.

Remark 4.1 The partial stability theory is used in the proofs of Theorem 4.1 and 4.2. On the other hand, as the usual approach the Barbalat lemma can be used to prove the

asymptotical stability of the error dynamics. It seems that using partial stability theory is convenient.

Remark 4.2 Since the adaptive law is $\dot{\hat{L}} = \|\mathbf{e}\|^2 \geq 0$. Therefore, \hat{L} and $\hat{L} - L$ are increasing functions of t and so is $\hat{L} + \varepsilon$. If ε or the initial value \hat{L}_0 of \hat{L} is large, then the feedback gain $\hat{L} + \varepsilon$ is always large. Hence, the larger \hat{L}_0 or ε the faster convergent rate of $\|\mathbf{e}\|$ is.

4.4 Numerical Illustrated Examples

Example 4.1 Unidirectional coupled autonomous system: Lorenz systems

$$\begin{aligned}\dot{x} &= -\sigma(x - y), \\ \dot{y} &= rx - y - xz, \\ \dot{z} &= xy - bz, \\ \dot{\hat{x}} &= -\sigma(\hat{x} - \hat{y}) - (\hat{L} + \varepsilon)(\hat{x} - x), \\ \dot{\hat{y}} &= r\hat{x} - \hat{y} - \hat{x}\hat{z} - (\hat{L} + \varepsilon)(\hat{y} - y), \\ \dot{\hat{z}} &= \hat{x}\hat{y} - b\hat{z} - (\hat{L} + \varepsilon)(\hat{z} - z), \\ \dot{\hat{L}} &= \|\mathbf{e}\|^2,\end{aligned}$$

where $\sigma = 10, r = 28, b = 8/3, \mathbf{x} = [x \ y \ z]^T$ and $\hat{\mathbf{x}} = [\hat{x} \ \hat{y} \ \hat{z}]^T$. Let the initial value be $[\mathbf{x}_0^T \ \hat{\mathbf{x}}_0^T \ \hat{L}_0]^T = [1 \ 1 \ 1 \ 0 \ 0 \ 0 \ 1]^T$ and $\varepsilon = 0.1$. The simulated results are shown in Fig. 4.1. Fig. 4.2 and Fig. 4.3 show the results for changed values $\hat{L}_0 = 25$ and $\varepsilon = 20$, respectively. The rates of convergence for the later two conditions are faster than the first one.

Example 4.2 Unidirectional coupled nonautonomous system: Duffing systems

$$\begin{aligned}\dot{x} &= y, \\ \dot{y} &= x - x^3 - \delta y + \gamma \cos \omega t, \\ \dot{\hat{x}} &= \hat{y} - (\hat{L} + \varepsilon)(\hat{x} - x), \\ \dot{\hat{y}} &= \hat{x} - \hat{x}^3 - \delta \hat{y} + \gamma \cos \omega t - (\hat{L} + \varepsilon)(\hat{y} - y), \\ \dot{\hat{L}} &= \|\mathbf{e}\|^2,\end{aligned}$$

where $\omega = 1, \delta = 0.25, \gamma = 0.4, \mathbf{x} = [x \ y]^T$ and $\hat{\mathbf{x}} = [\hat{x} \ \hat{y}]^T$. Let the initial value be $[\mathbf{x}_0^T \ \hat{\mathbf{x}}_0^T \ \hat{L}_0]^T = [1 \ 1 \ 0.1 \ 0.1 \ 1]^T$ and $\varepsilon = 0.1$. The simulated results are shown in Fig. 4.4. Figs. 4.5 shows the results for changed values $\hat{L}_0 = 5$. Set $\varepsilon = 8$ and $\hat{L}_0 = 1$, the

simulated results are shown in Fig. 4.6. The rates of convergence for the later two conditions are faster than the first one.

Example 4.3 Mutual coupled autonomous system: Lorenz systems

$$\begin{aligned}\dot{x} &= -\sigma(x-y) - (\hat{L} + \varepsilon)(x - \hat{x}), \\ \dot{y} &= rx - y - xz - (\hat{L} + \varepsilon)(y - \hat{y}), \\ \dot{z} &= xy - bz - (\hat{L} + \varepsilon)(z - \hat{z}), \\ \dot{\hat{x}} &= -\sigma(\hat{x} - \hat{y}) - (\hat{L} + \varepsilon)(\hat{x} - x), \\ \dot{\hat{y}} &= r\hat{x} - \hat{y} - \hat{x}\hat{z} - (\hat{L} + \varepsilon)(\hat{y} - y), \\ \dot{\hat{z}} &= \hat{x}\hat{y} - b\hat{z} - (\hat{L} + \varepsilon)(\hat{z} - z), \\ \dot{\hat{L}} &= \|\mathbf{e}\|^2,\end{aligned}$$

where $\sigma = 10, r = 28, b = 8/3, \mathbf{x} = [x \ y \ z]^T$ and $\hat{\mathbf{x}} = [\hat{x} \ \hat{y} \ \hat{z}]^T$. Let the initial value be $[\mathbf{x}_0^T \ \hat{\mathbf{x}}_0^T \ \hat{L}_0]^T = [1 \ 1 \ 1 \ 0 \ 0 \ 0 \ 1]^T$ and $\varepsilon = 0.1$. The simulated results are shown in Fig. 4.7. Fig. 4.8 and Fig. 4.9 show the results for changed values $\hat{L}_0 = 20$ and $\varepsilon = 18$, respectively. The rates of convergence for the later two conditions are faster than the first one.

Example 4.4 Mutual coupled nonautonomous system: Duffing systems

$$\begin{aligned}\dot{x} &= y - 0.5(\hat{L} + \varepsilon)(x - \hat{x}), \\ \dot{y} &= x - x^3 - \delta y + \gamma \cos \omega t - 0.5(\hat{L} + \varepsilon)(y - \hat{y}), \\ \dot{\hat{x}} &= \hat{y} - 0.5(\hat{L} + \varepsilon)(\hat{x} - x), \\ \dot{\hat{y}} &= \hat{x} - \hat{x}^3 - \delta \hat{y} + \gamma \cos \omega t - 0.5(\hat{L} + \varepsilon)(\hat{y} - y), \\ \dot{\hat{L}} &= \|\mathbf{e}\|^2,\end{aligned}$$

where $\omega = 1, \delta = 0.25, \gamma = 0.4, \mathbf{x} = [x \ y]^T$ and $\hat{\mathbf{x}} = [\hat{x} \ \hat{y}]^T$. Let the initial value be $[\mathbf{x}_0^T \ \hat{\mathbf{x}}_0^T \ \hat{L}_0]^T = [1 \ 1 \ 0 \ 0 \ 1]^T$ and $\varepsilon = 0.1$. The simulated results are shown in Fig. 4.10. Figs. 4.11 and 4.12 show the results for changed values $\hat{L}_0 = 5$ and $\varepsilon = 3$, respectively. The rates of convergence for the later two conditions are faster than the first one.

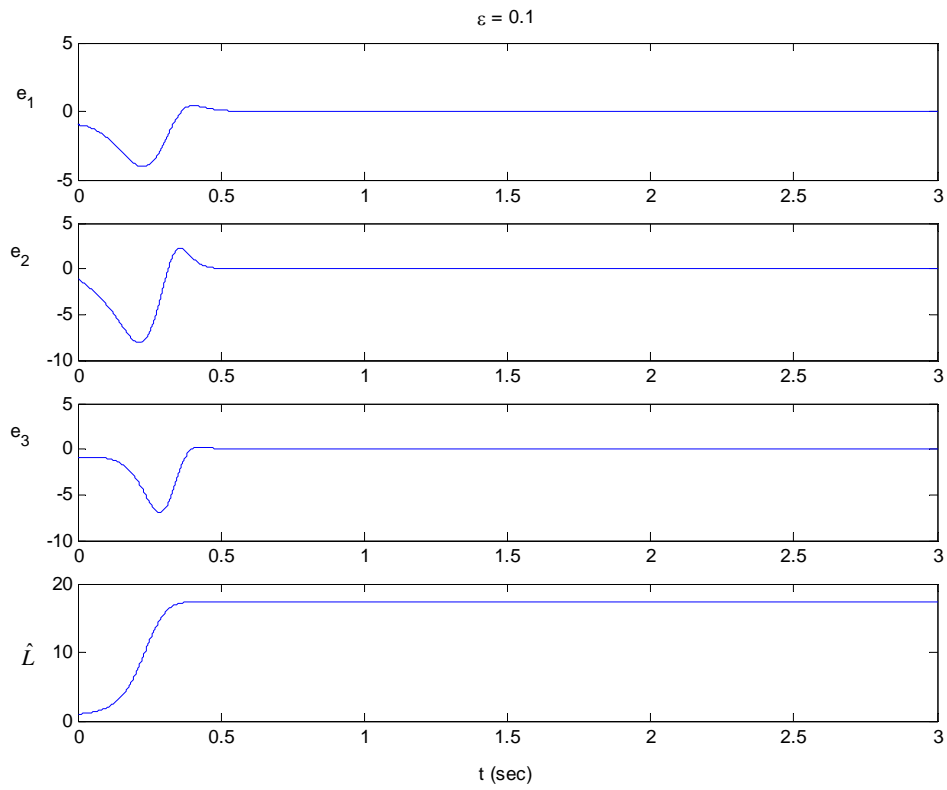


Fig. 4.1 State errors and estimated Lipschitz constant versus time for $\hat{L}_0 = 1$ and $\varepsilon = 0.1$ of unidirectional coupled Lorenz systems.

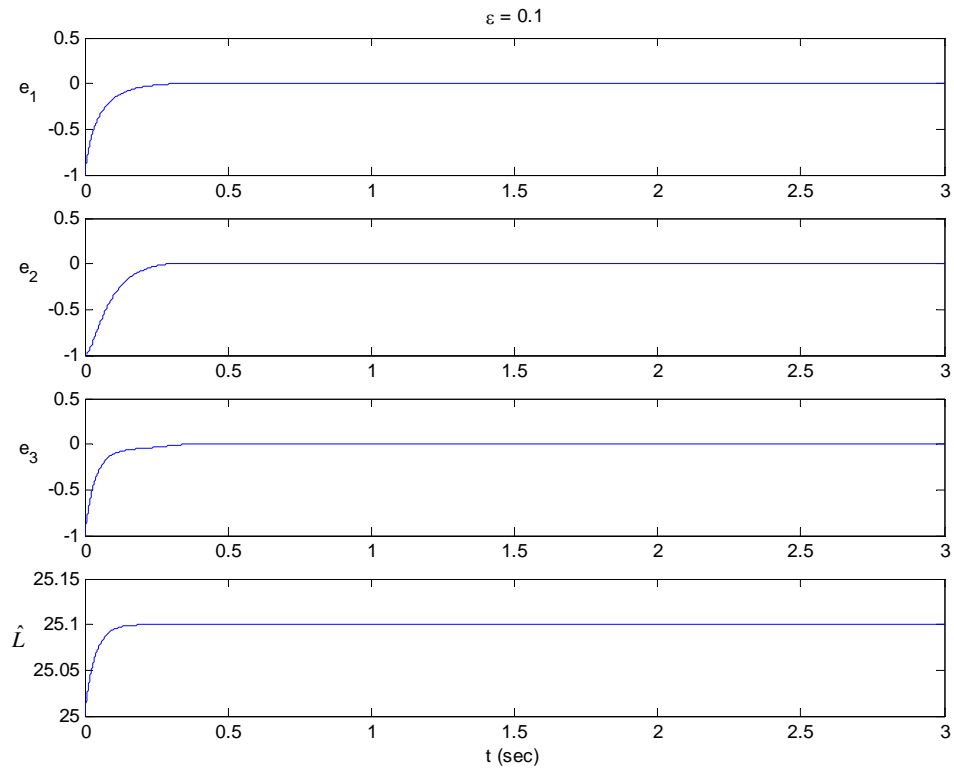


Fig. 4.2 State errors and estimated Lipschitz constant versus time for $\hat{L}_0 = 25$ and $\varepsilon = 0.1$ of unidirectional coupled Lorenz systems.

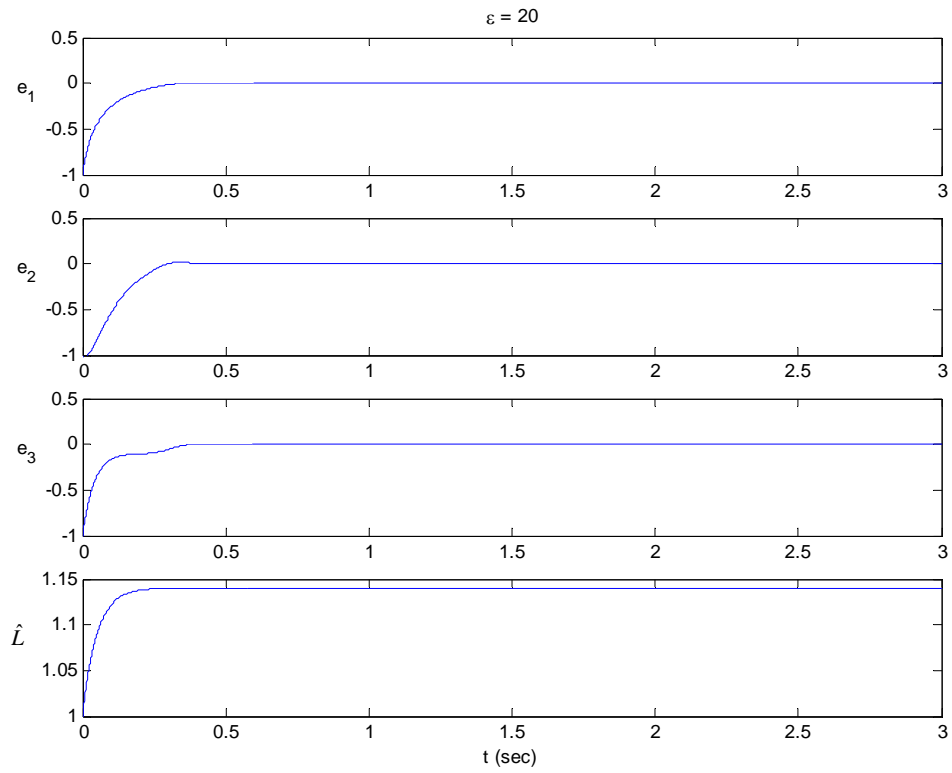


Fig. 4.3 State errors and estimated Lipschitz constant versus time for $\hat{L}_0 = 1$ and $\varepsilon = 20$ of unidirectional coupled Lorenz systems.

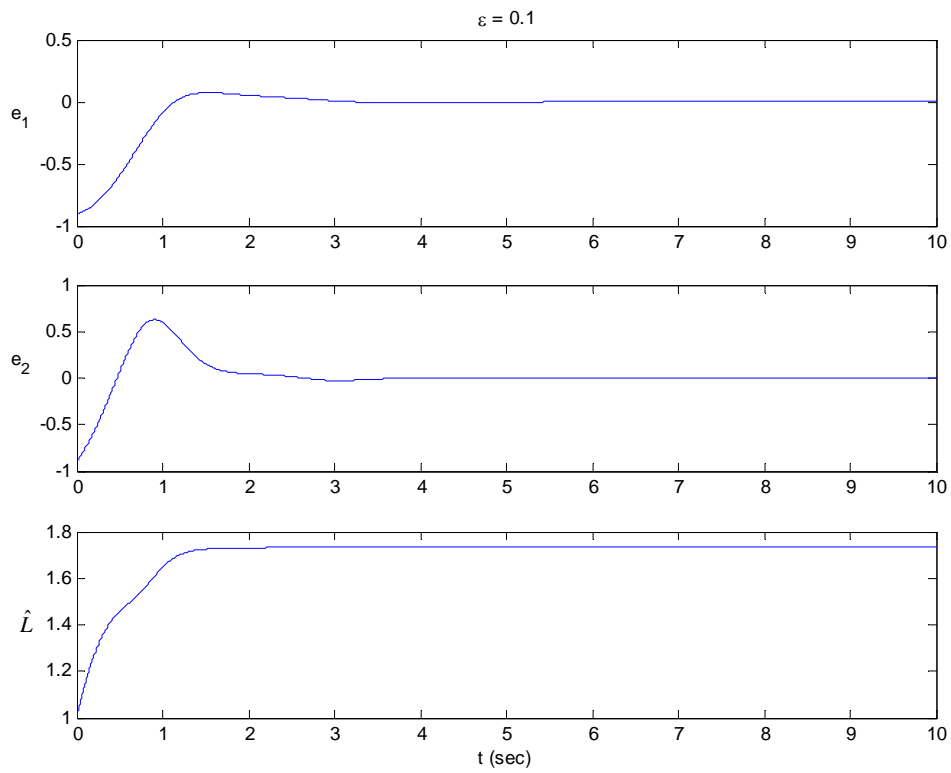


Fig. 4.4 State errors and estimated Lipschitz constant versus time for $\hat{L}_0 = 1$ and $\varepsilon = 0.1$ of unidirectional coupled Duffing systems.

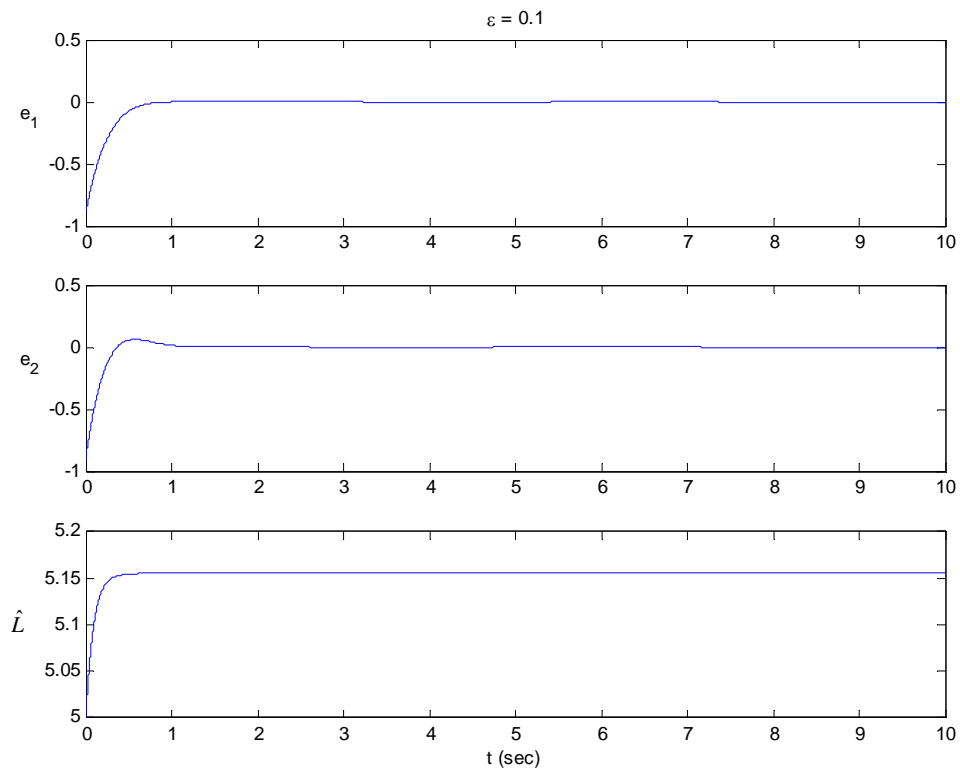


Fig. 4.5 State errors and estimated Lipschitz constant versus time for $\hat{L}_0 = 5$ and $\varepsilon = 0.1$ of unidirectional coupled Duffing systems.

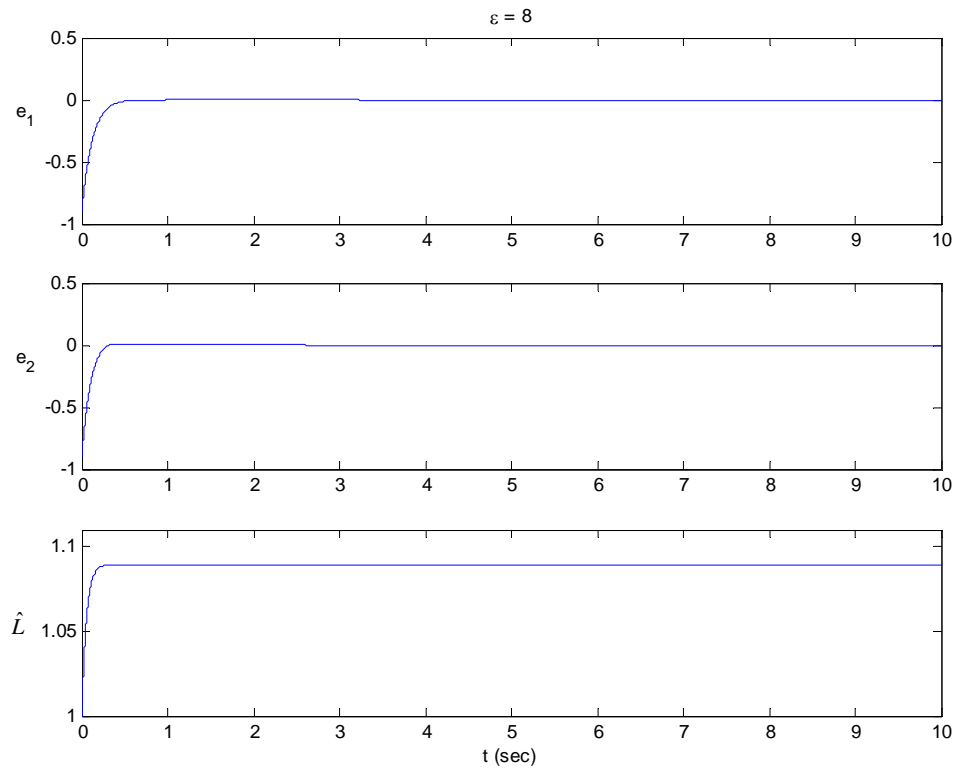


Fig. 4.6 State errors and estimated Lipschitz constant versus time for $\hat{L}_0 = 1$ and $\varepsilon = 8$ of unidirectional coupled Duffing systems.

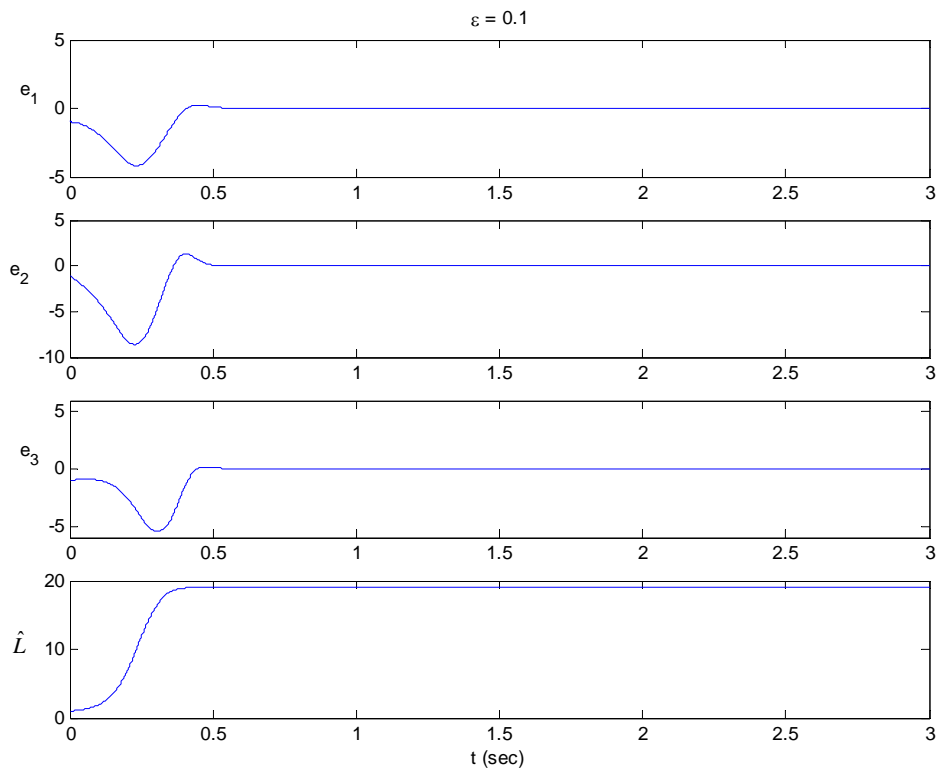


Fig. 4.7 State errors and estimated Lipschitz constant versus time for $\hat{L}_0 = 1$ and $\varepsilon = 0.1$ of mutual coupled Lorenz systems.

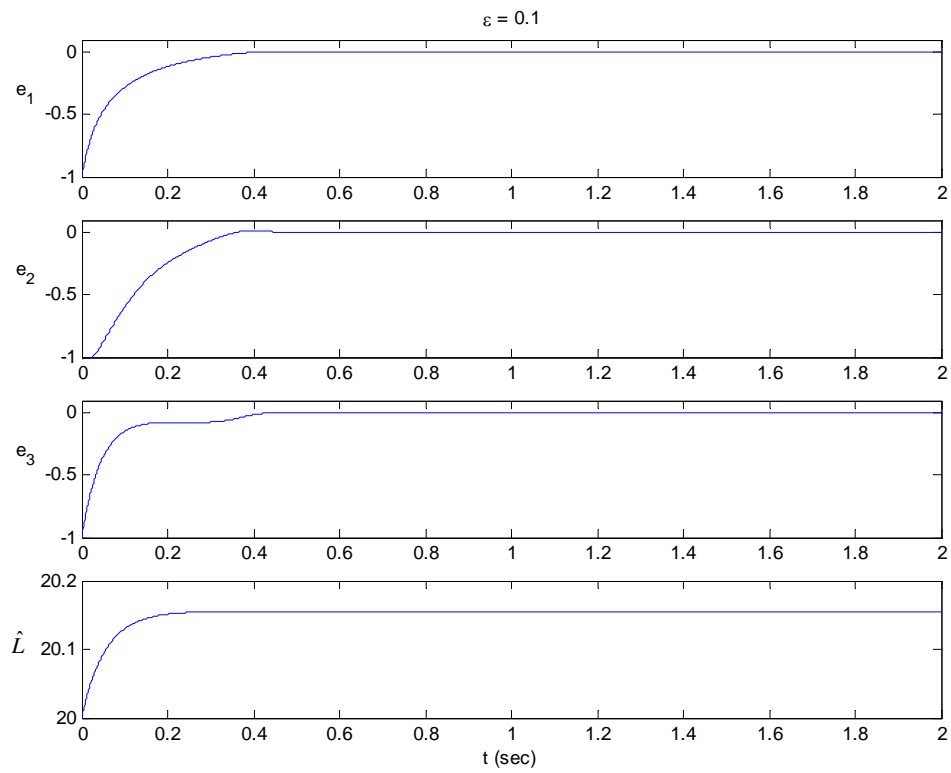


Fig. 4.8 State errors and estimated Lipschitz constant versus time for $\hat{L}_0 = 20$ and $\varepsilon = 0.1$ of mutual coupled Lorenz systems.

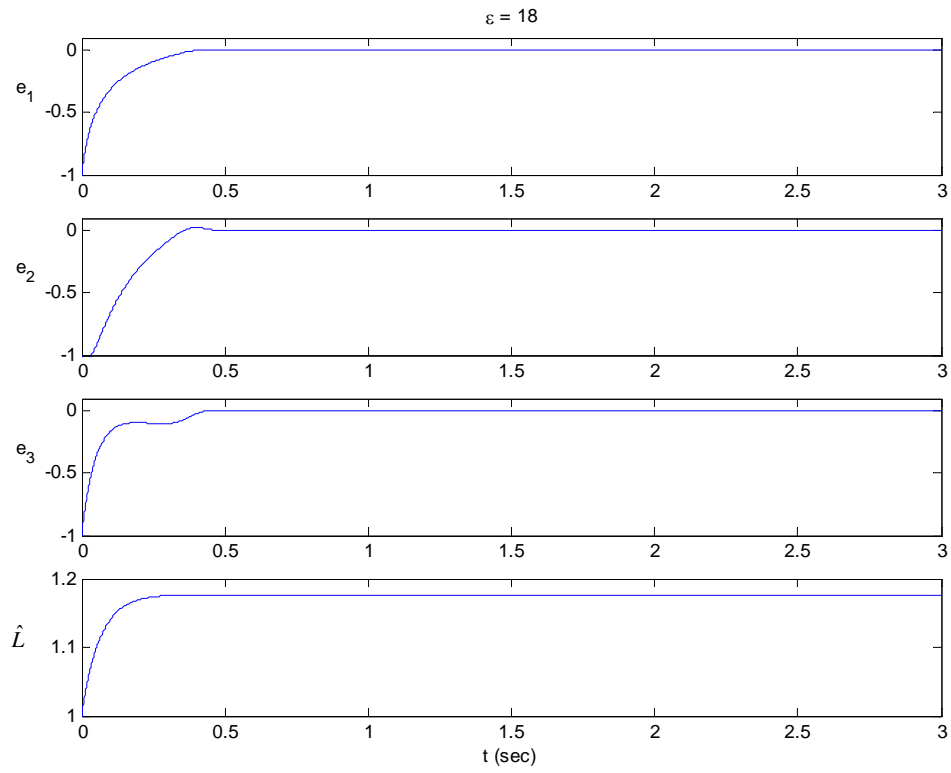


Fig. 4.9 State errors and estimated Lipschitz constant versus time for $\hat{L}_0 = 1$ and $\varepsilon = 18$ of mutual coupled Lorenz systems.

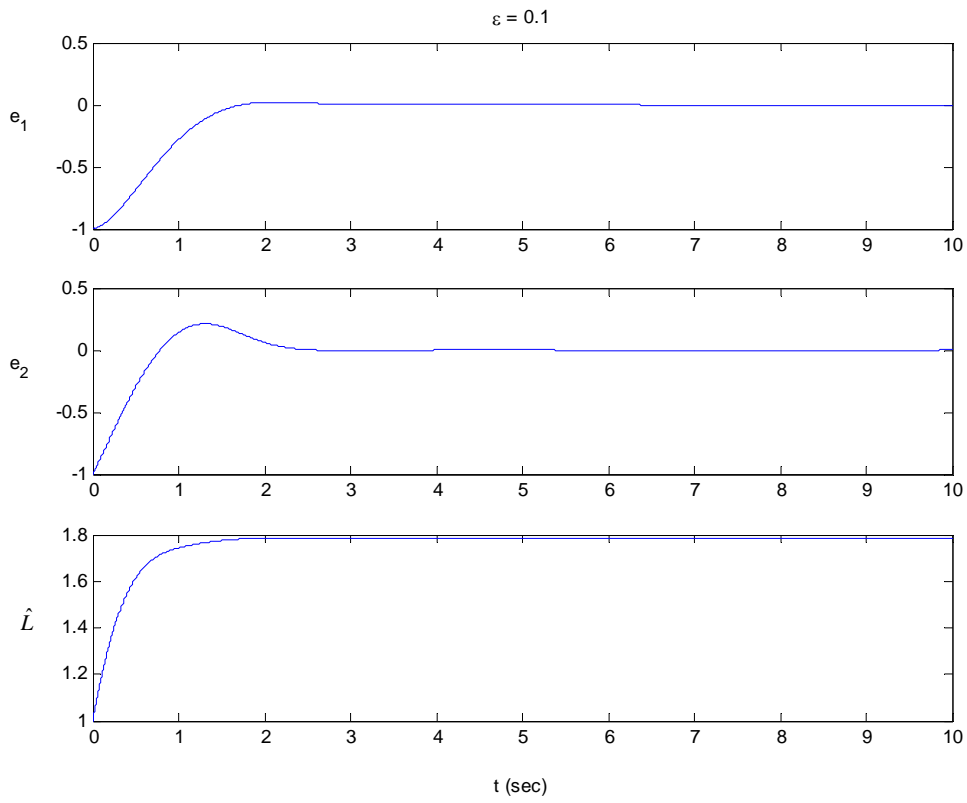


Fig. 4.10 State errors and estimated Lipschitz constant versus time for $\hat{L}_0 = 1$ and $\varepsilon = 0.1$ of mutual coupled Duffing systems

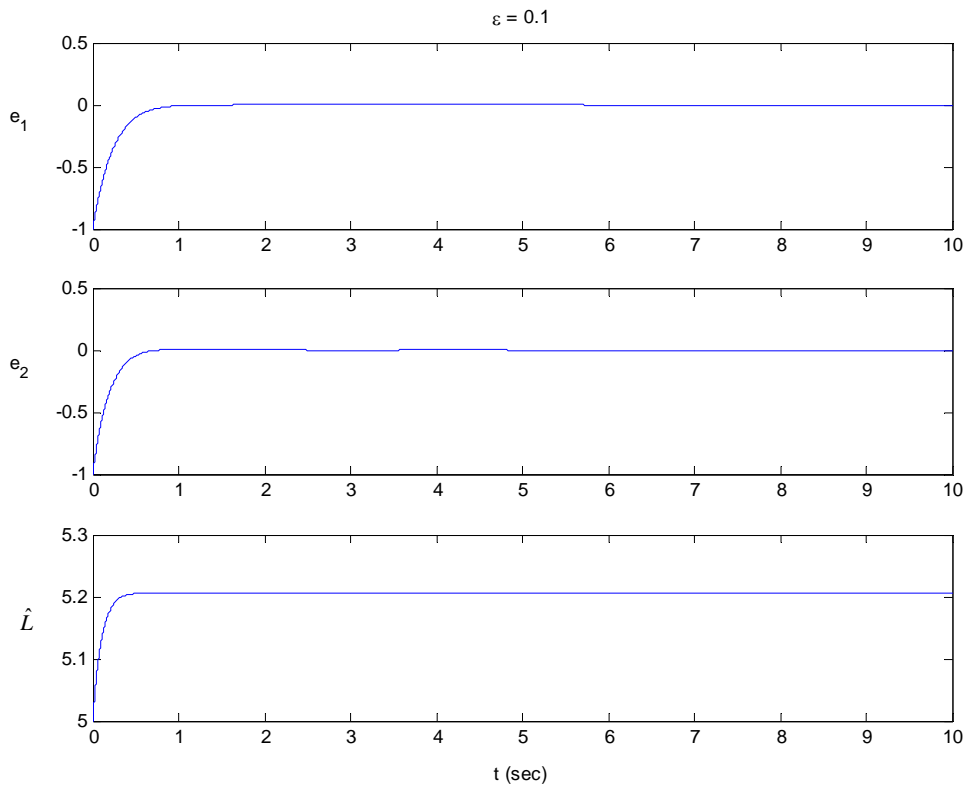


Fig. 4.11 State errors and estimated Lipschitz constant versus time for $\hat{L}_0 = 5$ and $\varepsilon = 0.1$ of mutual coupled Duffing systems.

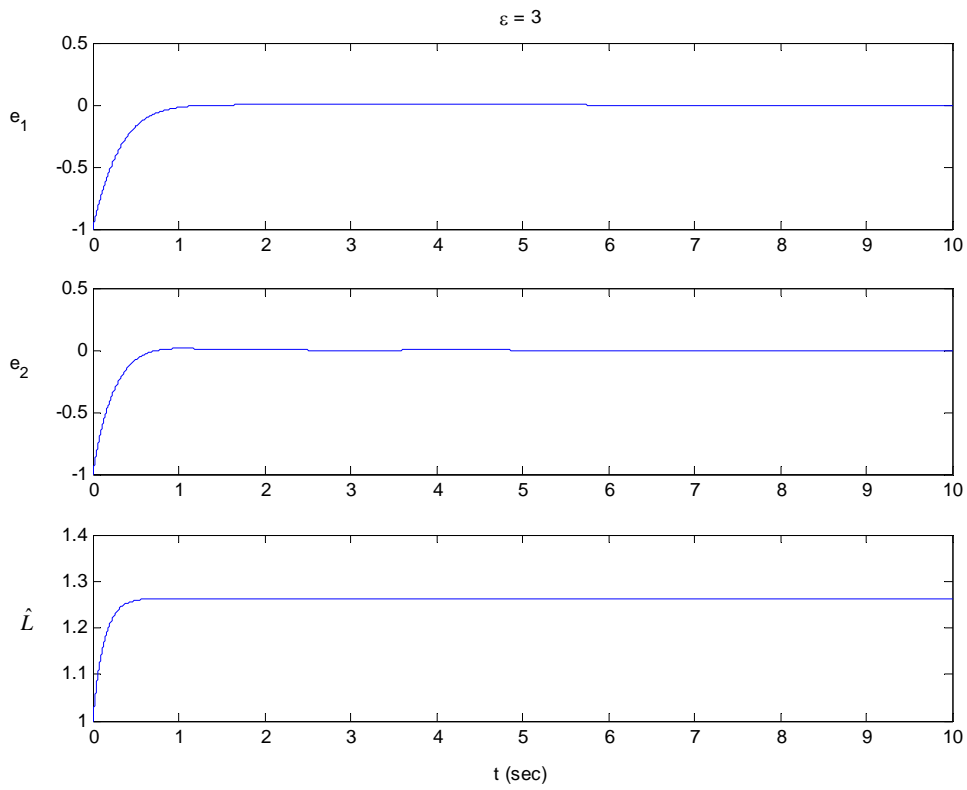


Fig. 4.12 State errors and estimated Lipschitz constant versus time for $\hat{L}_0 = 1$ and $\varepsilon = 3$ of mutual coupled Duffing systems.

Chapter 5

Generalized Synchronization of Coupled Chaotic Systems

5.1 Introduction

In the foregoing three chapters, the synchronization discussed indicates the identical synchronization (or complete synchronization). Besides the identical synchronization, there are many other types of synchronization, such as phase synchronization, lag synchronization, anticipated synchronization and generalized synchronization. In this chapter, the effort will be concentrated on generalized synchronization which means that there is a functional relation between the states of driving and response systems as time goes to infinity.

Similar as the contents in the chapter 2 to chapter 4, a scheme to achieve chaos generalized synchronization via partial stability will be proposed in this chapter. One theorem is proven to ensure the occurrence of generalized synchronization for a general kind of unidirectional coupled nonautonomous systems by linear feedback. The result works for both regular and chaotic systems. Finally, two numerical examples are simulated to illustrate the theoretical analysis.

5.2 Theoretical Analysis

Consider the following unidirectional coupled nonautonomous systems

$$\begin{aligned}\dot{\mathbf{x}} &= \mathbf{f}(t, \mathbf{x}), \\ \dot{\hat{\mathbf{z}}} &= \mathbf{g}(t, \hat{\mathbf{z}}) + \mathbf{u}(t, \hat{\mathbf{z}}, \mathbf{x}),\end{aligned}\tag{5.1}$$

where $\mathbf{x}, \hat{\mathbf{z}} \in \mathbb{R}^n$. The vector value functions $\mathbf{f}, \mathbf{g}: \Omega_1 \subset \mathbb{R} \times \mathbb{R}^n \rightarrow \mathbb{R}^n$, $\mathbf{u}: \Omega_2 \subset \mathbb{R} \times \mathbb{R}^{2n} \rightarrow \mathbb{R}^n$ satisfy Lipschitz condition. Ω_1 and Ω_2 are domains containing the origin. Assume that the solutions of Eq. (5.1) have *a priori* bounds then they must exist for infinite time. That is, for given $(t_0, \mathbf{x}_0, \hat{\mathbf{z}}_0) \in \Omega_1 \cap \Omega_2$ the solution $\left[\mathbf{x}^T(t; t_0, \mathbf{x}_0, \hat{\mathbf{z}}_0) \quad \hat{\mathbf{z}}^T(t; t_0, \mathbf{x}_0, \hat{\mathbf{z}}_0) \right]^T$ of Eq. (5.1) exists for $t \geq t_0$. At the first, we recall the definition of generalized synchronization.

Definition 5.1 *The system (5.1) is generalized synchronized if there is a continuous*

function $H : \mathbb{R}^n \rightarrow \mathbb{R}^n$ s.t. $\lim_{t \rightarrow \infty} \|H[\mathbf{x}(t; t_0, \mathbf{x}_0, \hat{\mathbf{z}}_0)] - \hat{\mathbf{z}}(t; t_0, \mathbf{x}_0, \hat{\mathbf{z}}_0)\| = 0$ with $(t_0, \mathbf{x}_0, \hat{\mathbf{z}}_0) \in \Omega_1 \cap \Omega_2$.

In Eq. (5.1) \mathbf{u} is the coupling function or the controlling term. In order to investigate the transversal stability of synchronization manifold, define $\mathbf{z} = H(\mathbf{x})$ and $\mathbf{e} = \hat{\mathbf{z}} - \mathbf{z}$ to be the state error. Herein, the function $H \in C^1$ is differentiable and can be arbitrary assigned to increase the complication of synchronization. Then the error equations can be written as

$$\dot{\mathbf{e}} = \dot{\hat{\mathbf{z}}} - \dot{\mathbf{z}} = \mathbf{g}(t, \hat{\mathbf{z}}) + \mathbf{u}(t, \hat{\mathbf{z}}, \mathbf{x}) - \dot{H}(\mathbf{x}),$$

where

$$\dot{H}(\mathbf{x}) = \frac{\partial H}{\partial \mathbf{x}} \dot{\mathbf{x}} = \frac{\partial H}{\partial \mathbf{x}} \mathbf{f}(t, \mathbf{x}).$$

So we have

$$\dot{\mathbf{e}} = \mathbf{g}(t, \hat{\mathbf{z}}) - \frac{\partial H}{\partial \mathbf{x}} \mathbf{f}(t, \mathbf{x}) + \mathbf{u}(t, \hat{\mathbf{z}}, \mathbf{x}). \quad (5.2)$$

Notice that since the right hand side of Eq. (5.2) is not only a function of t and error \mathbf{e} but also a function of \mathbf{x} . As a result, the traditional Lyapunov direct method can not be used. On the other hand, the variational equation or Lyapunov exponents may be used to clarify transversal stability. As mentioned before, there is a drawback that we can only calculate finite evolution time in computer simulation but infinite evolution time is needed by definition of Lyapunov exponent.

Herein, we add the upper half (lower half also works) of Eq. (5.1) with $\hat{\mathbf{z}}$ replaced by $\hat{\mathbf{z}} = \mathbf{e} + \mathbf{z}$ to Eq. (5.2), then an extended equation is obtained as following

$$\begin{aligned} \dot{\mathbf{x}} &= \mathbf{f}(t, \mathbf{x}), \\ \dot{\mathbf{e}} &= \mathbf{g}(t, \mathbf{e} + \mathbf{z}) - \frac{\partial H}{\partial \mathbf{x}} \mathbf{f}(t, \mathbf{x}) + \mathbf{u}(t, \mathbf{e} + \mathbf{z}, \mathbf{x}). \end{aligned} \quad (5.3)$$

If the partial variables \mathbf{e} in Eq. (5.3) are asymptotically stable about $\mathbf{e} = \mathbf{0}$, the synchronization manifold is stable in transversal directions. This can be done via stability with respect to partial variables.

In the following, we choose $\mathbf{u}(t, \hat{\mathbf{z}}, \mathbf{z}) = \Gamma(\mathbf{z} - \hat{\mathbf{z}})$ and $\mathbf{g}(t, \mathbf{z}) = \frac{\partial H}{\partial \mathbf{x}} \mathbf{f}(t, \mathbf{x})$, where $\Gamma \in M_{n \times n}$ is a constant matrix whose entries represent the coupling strength of the linear feedback term $(\mathbf{z} - \hat{\mathbf{z}})$. Then the Eq. (5.3) becomes

$$\begin{aligned}\dot{\mathbf{x}} &= \mathbf{f}(t, \mathbf{x}), \\ \dot{\mathbf{e}} &= \mathbf{g}(t, \mathbf{e} + \mathbf{z}) - \mathbf{g}(t, \mathbf{z}) - \Gamma \mathbf{e}.\end{aligned}\tag{5.4}$$

where $\mathbf{0}$ is still an equilibrium point of the second equation of Eqs. (5.4) as synchronization occurs.

Theorem 5.1 *The partial state \mathbf{e} asymptotically approaches to $\mathbf{0}$ in Eq. (5.4) if $L\mathbf{I}_n - \Gamma$ is negative definite, i.e. the system in Eq. (5.1) is in generalized synchronization if $L\mathbf{I}_n - \Gamma$ is negative definite.*

Proof Choose a function $V(\mathbf{x}, \mathbf{e}) = \frac{1}{2} \mathbf{e}^T \mathbf{e}$ that is positive definite with respect to \mathbf{e} and with infinitesimal upper bound. Then its time derivative along the solution of Eq. (5.3) is

$$\begin{aligned}\dot{V} &= \mathbf{e}^T [\mathbf{g}(t, \mathbf{e} + \mathbf{z}) - \mathbf{g}(t, \mathbf{z}) - \Gamma \mathbf{e}] \\ &\leq \mathbf{e}^T [L\mathbf{I}_n - \Gamma] \mathbf{e}.\end{aligned}$$

If $L\mathbf{I}_n - \Gamma$ is negative definite, \dot{V} is negative definite. Then the partial state \mathbf{e} uniformly asymptotically approaches to $\mathbf{0}$ in Eq. (5.4) by partial stability theory. Hence the system in Eq. (5.1) is in generalized synchronization if $L\mathbf{I}_n - \Gamma$ is negative definite.

Remark 5.1 $L\mathbf{I}_n - \Gamma$ is negative definite if and only if all its eigenvalues are negative. For the case $\Gamma = \text{diag}(\gamma_1, \gamma_2, \dots, \gamma_n)$ with $\gamma_i > 0$, $i = 1, \dots, n$, synchronization occurs if $\gamma_{\min} > L$, where $\gamma_{\min} \leq \gamma_i, i = 1, \dots, n$. This is because the time derivative of $V(\mathbf{x}_1, \mathbf{e})$ can be written as $\dot{V}(\mathbf{x}_1, \mathbf{e}) \leq (L - \gamma_{\min}) \|\mathbf{e}\|^2$. The criterion is global if \mathbf{f} is globally Lipschitz.

5.3 Numerical Illustrated Examples

Example 5.1 Autonomous case: Lorenz systems

$$\begin{aligned}\dot{x}_1 &= -\sigma(x_1 - x_2) \triangleq f_1(\mathbf{x}), \\ \dot{x}_2 &= rx_1 - x_2 - x_1x_3 \triangleq f_2(\mathbf{x}), \\ \dot{x}_3 &= x_1x_2 - bx_3 \triangleq f_3(\mathbf{x}),\end{aligned}$$

where $\sigma = 10, r = 28, b = 8/3, \mathbf{x} = [x_1 \ x_2 \ x_3]^T$. To apply the theorem given in this chapter, one needs to estimate the Lipschitz constant at the beginning. By

Cauchy-Schwarz inequality, it can be derived for any $\mathbf{x}_2 = [x_{21} \ x_{22} \ x_{23}]^T$, $\mathbf{x}_1 = [x_{11} \ x_{12} \ x_{13}]^T$, we have

$$\begin{aligned} |f_1(\mathbf{x}_2) - f_1(\mathbf{x}_1)| &\leq \|[-\sigma \ \sigma \ 0]\| \|\mathbf{x}_2 - \mathbf{x}_1\|, \\ |f_2(\mathbf{x}_2) - f_2(\mathbf{x}_1)| &\leq \|[r + B_3 \ -1 \ B_1]\| \|\mathbf{x}_2 - \mathbf{x}_1\|, \\ |f_3(\mathbf{x}_2) - f_3(\mathbf{x}_1)| &\leq \|[B_2 \ B_1 \ -b]\| \|\mathbf{x}_2 - \mathbf{x}_1\|, \end{aligned}$$

where $|x_{ij}(t)| \leq B_j$, $\forall t > t_0$, $i = 1, 2$, $j = 1, 2, 3$. Hence, a Lipschitz constant can be obtained as

$$L = \sqrt{\|[-\sigma \ \sigma \ 0]\|^2 + \|[r + B_3 \ -1 \ B_1]\|^2 + \|[B_2 \ B_1 \ -b]\|^2}.$$

From numerical simulation, $B_1 = 20$, $B_2 = 28$, $B_3 = 49$, then $L = 87.87$. If we choose $\mathbf{z} = \Phi(\mathbf{x}) = \mathbf{A}\mathbf{x} + \mathbf{b}$ to be an affine mapping, then the response system becomes

$$\dot{\hat{\mathbf{z}}} = \mathbf{A} \mathbf{f}(\Phi^{-1}(\hat{\mathbf{z}})) - \Gamma(\hat{\mathbf{z}} - \Phi(\mathbf{x})),$$

where $\Gamma = \text{diag}\{\gamma, \dots, \gamma\}$ and $\hat{\mathbf{z}} = [\hat{z}_1 \ \hat{z}_2 \ \hat{z}_3]^T$. $L\mathbf{I}_n - \Gamma$ is negative definite if $\gamma = 88$. First, select Φ be a reflection, that is $\mathbf{A} = -\mathbf{I}$ and $\mathbf{b} = \mathbf{0}$. With the initial value $[\mathbf{x}_0^T \ \hat{\mathbf{z}}_0^T]^T = [10 \ 10 \ 10 \ 0.5 \ 0.5 \ 0.5]^T$, the simulated results are shown in Fig.5.1-5.4. As expectation, the projections of synchronized manifold in Fig.5.2 are diagonal-like and reflected to vertical axis. Compare Fig.5.4 with Fig.5.3, the phase portrait of response system in Fig.5.4 is reflected to the phase portrait of driving system in Fig.5.3. This case is also called anti-synchronization of chaos. With the same initial condition, let

$$\mathbf{A} = \begin{bmatrix} 1 & -1 & 0 \\ 0.1 & 2 & 1 \\ 0.3 & 1 & 2 \end{bmatrix} \text{ and } \mathbf{b} = \begin{bmatrix} 0 \\ 0 \\ -50 \end{bmatrix},$$

the simulated results are shown in Fig. 5.5 and Fig. 5.7, respectively. The projections of synchronized manifold are no longer diagonal-like but more complicated.

Example 5.2 Nonautonomous case: An extended equation of the coupled Duffing systems is written as

$$\begin{aligned} \dot{x}_1 &= x_2 \triangleq f_1(\mathbf{x}), \\ \dot{x}_2 &= x_1 - x_1^3 - \delta x_2 + \alpha \cos \omega t \triangleq f_2(\mathbf{x}), \\ \dot{\hat{\mathbf{z}}} &= \mathbf{A} \mathbf{f}(\Phi^{-1}(\hat{\mathbf{z}})) - \Gamma(\hat{\mathbf{z}} - \Phi(\mathbf{x})), \end{aligned}$$

where $\omega = 1$, $\delta = 0.25$, $\alpha = 0.4$, $\mathbf{x} = [x_1 \ x_2]^T$, $\hat{\mathbf{z}} = [\hat{z}_1 \ \hat{z}_2]^T$, $\Gamma = \text{diag}\{\gamma, \dots, \gamma\}$ and

$\mathbf{z} = \Phi(\mathbf{x}) = \mathbf{A}\mathbf{x} + \mathbf{b}$. By Cauchy-Schwarz inequality, it can be derived for any

$$\mathbf{x}_2 = [x_{21} \ x_{22}]^T, \mathbf{x}_1 = [x_{11} \ x_{12}]^T$$

$$|f_1(\mathbf{x}_2) - f_1(\mathbf{x}_1)| \leq \|\mathbf{x}_2 - \mathbf{x}_1\|,$$

$$|f_2(\mathbf{x}_2) - f_2(\mathbf{x}_1)| \leq \left\| \begin{bmatrix} 1+3B_1^2 & -\delta \end{bmatrix} \right\| \|\mathbf{x}_2 - \mathbf{x}_1\|,$$

where $|x_{ij}(t)| \leq B_1, |y_{ij}(t)| \leq B_2, \forall t > t_0, i=1, 2, j=1, 2$. Hence, a Lipschitz constant can be obtained as

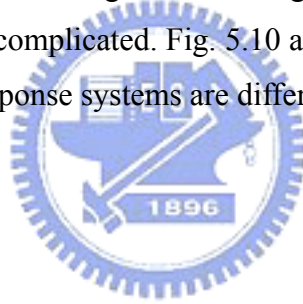
$$L = \sqrt{1 + \left\| \begin{bmatrix} 1+3B_1^2 & -\delta \end{bmatrix} \right\|^2} .$$

From numerical simulation, $B_1 = 1.5, B_2 = 0.9$, then $L = 7.82$. Choose

$$\mathbf{A} = \begin{bmatrix} 1 & 0.5 \\ 1.8 & 1 \end{bmatrix}, \mathbf{b} = \begin{bmatrix} 5 \\ 5 \end{bmatrix},$$

and the initial value $[\mathbf{x}_0^T \ \hat{\mathbf{z}}_0^T]^T = [1 \ 1 \ 0.1 \ 0.1]^T$. $L\mathbf{I}_n - \Gamma$ is negative definite if $\gamma = 8$.

The simulated results are shown in Fig. 5.8-5.11. Fig. 5.9 shows that the projections of synchronized manifold are complicated. Fig. 5.10 and Fig. 5.11 show that the phase portraits of the driving and response systems are different.



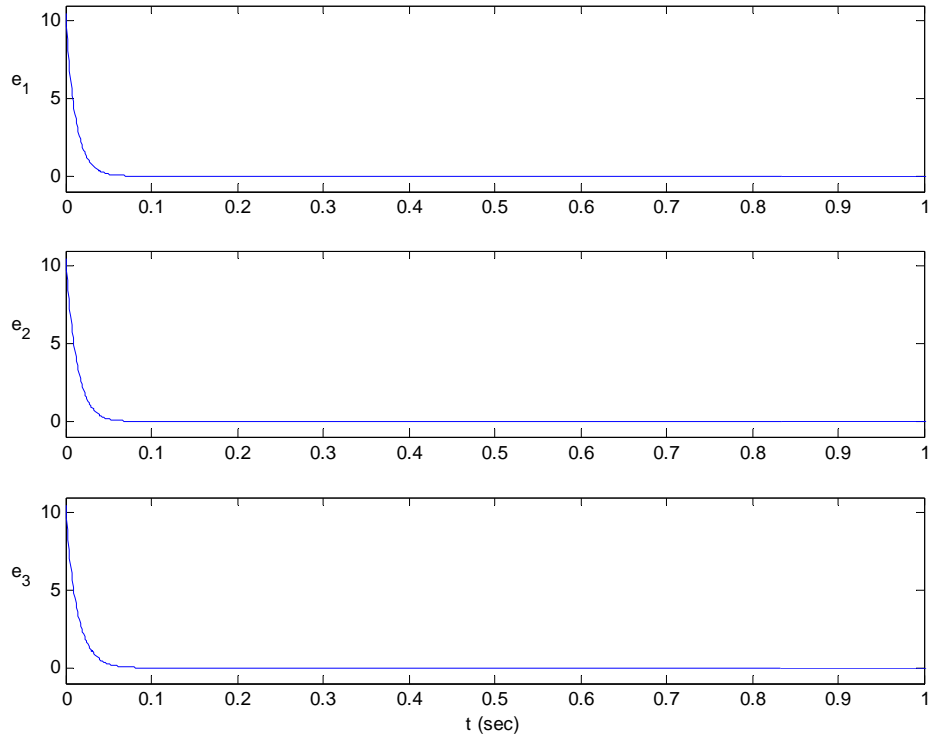


Fig. 5.1 e_1, e_2 and e_3 versus time.



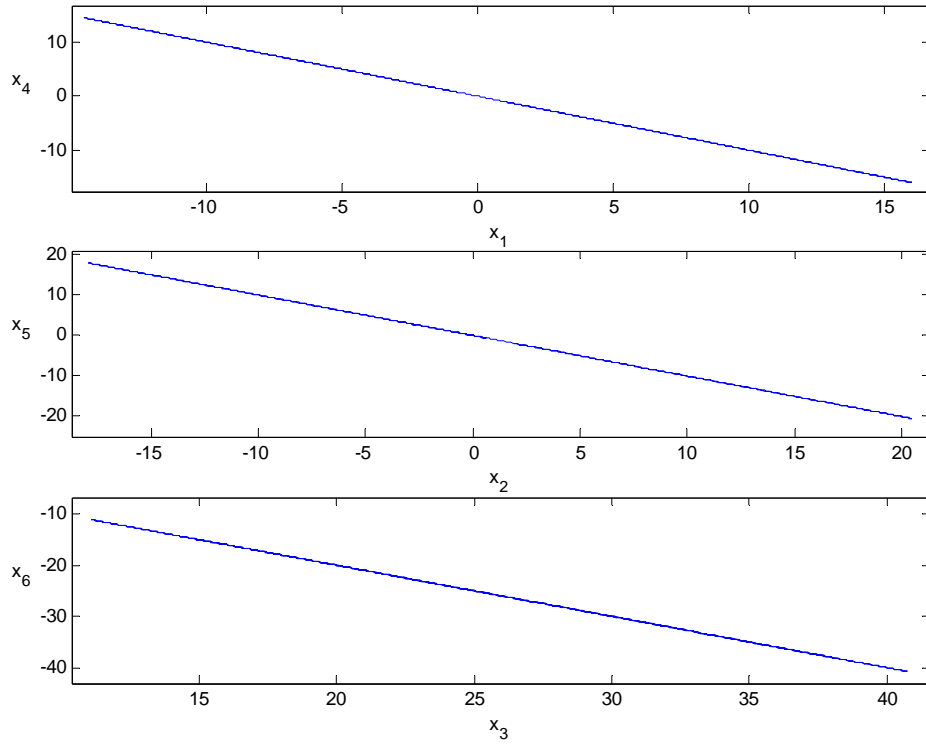


Fig. 5.2 Projections of synchronized manifold.

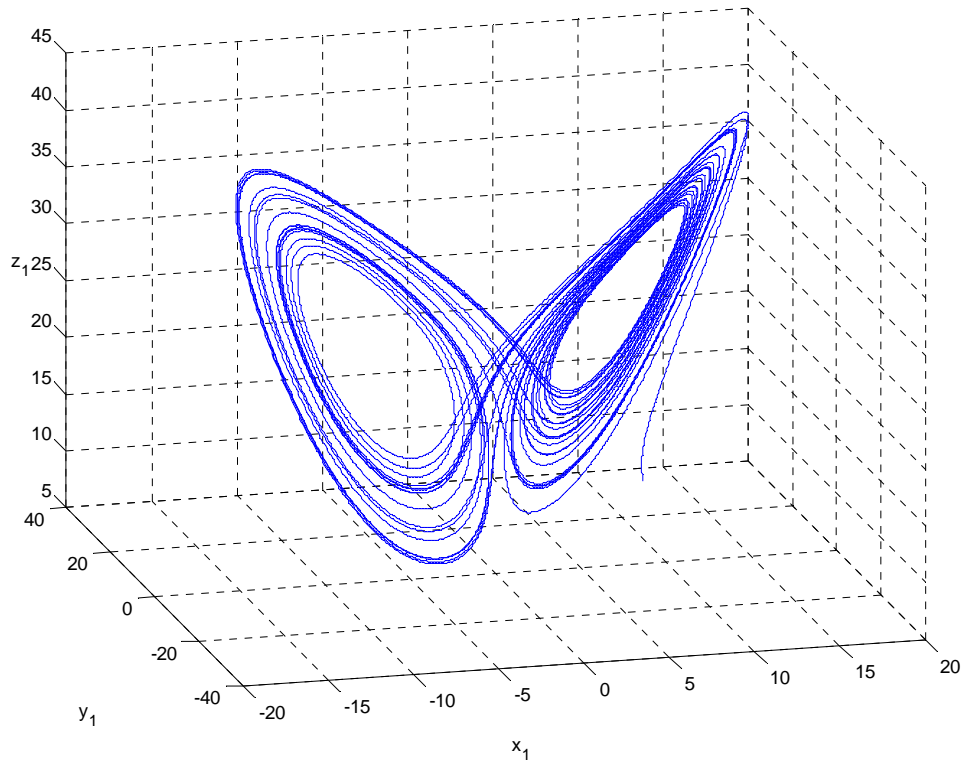


Fig. 5.3 Phase portrait of the driving system.

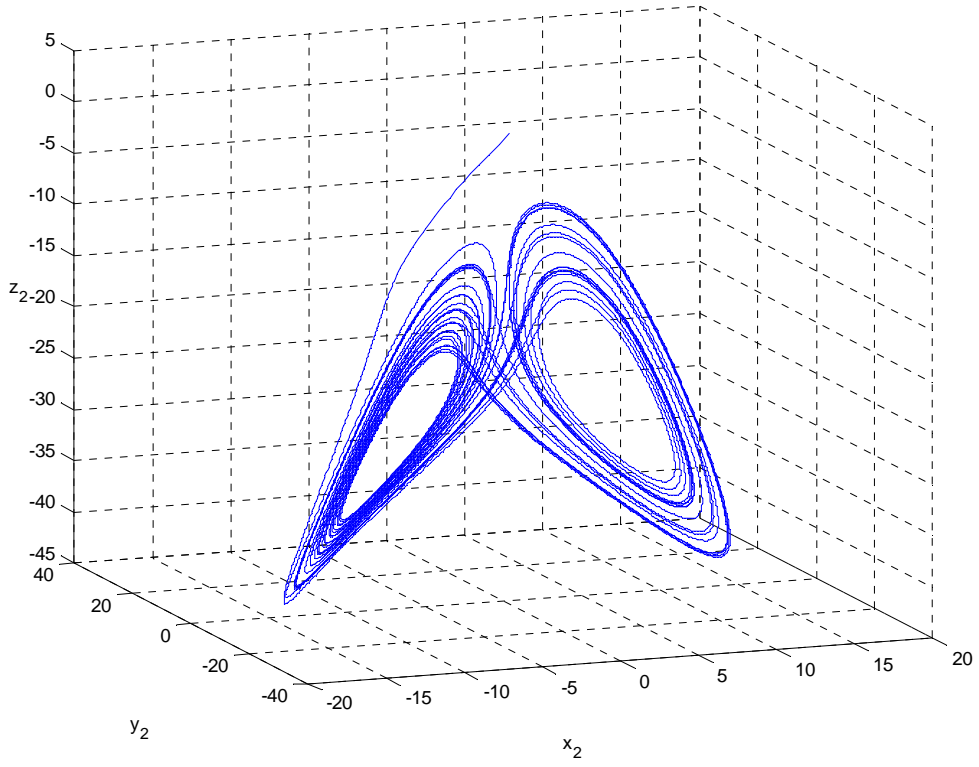


Fig. 5.4 Phase portrait of the response system.

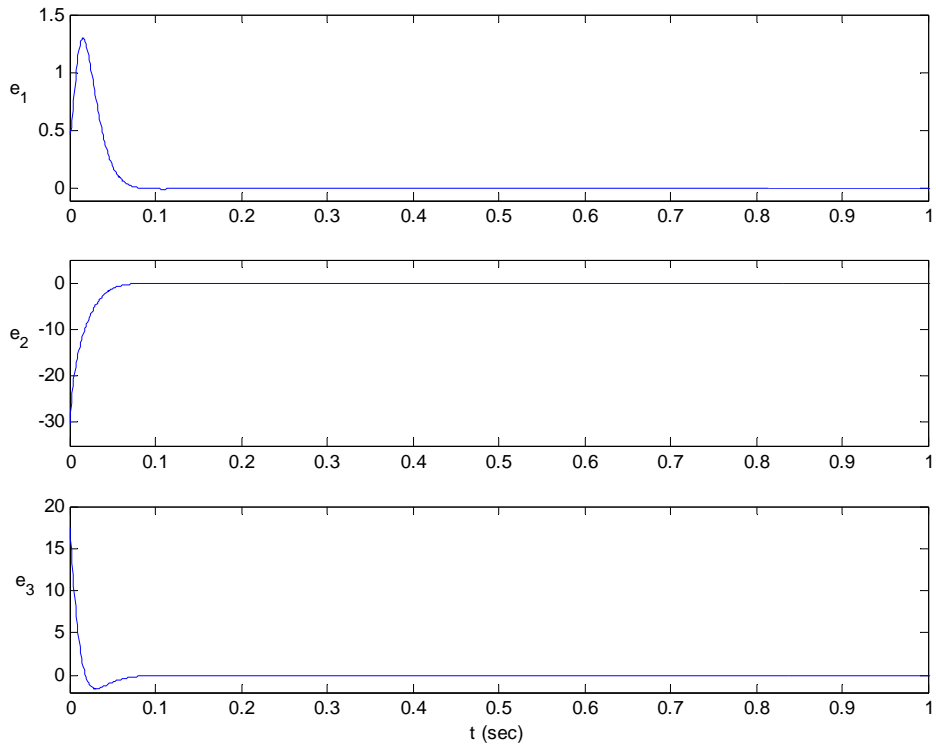


Fig. 5.5 e_1, e_2 and e_3 versus time.

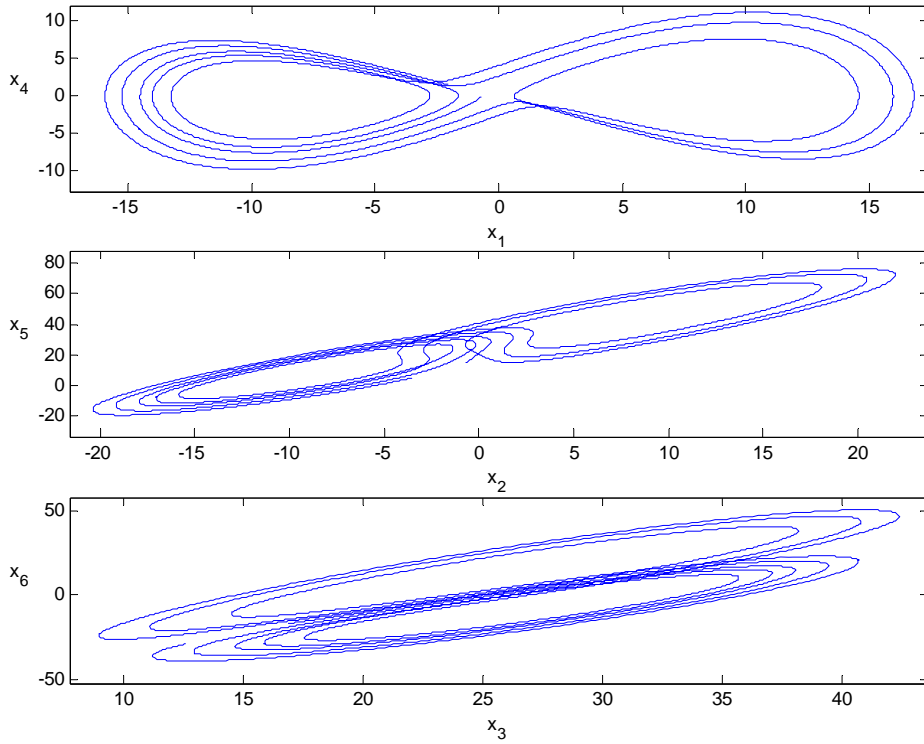


Fig. 5.6 Projections of synchronized manifold.



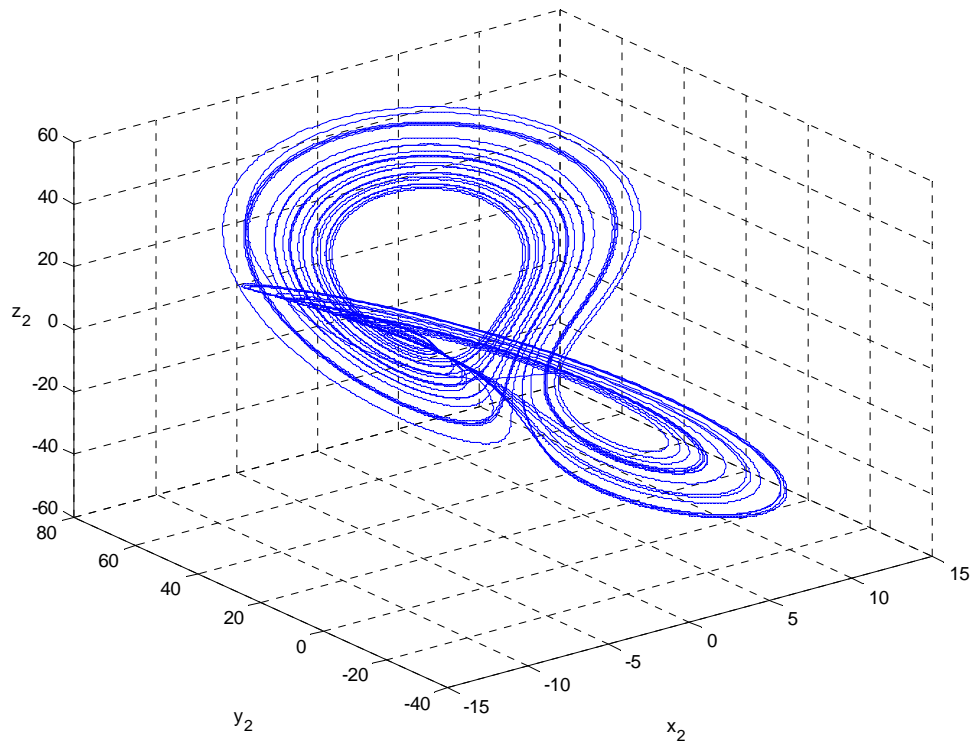


Fig. 5.7 Phase portrait of the response system.

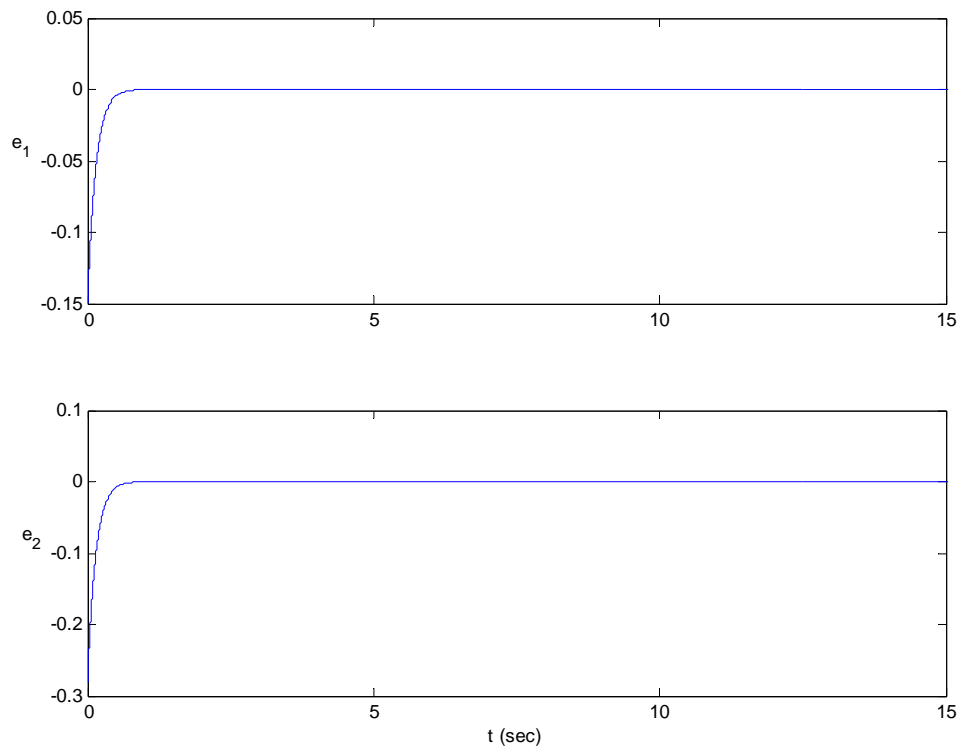


Fig. 5.8 e_1 and e_2 versus time.

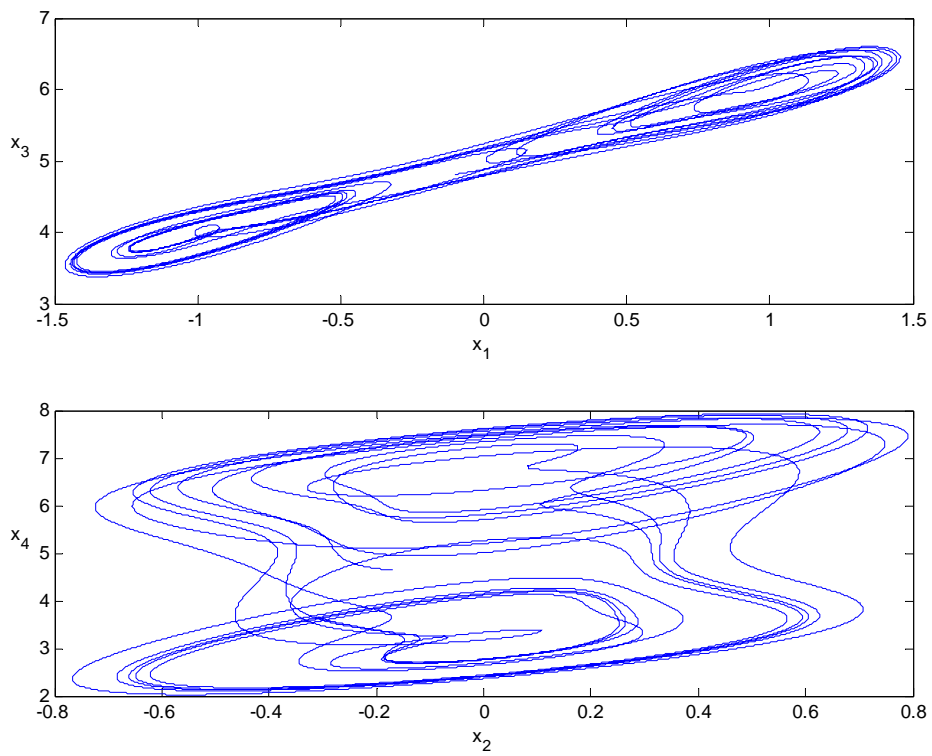


Fig. 5.9 Projections of synchronized manifold.

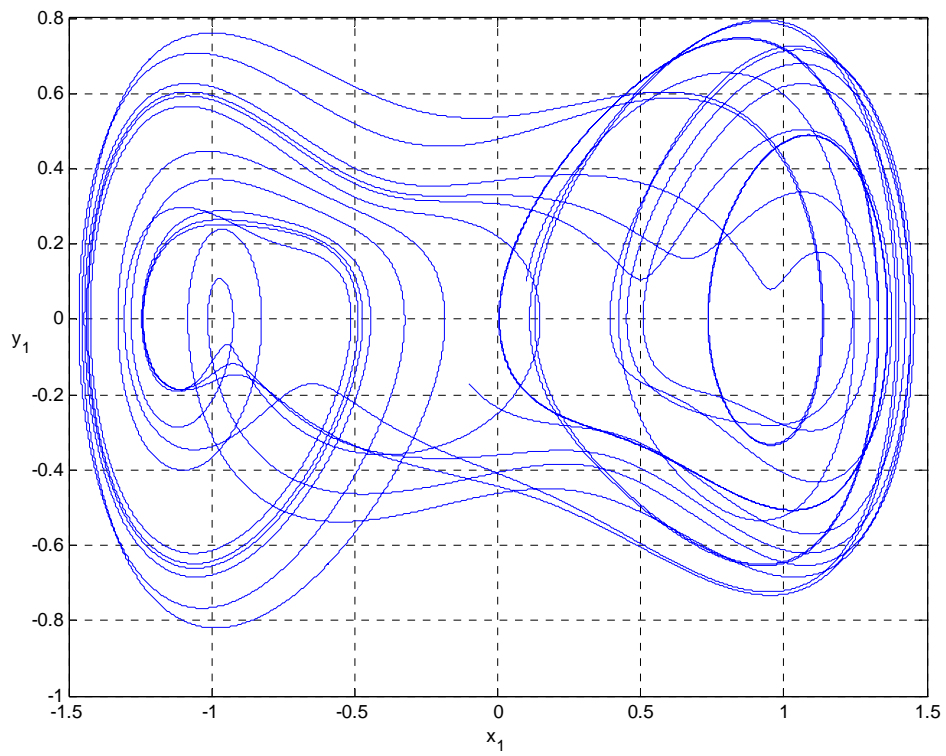


Fig. 5.10 Phase portrait of the driving system.

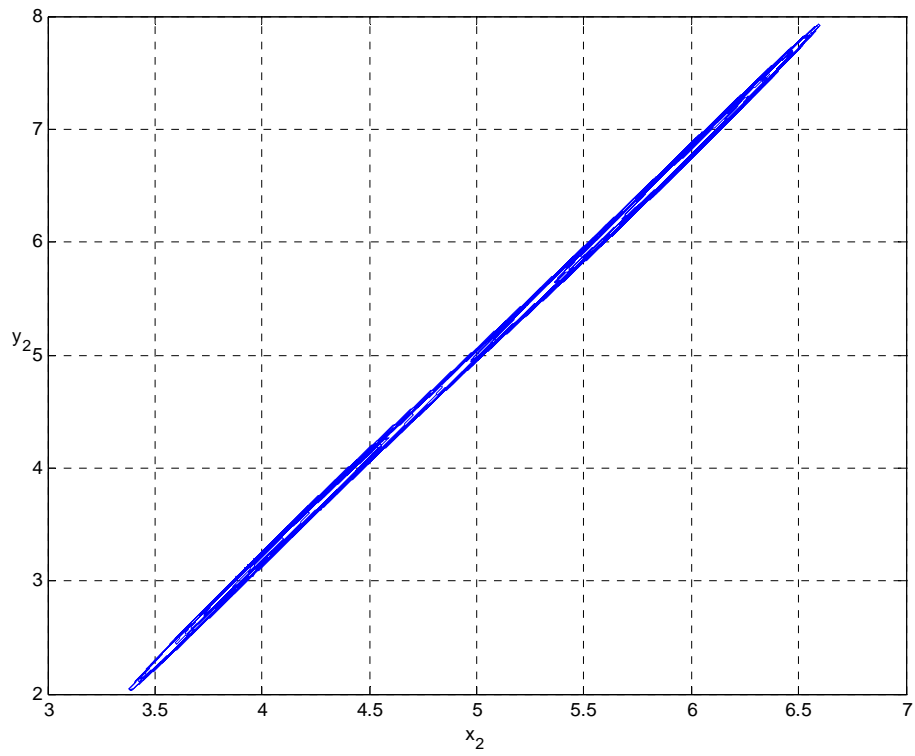


Fig. 5.11 Phase portrait of the response system.

Chapter 6

Conclusions

Chaos synchronization is an important research topic in these years. There are several methods to guarantee the emergence of chaos synchronization but there is no easy unified criterion in general. Most of them are suitable for a specific kind of system or even for a special system. Herein, a general scheme for both unidirectional and mutual coupled systems is proposed to achieve chaos synchronization via partial stability theory. It can overcome two drawbacks. First, it is difficult to use the traditional Lyapunov method since the state error equation is not a pure function of state error in general. Second, zero crossing of Lyapunov exponent whose definition needs infinite evolution time is used as a criterion of chaos synchronization widely but we can only calculate finite evolution time in computer simulation. The benefit of this scheme is that the usage of the partial stability theory is similar to the traditional Lyapunov method. Superficially, the order of the error dynamic equation is enlarged since it is replaced by an extended equation in this scheme. But only partial variables are manipulated in actual. Furthermore, many control techniques can be applied to synchronize coupled systems in this scheme.

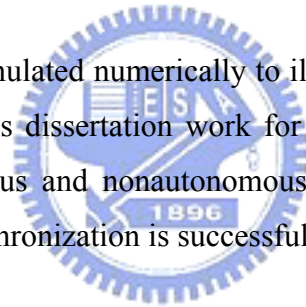
Follows the procedure of the proposed scheme, the unidirectional coupled systems are discussed first and three sufficient criteria are derived. One of them is suitable for systems without perturbation and the other two are suitable for systems under two kinds of perturbations, vanishing and nonvanishing, respectively. Second, the effort is concentrated on synchronization of mutual coupled systems. Similar to the unidirectional case, three theorems are proven to ensure the occurrence of synchronization. One of them is suitable for systems without perturbation and the other two are suitable for systems under two kinds of perturbations, vanishing and nonvanishing, respectively.

In previous six criteria, to guarantee the emergence of synchronization a matrix equation should be satisfied and the estimation of Lipschitz constant is needed. Moreover, the estimate of Lipschitz constant is often conservative. To overcome these two shortcomings, this matrix equation and the estimation of Lipschitz constant are replaced by adopting an adaptive coupling gain and an adaptive estimator,

respectively. As a result, a simple and convenient adaptive synchronization of chaotic systems is realized for both unidirectional and mutual coupled systems. It is easier and more convenient to use this method for synchronization of both unidirectional and mutual coupled systems than the six theorems in chapter 2 and 3. Furthermore, to increase the convergent rate of state error dynamics we only need to set a larger initial condition of the adaptive equation.

The synchronization discussed indicates the identical synchronization (or complete synchronization) in the foregoing results. Another kind of synchronization called generalized synchronization which means that there is a functional relation between the states of driving and response systems as time goes to infinity are studied in the chapter 5. This function can increase the complication of synchronization. Similar to the chapter 2, a scheme to achieve chaos generalized synchronization via partial stability is proposed. One theorem is proven to ensure generalized synchronization for a general kind of unidirectional coupled nonautonomous systems by linear feedback.

Several examples are simulated numerically to illustrate the theoretical analyses. All the criteria derived in this dissertation work for regular and chaotic, linear and nonlinear systems, autonomous and nonautonomous systems. Hence, the proposed scheme to achieve chaos synchronization is successful.



Appendix

The content of this appendix follows [78-80]. Consider a differential system

$$\dot{\mathbf{x}} = \mathbf{f}(t, \mathbf{x}), \quad (\text{A1})$$

where $\mathbf{f} : [t_0, \infty) \times \Omega \rightarrow \mathbb{R}^n$, $\mathbf{f}(t, \mathbf{0}) = \mathbf{0} \quad \forall t \in I \triangleq [t_0, \infty)$ and $\Omega \subset \mathbb{R}^n$ is a region containing the origin. Assume that \mathbf{f} is smooth enough to ensure that the solution of (A1) exists uniquely. To shorten the notation, write $\mathbf{x} = (y_1, \dots, y_m, z_1, \dots, z_{n-m})^T$,

$$\|\mathbf{y}\| = \left(\sum_{i=1}^m y_i^2 \right)^{1/2}, \quad \|\mathbf{z}\| = \left(\sum_{i=1}^{n-m} z_i^2 \right)^{1/2} \quad \text{and} \quad \|\mathbf{x}\| = \left(\sum_{i=1}^n x_i^2 \right)^{1/2} = (\|\mathbf{y}\| + \|\mathbf{z}\|)^{1/2} \quad \text{with} \quad 0 < m \leq n.$$

We assume that the solution of (A1) is \mathbf{z} -extendable, i.e. any solution of (A1) exists for all $t \geq t_0$ and $\|\mathbf{y}(t)\| \leq H$, H is a constant. Write $Q = \{(t, \mathbf{x}) \mid t \geq t_0, \|\mathbf{y}\| \leq H, 0 \leq \|\mathbf{z}\| < +\infty\}$ and $\tilde{Q} = \{(t, \mathbf{x}) \mid t \geq t_0, \|\mathbf{x}\| < \infty\}$.

Definition A1 *The solution of (A1) is stable with respect to \mathbf{y} (\mathbf{y} -stable) if $\forall \varepsilon > 0$, $\forall t_0 \in [0, \infty)$, $\exists \delta(t_0, \varepsilon) > 0$, $\forall \mathbf{x}_0 \in B_\delta := \{\mathbf{x} \mid \|\mathbf{x}\| < \delta(t_0, \varepsilon)\}$ such that $\|\mathbf{y}(t, t_0, \mathbf{x}_0)\| < \varepsilon \quad \forall t \geq t_0$. The solution of (A1) is uniformly \mathbf{y} -stable if $\delta(t_0, \varepsilon)$ is independent of t_0 in the definition of \mathbf{y} -stable.*

The solution of (A1) is asymptotically stable with respect to \mathbf{y} (asymptotically \mathbf{y} -stable) if it is (1) \mathbf{y} -stable and (2) \mathbf{y} -attractive, i.e. $\forall t_0 \in [0, \infty)$, $\exists \delta'(t_0) > 0$, $\forall \varepsilon' > 0$, $\forall \mathbf{x}_0 \in B_{\delta'} := \{\mathbf{z} \mid \|\mathbf{z}\| < \delta'(t_0)\}$, $\exists T(t_0, \mathbf{x}_0, \varepsilon')$ such that $\|\mathbf{y}(t, t_0, \mathbf{x}_0)\| < \varepsilon' \quad \forall t \geq t_0 + T$. The solution of (A1) is uniformly asymptotically \mathbf{y} -stable if it is (1) uniformly \mathbf{y} -stable and (2) uniformly \mathbf{y} -attractive, i.e. $\delta'(t_0, \varepsilon')$ is independent of t_0 and $T(t_0, \mathbf{x}_0, \varepsilon')$ is independent of t_0, \mathbf{x}_0 in the definition of \mathbf{y} -attractive.

The solution of (A1) is globally \mathbf{y} -attractive if $B_\delta = \mathbb{R}^n$ in the definition of \mathbf{y} -attractive. Furthermore, if $B_\delta = \mathbb{R}^n$ and $\exists \delta'(t_0) > 0$ can be replaced by $\forall \delta$ the solution of (A1) is globally uniformly \mathbf{y} -attractive. The solution of (A1) is globally asymptotically \mathbf{y} -stable if it is (1) \mathbf{y} -stable and (2) globally \mathbf{y} -attractive. The solution

of (A1) is globally uniformly asymptotically \mathbf{y} - stable if it is (1) uniformly \mathbf{y} -stable and (2) globally uniformly \mathbf{y} -attractive.

The next definition extended the notation of definite functions to partial variables. Let $V(t, \mathbf{x}) \in C([t_0, \infty) \times \mathbb{R}^n, \mathbb{R})$ with $V(t, \mathbf{0}) = \mathbf{0}$ and V is in the domain Q .

Definition A2 A t implicit positive (negative) semi-definite function $V(\mathbf{x})$ is called positive (negative) definite with respect to \mathbf{y} if $V(\mathbf{x})$ can vanish only when $\mathbf{y} = \mathbf{0}$.

A positive (negative) semi-definite function $V(t, \mathbf{x})$ is called positive (negative) definite with respect to \mathbf{y} if there is a positive (negative) definite function $W(\mathbf{y})$ such that $V(t, \mathbf{x}) \geq W(\mathbf{y})$ ($V(t, \mathbf{x}) \leq W(\mathbf{y})$).

Definition A3 A function $V(t, \mathbf{x})$ is called bounded if $\exists M > 0$ such that $|V(t, \mathbf{x})| \leq M$. A bounded function $V(t, \mathbf{x})$ possesses an infinitesimal upper bound if $\forall \tilde{\varepsilon} > 0, \exists \tilde{\delta}(\tilde{\varepsilon}) > 0$, for $t \geq t_0$ and $\|\mathbf{x}\| < \tilde{\delta}(\tilde{\varepsilon})$ such that $|V(t, \mathbf{x})| \leq \tilde{\varepsilon}$. A bounded function $V(t, \mathbf{x})$ possesses an infinitesimal upper bound with respect to x_1, \dots, x_k ($m \leq k \leq n$) if $\forall \tilde{\varepsilon} > 0, \exists \tilde{\delta}(\tilde{\varepsilon}) > 0$, for $t \geq t_0$, $\sum_{i=1}^k x_i^2 < \tilde{\delta}$, $-\infty < x_{k+1}^2 + \dots + x_n^2 < \infty$ such that $|V(t, \mathbf{x})| \leq \tilde{\varepsilon}$.

Theorem A1 Suppose there exists a positive definite function $V(t, \mathbf{x})$ with respect to x_1, \dots, x_k ($k \leq n$) such that $\dot{V}(t, \mathbf{x})$ is positive semi-definite or vanishes, then the undisturbed motion is stable with respect to x_1, \dots, x_k ($k \leq n$).

Theorem A2 Suppose there exists a positive definite function $V(t, \mathbf{x})$ with respect to x_1, \dots, x_k ($k \leq n$) such that $V(t, \mathbf{x})$ possesses an infinitesimal upper bound and $\dot{V}(t, \mathbf{x})$ is positive definite with respect to x_1, \dots, x_k , then the undisturbed motion is asymptotically stable with respect to x_1, \dots, x_k .

Theorem A3 Suppose there exist a function $V : [0, \infty) \times \Omega \times \mathbb{R}^m \rightarrow \mathbb{R}$ such that for some functions $a, b, c \in \mathcal{K}$ and every $(t, \mathbf{x}) \in Q$:

$$(i) \quad a(\|\mathbf{y}\|) \leq V(t, \mathbf{x}), V(t, \mathbf{0}) = \mathbf{0},$$

$$(ii) \quad V(t, \mathbf{x}) \leq b \left(\left(\sum_{i=1}^k x_i^2 \right)^{1/2} \right), m \leq k \leq n,$$

$$(iii) \quad \dot{V}(t, \mathbf{x}) \leq -c \left(\left(\sum_{i=1}^k x_i^2 \right)^{1/2} \right),$$

then the origin is uniformly asymptotically y-stable.

Theorem A4 Suppose there exist a function $V : [0, \infty) \times \Omega \times \mathbb{R}^m \rightarrow \mathbb{R}$ such that for some functions $a, b, c \in \mathcal{K}$, $a : \mathbb{R}^+ \rightarrow \mathbb{R}^+$ with $r \rightarrow +\infty \Rightarrow a(r) \rightarrow +\infty$ and every $(t, \mathbf{x}) \in \tilde{Q}$:

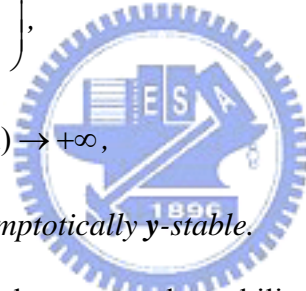
$$(i) \quad a(\|\mathbf{y}\|) \leq V(t, \mathbf{x}), V(t, \mathbf{0}) = \mathbf{0},$$

$$(ii) \quad V(t, \mathbf{x}) \leq b \left(\left(\sum_{i=1}^k x_i^2 \right)^{1/2} \right), m \leq k \leq n,$$

$$(iii) \quad \dot{V}(t, \mathbf{x}) \leq -c \left(\left(\sum_{i=1}^k x_i^2 \right)^{1/2} \right),$$

$$(iv) \quad \sum_{i=1}^n x_i^2 \rightarrow +\infty \Rightarrow V(t, \mathbf{x}) \rightarrow +\infty,$$

then the origin is globally asymptotically y-stable.



If there is perturbation in the system, the stability of motion is different. Consider differential equation of a system under constantly acting perturbation

$$\dot{\mathbf{x}} = \mathbf{f}(t, \mathbf{x}) + \mathbf{R}(t, \mathbf{x}), \quad (A2)$$

where $\mathbf{R}(t, \mathbf{x}) \in [I \times \Omega, \mathbb{R}]$ with $\mathbf{R}(t, \mathbf{0}) \neq \mathbf{0}$ in general. Assume that the solution $\mathbf{x}(t; t_0, \mathbf{x}_0)$ exists for infinitely time.

Definition A4 The motion $\mathbf{x} = \mathbf{0}$ of system (A1) is said to be y-stable under constantly acting perturbation small at each instant, if $\forall \varepsilon > 0$, $t_0 > 0$, $\exists \delta_1(\varepsilon, t_0) > 0$, $\delta_2(\varepsilon, t_0) > 0$ such that whenever $\|\mathbf{x}_0\| < \delta_1(\varepsilon, t_0)$ and $\|\mathbf{R}(t, \mathbf{x})\| < \delta_2(\varepsilon, t_0)$, the partial solution $\mathbf{y}(t; t_0, \mathbf{x}_0)$ satisfy $\|\mathbf{y}(t; t_0, \mathbf{x}_0)\| < \varepsilon$. The motion $\mathbf{x} = \mathbf{0}$ of system (A1) is said to be y-stable under constantly acting perturbation small on the average, if $\forall \varepsilon > 0$, $t_0 > 0$, $\forall T > 0$, $\exists \delta_1(\varepsilon, t_0, T) > 0$, $\delta_2(\varepsilon, t_0, T) > 0$ such that whenever $\|\mathbf{x}_0\| < \delta_1(\varepsilon, t_0, T)$ and

$$\int_t^{t+T} \sup \{ \|\mathbf{R}(\tau, \mathbf{x})\| \} d\tau \leq \delta_2(\varepsilon, t_0, T) \quad \forall t \in I$$

, the partial solution $\mathbf{y}(t; t_0, \mathbf{x}_0)$ satisfy $\|\mathbf{y}(t; t_0, \mathbf{x}_0)\| < \varepsilon$.

If δ_1, δ_2 do not dependent on t_0 , the \mathbf{y} -stable under constantly acting perturbation, small at each instant, are uniform. This is also called *total stability*.

Theorem A5 Suppose there exist a function $V : [0, \infty) \times \Omega \times \mathbb{R}^m \rightarrow \mathbb{R}$ such that for some functions $a, b, c \in \mathcal{K}$ and every $(t, \mathbf{x}) \in \tilde{Q}$:

$$(i) \quad \left\| \frac{\partial V}{\partial \mathbf{x}} \right\| \leq N = \text{constant},$$

$$(ii) \quad a(\|\mathbf{y}\|) \leq V(t, \mathbf{x}) \leq b\left(\left(\sum_{i=1}^k x_i^2\right)^{1/2}\right), m \leq k \leq n,$$

$$(iii) \quad \dot{V}(t, \mathbf{x}) \leq -c\left(\left(\sum_{i=1}^k x_i^2\right)^{1/2}\right),$$

then the solution of system (A2) is \mathbf{y} -stable under constantly acting perturbation small at each instant.

Theorem A6 Suppose there exist a function $V : [0, \infty) \times \Omega \times \mathbb{R}^m \rightarrow \mathbb{R}$ such that for some functions $a, b, c \in \mathcal{K}$ and every $(t, \mathbf{x}) \in \tilde{Q}$:

$$(i) \quad \left\| \frac{\partial V}{\partial \mathbf{x}} \right\| \leq N = \text{constant},$$

$$(ii) \quad a(\|\mathbf{y}\|) \leq V(t, \mathbf{x}) \leq b(\|\mathbf{y}\|),$$

$$(iii) \quad \dot{V}(t, \mathbf{x}) \leq -c(\|\mathbf{y}\|),$$

then the solution of system (A2) is \mathbf{y} -stable under constantly acting perturbation small on the average.

Corollary A1 The functions \mathbf{f} and $D\mathbf{f}(\mathbf{x})$ are continuous and bounded in Q . If the invariant set $\{\mathbf{x} | \mathbf{y} = \mathbf{0}\}$ is uniformly asymptotically stable, then it is uniformly stable under constantly acting perturbation small on the average.

References

- [1]. H. Fujisaka and T. Yamada, “Stability theory of synchronized motion in coupled-oscillator systems”, *Prog. Theor. Phys.* **69**, 32-47 (1983).
- [2]. V. S. Afraimovich, N. N. Verichev and M. I. Robinovich, “Stochastic synchronization of oscillation in dissipative systems”, *Radiophys. Quantum Electron.* **29**, 795 (1986).
- [3]. L. M. Pecora and T. L. Carroll, “Synchronization in chaotic systems”, *Phys. Rev. Lett.* **64**, 821-824 (1990).
- [4]. L. M. Pecora and T. L. Carroll, “Driving systems with chaotic signals”, *Phys. Rev. A* **44**, 2374-2383 (1991).
- [5]. R. He. and P. G. Vaidya, “Analysis and synthesis of synchronous periodic and chaotic systems”, *Phys. Rev. A* **46**, 7387 (1992).
- [6]. L. M. Pecora and T. L. Carroll, “Cascading synchronized chaotic systems”, *Physica D* **67**, 126 (1993).
- [7]. M. Ding and Ott, “Enhancing synchronism of chaotic systems”, *Phys. Rev. E* **49**, 945 (1994).
- [8]. K. Murali and M. Lakshmanan, “Drive-response scenario of chaos synchronization in identical nonlinear systems”, *Phys. Rev. E* **49**, 4882 (1994).
- [9]. C. W. Wu and L. O. Chua, “A unified framework for synchronization and control of dynamical systems”, *Int. J. Bifurcation and Chaos* **4**, 979 (1994).
- [10]. T. L. Carroll and L. M. Pecora, “Synchronizing nonautonomous chaotic circuits”, *IEEE Trans. Circuits Syst. II* **40**, 646 (1993).
- [11]. K. Pyragas, “Weak and strong synchronization of chaos”, *Phys. Rev. E* **54**, 4508 (1996).
- [12]. T. Kapitaniak, M. Sekieta and M. Ogorzolek, “Monotone synchronization of chaos”, *Int. J. Bifurcation and Chaos* **6**, 211 (1996).
- [13]. T. L. Carroll and L. M. Pecora, “Master stability functions for synchronized coupled systems”, *Int. J. Bifurcation and Chaos* **9**, 2315 (1999).
- [14]. G. S. Santoboni, S. R. Bishop and A. Varone, “Transient time in unidirectional synchronization”, *Int. J. Bifurcation and Chaos* **9**, 2345 (1999).
- [15]. L. Kocarev, U. Parlitz and R. Brown, “A unifying definition of synchronization

- for dynamical systems”, Phys. Rev. E **61**, 3716 (2000).
- [16]. T. L. Carroll and L. M. Pecora, “Synchronizing chaotic circuits”, IEEE Trans. CAS. **38**, 453 (1991).
- [17]. G. Millerioux and J. Daafouz, “Global chaos synchronization and robust filtering in noisy content”, IEEE Trans. Circuits Syst.- I **48**, 1170 (2001).
- [18]. K. M. Cuomo and A. V. Oppenheim, “Circuit implementation of synchronized chaos with applications to communications”, Phys. Rev. Lett. **71**, 65 (1993).
- [19]. C. W. Wu and L. O. Chua, “A simple way to synchronize chaotic systems with applications to secure communication systems”, Int. J. Bifurcation and Chaos **3**, 1619 (1993).
- [20]. K. M. Short, “Steps toward unmasking secure communications”, Int. J. Bifurcation and Chaos **4**, 959 (1994).
- [21]. G. Perez and H. A. Cerdeira, “Extracting messages masked by chaos”, Phys. Rev. Lett. **74**, 1970 (1995).
- [22]. K. M. Cuomo, “Synthesizing self-synchronizing chaotic systems”, Int. J. Bifurcation and Chaos **3**, 1327 (1993).
- [23]. K. M. Cuomo, A. V. Oppenheim and S. H. Strogatz, “Synchronization of Lorenz-based chaotic circuits with applications to communications”, IEEE Trans. Circuits Syst. **40**, 626 (1993).
- [24]. J. H. Peng, E. J. Ding, M. Ding and W. Yang, “Synchronizing hyperchaos with a scalar transmitted signal”, Phys. Rev. Lett. **76**, 904 (1996).
- [25]. C. Williams, “Chaotic communications over radio channels”, IEEE Trans. Circuits Syst.- I **48**, 1394 (2001).
- [26]. H. Puebla and J. Alvarez-Ramirez, “Stability of inverse-system approaches in coherent chaotic communications”, IEEE Trans. Circuits Syst.- I **48**, 1413 (2001).
- [27]. N. F. Rulkov *et. al.*, “Digital communication using chaotic-pulse-position modulation”, IEEE Trans. Circuits Syst.- I **48**, 1436 (2001).
- [28]. G. Mazzini, R. Rovatti and G. Setti, “Chaos-based asynchronous Ds-CDMA systems and enhanced rake receivers: measuring the improvements”, IEEE Trans. Circuits Syst.- I **48**, 1445 (2001).
- [29]. M. Delgado-Restituto and A. Rodriguez-Vazquez, “Mixed-signal Map-configurable integrated chaos generator for chaotic communications”, IEEE

- Trans. Circuits Syst.- I **48**, 1462 (2001).
- [30]. J. Liu M. H. F. Chen and S. Tang, “Optical-communication systems based on chaos in semiconductor Lasers”, IEEE Trans. Circuits Syst.- I **48**, 1475 (2001).
- [31]. Y. Liu *et. al.*, “Communication using synchronization of optical-feedback-induced chaos in semiconductor lasers”, IEEE Trans. Circuits Syst.- I **48**, 1484 (2001).
- [32]. J. Garcia-Ojalvo and R. Roy, “Parallel communication with optical spatiotemporal chaos”, IEEE Trans. Circuits Syst.- I **48**, 1491 (2001).
- [33]. F. Dachselt and W. Schwarz, “Chaos and cryptography”, IEEE Trans. Circuits Syst.- I **48**, 1498 (2001).
- [34]. Z. Galias and G. M. Maggio, “Quadrature chaos-shift keying: theory and performance analysis”, IEEE Trans. Circuits Syst.- I **48**, 1510 (2001).
- [35]. T. L. Carroll, “Noise-robust synchronized chaotic communications”, IEEE Trans. Circuits Syst.- I **48**, 1519 (2001).
- [36]. P. Davis, Y. Liu and T. Aida, “Chaotic wavelength-hopping device for multiwavelength optical communications”, IEEE Trans. Circuits Syst.- I **48**, 1523 (2001).
- [37]. O. Morgül and E. Solak, “Observer based synchronization of chaotic systems”, Phys. Rev. E **54**, 4803-4811 (1996).
- [38]. H. Nijmeijer and I. M. Y. Mareels, “An observer looks at synchronization”, IEEE Trans. Circuits Syst.- I **44**, 882-890 (1997).
- [39]. G. Grassi and S. Mascolo, “Nonlinear observer design to synchronize hyperchaotic systems via a scalar signal”, IEEE Trans. Circuits Syst.- I **44**, 1011-1014 (1997).
- [40]. G. Grassi and S. Mascolo, “Synchronizing hyperchaotic systems by observer design”, IEEE Trans. Circuits Syst.- II **46**, 478-483 (1999).
- [41]. A. Azemi and E. E. Yaz, “Sliding-mode adaptive observer approach to chaotic synchronization”, J. Dynamics, Measurement and Control, Transactions of ASME **122**, pp. 758-765 (2000).
- [42]. M. Feki, “Observer-based exact synchronization of ideal and mismatched chaotic systems”, Physics Letters A **309**, pp. 53-60 (2003)
- [43]. M. Feki, “Synchronization of chaotic systems with parameter uncertainties using

- sliding observers”, *Int. J. Bifurcation and Chaos* **14**, pp. 2467-2475 (2004).
- [44]. J.-S. Lin, J.-J. Yan and T.-L. Liao, “Chaotic synchronization via adaptive sliding mode observers subject to input nonlinearity”, *Chaos, Solitons & Fractals* **24**, pp. 371-381 (2005).
- [45]. R. Femat, J. Alvarez-Ramirez and G. Fernandez-Anaya, “Adaptive synchronization of high-order chaotic systems: a feedback with low-order parameterization”, *Physica D* **139**, 231-246 (2000).
- [46]. Lian *et. al.*, “Adaptive synchronization design for chaotic systems via a scalar signal”, *IEEE Trans. Circuits Syst.-I* **49**, 17-27 (2002).
- [47]. C. Wang and S. S. Ge, “Synchronization of two uncertain chaotic systems via adaptive backstepping”, *Int. J. Bifurcation and Chaos* **11**, 1743-1751 (2001).
- [48]. C. Wang and S. S. Ge, “Adaptive synchronization of chaotic systems via backstepping design”, *Chaos, Solitons & Fractals* **12**, pp. 1199-1206 (2001).
- [49]. Y. Hong, H. Qin and G. Chen, “Adaptive synchronization of chaotic systems via state or output feedback control”, *Int. J. Bifurcation and Chaos* **11**, pp. 1149-1158 (2001).
- [50]. X. Tan, J. Zhang and Y. Yang, “Synchronizing chaotic systems using backstepping design”, *Chaos, Solitons & Fractals* **16**, pp. 37-45 (2003).
- [51]. Z. Li, G. Chen S. Shi and C. Han, “Robust adaptive tracking control for a class of uncertain chaotic systems”, *Physics Letters A* **310**, pp. 40-43 (2003).
- [52]. S. Chen, J. Hu, C. Wang and J. Lü, “Adaptive synchronization of uncertain Rössler hyperchaotic system based on parameter identification”, *Physics Letters A* **321**, pp. 50-55 (2004).
- [53]. Y. Yu and S. Zhang, “Adaptive backstepping synchronization of uncertain chaotic system”, *Chaos, Solitons & Fractals* **21**, pp. 643-649 (2004).
- [54]. S. Bowong and F. M. M. Kakmeni, “Synchronization of uncertain chaotic systems via backstepping approach”, *Chaos, Solitons & Fractals* **21**, pp. 999-1011 (2004).
- [55]. T. Yang and H. H. Shao, “Synchronizing chaotic dynamics with uncertainties based on a sliding mode control design”, *Phys. Rev. E* **65**, 046210 (2002).
- [56]. Z. Li and S. Shi, “Robust adaptive synchronization of Rossler and Chen chaotic systems via sliding technique”, *Physics Letters A* **311**, pp. 389-395 (2003).
- [57]. C.-C. Wang and J.-P. Su, “A new adaptive variable structure control for chaotic

- synchronization and secure communication”, *Chaos, Solitons & Fractals* **20**, pp. 967-977 (2004).
- [58]. H.-T. Yau, “Design of adaptive sliding mode controller for chaos synchronization with uncertainties”, *Chaos, Solitons & Fractals* **22**, pp. 341-347 (2004).
- [59]. T. Yang and L. O. Chua, “Impulsive stabilization for control and synchronization of chaotic systems: Theory and application to secure communication”, *IEEE Trans. Circuits Syst.- I* **44**, pp. 976-988 (1997).
- [60]. W. Xie, C. Wen and Z. Li, “Impulsive control for stabilization and synchronization of Lorenz systems”, *Physics Letters A* **275**, pp. 67-72 (2000).
- [61]. T. Yang and L. O. Chua, “Practical stability of impulsive synchronization between two nonautonomous chaotic systems”, *Int. J. Bifurcation and Chaos* **10**, pp. 859-867 (2001).
- [62]. Z. G. Li *et. al.*, “The stabilization and synchronization of Chua’s oscillators via impulsive control”, *IEEE Trans. Circuits Syst.- I* **48**, pp. 1351-1355 (2001).
- [63]. J. Sun, Y. Zhang and Q. Wu, “Less conservative conditions for asymptotic stability of impulsive control systems”, *IEEE Trans. Automatic Control* **48**, pp. 829-831 (2003).
- [64]. S. Chen, Q. Yang and C. Wang, “Impulsive control and synchronization of unified chaotic system”, *Chaos, Solitons & Fractals* **20**, pp. 751-758 (2004).
- [65]. C. Li, X. Liao and R. Zhang, “Impulsive synchronization of nonlinear coupled chaotic systems”, *Physics Letters A* **328**, pp. 47-50 (2004).
- [66]. X. Yu and Y. Song, “Chaos synchronization via controlling partial state of chaotic systems”, *Int. J. Bifurcation and Chaos* **11**, 1737-1741 (2001).
- [67]. X.-F. Wang, Z.-Q. Wang and G.-R. Chen, “A new criterion for synchronization of coupled chaotic oscillators with application to Chua’s circuits”, *Int. J. Bifurcation and Chaos* **9**, pp. 1169-1174 (1999).
- [68]. R. Tonelli, Y. Lai and C. Grebogi, “Feedback synchronization using pole-placement control”, *Int. J. Bifurcation and Chaos* **10**, 2611-2617 (2000).
- [69]. G. Grassi and S. Mascolo, “Synchronizing high dimensional chaotic systems via eigenvalue placement with application to neural networks”, *Int. J. Bifurcation and Chaos* **9**, 705-711 (1999).
- [70]. J.-Q. Fang, Y. Hong and G. Chen, “Switching manifold approach to chaos

- synchronization”, Phys. Rev. E **59**, R2523 (1999).
- [71]. S. Chen *et. al.*, “A stable-manifold-based method for chaos control and synchronization”, Chaos, Solitons & Fractals **20**, pp.947-954 (2004).
- [72]. J. Cao, H. X. Li and D. W. C. Ho, “Synchronization criteria of Lur’e Systems with time-delay feedback control”, Chaos, Solitons & Fractals **23**, pp.1285-1298 (2005).
- [73]. N. F. Rulkov *et. al.*, “Generalized synchronization of chaos indirectionally coupled chaotic systems”, Phys. Rev. E **51**, 980-994 (1995).
- [74]. H. D. I. Abarbanel, N. F. Rulkov and M. M. Sushchik, “Generalized synchronization of chaos: The auxiliary approach”, Phys. Rev. E **53**, 4528-4535 (1996).
- [75]. L. Kocarev and U. Parlitz, “Generalized synchronization, predictability, and equivalence of unidirectional coupled dynamical systems”, Phys. Rev. Lett. **76**, 1816-1819 (1996).
- [76]. L. M. Pecora, T. L. Carroll and J. F. Heagy, “Statistics for mathematical properties of maps between time series embeddings”, Phys. Rev. E **52**, 3420-3439 (1995).
- [77]. B. R. Hunt, E. Ott and J. A. Yorke, “Differentiable generalized synchronization of chaos”, Phys. Rev. E **55**, 4029-4034 (1997).
- [78]. V. V. Rumjantsev, Vestnik Moskov. Univ. Ser. I Mat. Meh. **4**, 9-16 (1957).
- [79]. N. Rouche, P. Habets and M. Laloy, *Stability Theory by Liapunov’s Direct Method*, 1977.
- [80]. V. V. Rumjantsev and A. S. Oziraner, *Stability and Stabilization of Motion with respect to Part of the Variables*, Nauka, 1987 (in Russian).
- [81]. K. Josić, “Invariant manifolds and synchronization of coupled dynamical systems”, Phys. Rev. Lett. **80**, 3053-3056 (1998).
- [82]. R. Femat and G. Solis-Perales, “On the chaos synchronization phenomena”, Phys. Lett. A **262**, 50 (1999).

Paper List

1. Zheng-Ming Ge and Yen-Sheng Chen, 2005, "Synchronization of Mutual Coupled Chaotic Systems via Partial Stability Theory", submitted to Physics Lett. A.
2. Zheng-Ming Ge and Yen-Sheng Chen, 2004, "Synchronization of Unidirectional Coupled Chaotic Systems via Partial Stability", Chaos, Solitons & Fractals **21**, pp.101-111. (SCI, Impact Factor: 1.526)
3. Zheng-Ming Ge and Yen-Sheng Chen, 2005, "Adaptive Synchronization of Unidirectional and Mutual Coupled Chaotic Systems", Chaos, Solitons & Fractals **26**, pp.881-888. (SCI, Impact Factor: 1.526)
4. Zheng-Ming Ge and Yen-Sheng Chen, 2005, "Diffeomorphic Synchronization of Unidirectional and Mutual Coupled Chaotic Systems", submitted to Chaos, Solitons & Fractals.
5. Zheng-Ming Ge, Tsung-Chih Yu and Yen-Sheng Chen, 2003, "Chaos Synchronization of a Horizontal Platform System", Journal of Sound and Vibration **268**, pp.731-749. (SCI, Impact Factor: 0.828)
6. Zheng-Ming Ge, Chia-Yang Yu and Yen-Sheng Chen, 2004, "Chaos Synchronization and Anticontrol of a Rotationally Supported Simple Pendulum", JSME Int. J. Series C, Vol. **47**, No.1, pp.233-241. (SCI)
7. Zheng-Ming Ge, Chun-Chi Lin and Yen-Sheng Chen, 2004, "Chaos, Chaos Control and Synchronization of Vibrometer System", Proc. Instn Mech. Engrs Vol. **218**, Part C: J. Mechanical Engineer Science, pp.1001-1020. (SCI)
8. Zheng-Ming Ge, Jui-Wen Cheng and Yen-Sheng Chen, 2004, "Chaos Anticontrol and Synchronization of Three Time Scales Brushless DC Motor

- System”, *Chaos, Solitons & Fractals* **22**, pp.1165-1182. (SCI, Impact Factor: 1.526)
9. Zheng-Ming Ge, Ching-Ming Chang and Yen-Sheng Chen, 2004, “Anti-Control of Chaos of Single Time Scale Brushless DC Motors and Chaos Synchronization of Different Order Systems”, accepted for publication by *Chaos, Solitons & Fractals*. (SCI, Impact Factor: 1.526)
 10. Zheng-Ming Ge, Chun-Lai Hsiao and Yen-Sheng Chen, 2004, “Nonlinear dynamics and Chaos Control for a Time Delay Duffing System”, *Int. J. of Nonlinear Sciences and Numerical Simulation* **6**(2), pp.187-199. (SCI, Impact Factor: 0.483).
 11. Zheng-Ming Ge, Chun-Lai Hsiao and Yen-Sheng Chen, 2004, “Chaos and Chaos Control for a Two-Degree-of-Freedom Heavy Symmetric Gyroscope”, submitted to *Chaos, Solitons & Fractals*.

